Nicotinic acid-free diet and NAPRT inhibitors as a means to sensitize cancer cells to NAMPT inhibitors

PhD thesis

Department of Internal Medicine and Medical Specialties- DIMI

University of Genoa

Marie-Skłodowska Curie Actions- Horizon 2020

INTEGRATA

Presented by: Moustafa S. Ghanem

Supervised by: Professor Alessio Nencioni

August 2019 - February 2023

Content

Abstract

Depleting NAD levels in tumors by interrupting their NAD-biosynthetic routes is an attractive anti-cancer strategy. Yet, suppressing the predominant NAD-producing salvage pathway by nicotinamide phosphoribosyltransferase (NAMPT) inhibitors failed in clinical trials, indicating that tumors can exploit alternative NAD-biosynthetic routes to escape NAMPT blockade. In this regard, the contribution of the Preiss-Handler (PH) pathway to NAD production in tumors is gaining great momentum. This pathway utilizes nicotinic acid (NA) as a substrate, which can be obtained from the diet or the gut microbiome. Herein, we demonstrate that blocking the PH pathway with an NA-free diet restored the activity of the NAMPT inhibitor FK866 in an ovarian cancer xenograft model. This combined intervention significantly reduced tumor volumes, blunted NAD levels, and impaired the energy status and metabolic activity of the tumors, while showing no systemic toxicity. In addition, combining an NA-free diet with antibiotics (to eliminate microbiota-derived NA) delayed tumor progression in the absence of NAMPT inhibitors. Furthermore, we also aimed at identifying new inhibitors to the rate-limiting enzyme of the PH pathway nicotinic acid phosphoribosyltransferase (NAPRT). We took advantage of *in silico* screening techniques and were able to annotate and characterize two NAPRT inhibitors that showed anti-cancer efficacy at micromolar concentrations while possessing favorable drug-like profiles. Since some NAMPT inhibitors are being currently evaluated in clinical trials, this work provides a rationale to couple NA-free diets or NAPRT inhibitors with NAMPT inhibitors in cancer patients.

List of Abbreviations

2-HNA	2-hydroxynicotinic acid
3-MA	3-methyl adenine
5-HNA	5-hydroxynicotinic acid
6-HNA	6-hydroxynicotinic acid
ACMSD	α-amino-β-carboxymuconate-ε-semialdehyde decarboxylase
ADCs	Antibody-drug conjugates
AFMID	Arylformamidase
AK	Adenosine kinase
ALL	Acute lymphoblastic leukemia
AMPK	AMP kinase
ATL	Adult T-cell leukemia/lymphoma
ATTECs	Autophagosome-tethering compounds
BBB	Blood-brain barrier
CLL	Chronic lymphocytic leukemia
DMSO	Dimethyl sulfoxide
EGFR	Epidermal growth factor receptor
EMT	Epithelial-to-mesenchymal transition
ERCC1	Excision repair cross-complementation group 1
Foxo1	Forkhead box O1
G6PD	Glucose 6-phosphate dehydrogenase
GACAT3	Gastric cancer-associated transcript 3
GLUT1	Glucose transporter 1
HAAO	3-hydroxyanthranilate 3,4-dioxygenase
HDAC	Histone deacetylase
HMGA1	High-mobility group A
IDH1	Isocitrate dehydrogenase 1
IDO	Indoleamine-2,3-dioxygenase
KMO	Kynurenine 3-monooxygenase
KYNU	Kynureninase
LDH	Lactate dehydrogenase
Lnc-RNA	Long non-coding RNA
MAPK	MAP kinase
MARTs	Mono (ADP-ribosyl) transferases
NA	Nicotinic acid
NAAD	Nicotinic acid adenine dinucleotide
NAD	Nicotinamide adenine dinucleotide
NADSYN	NAD synthase
NAM	Nicotinamide
NAMN	Nicotinic acid mononucleotide
NAMPT	Nicotinamide phosphoribosyltransferase
NAPRT	Nicotinic acid phosphoribosyltransferase
NF-κB	Nuclear-factor kappa B
NMN	Nicotinamide mononucleotide

NMNAT	Nicotinamide mononucleotide adenylyl transferase
NMNH	Reduced nicotinamide mononucleotide
NMRK1/2	Nicotinamide riboside kinase
NNMT	Nicotinamide N-methyltransferase
NQO1	NAD(P)H:quinone oxidoreductase
NQO2	NRH:quinone oxidoreductase
NR	Nicotinamide riboside
NRH	Reduced nicotinamide riboside
NSCLC	Non-small cell lung cancer
PAK 4	Serine/threonine p21-activated kinase 4
PAM	Plasma-activated medium
PARP	Poly (ADP-ribose) polymerase
PBS	Phosphate buffer saline
PCN	Pyrazine carbonitrile
PDAC	Pancreatic ductal adenocarcinoma
Pgp	P-glycoprotein 1
PH	Preiss-Handler
PncA	Nicotinamidase
PPM1D	Protein phosphatase Mg2+/Mn2+-dependent 1D
PPP	Pentose phosphate pathway
PROTACs	Proteolysis-targeting chimeras
QA	Quinolinic acid
QAPRT	Quinolinic acid phosphoribosyltransferase
ROS	Reactive oxygen species
SARM1	Sterile Alpha And TIR Motif Containing 1
SASP	Senescence-associated secretory phenotype
SRB	Sulforhodamine B
TCA	Tricarboxylic acid
TCA	Trichloroacetic acid
TDO	Tryptophan-2,3-dioxygenase
TNBC	Triple-negative breast cancer
TRAIL	Tumor necrosis factor-related apoptosis-inducing ligand
WM	Waldenstrom macroglobulinemia

1.   Introduction

1.1.   NAD and its cellular roles

Nicotinamide adenine dinucleotide (NAD) is a ubiquitous pyridine metabolite that actively participates in a broad range of fundamental processes in living cells. Since its discovery in 1906[1], the crucial functions of NAD inside the cells have been described and well-established[2]. NAD serves as a redox cofactor in vital cellular metabolic processes intimately engaged in energy production such as glycolysis, the tricarboxylic acid (TCA) cycle (also known as Krebs cycle), oxidative phosphorylation and fatty acid oxidation[3,4]. NAD carries out this function by mediating the transfer of a hydride anion ($H^+ + 2$ e^-) through shuttling between the oxidized (NAD+) and reduced forms (NADH)[3,5]. For example, NAD is reduced into NADH during glycolysis and the TCA cycle whereas in oxidative phosphorylation, NADH is oxidized back to NAD+ by donating its electrons. The released electrons flow along the complexes of the electron transport chain which creates a proton gradient across the inner mitochondrial membrane and ultimately results in energy production in the form of ATP. Apart from its role as a cofactor, NAD also acts as a substrate for several NAD-consuming enzymes such as mono (ADP-ribosyl) transferases, poly (ADP-ribosyl) polymerases (PARPs), the NAD-dependent deac(et)ylases sirtuins (SIRT1-7), and the NAD glycohydrolases CD38, CD157 and SARM1[2,4–6]. Through catalyzing the breakdown of NAD into ADP-ribose, these enzymes orchestrate a broad range of critical cellular processes such as DNA repair (*e.g.* PARP1 and PARP2), mitochondrial homeostasis (*e.g.* SIRT3, SIRT4, and SIRT5), epigenetic regulation of gene expression through DNA modification (*e.g.* PAPR1) or post-

translational modifications of histones (*e.g.* SIRT1 and SIRT6), circadian rhythm (*e.g.* SIRT1 and SIRT6), calcium signaling (*e.g.* CD38), immune regulation (*e.g.* CD157), and neural degeneration (*e.g.* SARM1)[5,7]. Thus, through its dual role as a co-factor and co-substrate, NAD is considered to be a central molecule that links cellular metabolic and signaling pathways.

1.2. NAD biosynthesis in mammals

NAD homeostasis is tightly balanced between NAD generation and breakdown. To maintain adequate NAD levels, mammalian cells are capable of utilizing several NAD precursors where each precursor follows a distinct biosynthetic route to form NAD. The most prevalent NAD production route in virtually all body tissues is the salvage pathway (also called the amidated pathway) which starts from nicotinamide (NAM). In addition, a parallel NAD-production route operates in multiple tissues and is named the Preiss-Handler pathway upon its discoverers[8,9]. The PH pathway utilizes nicotinic acid (NA) as its precursor (hence it is also called the deamidated pathway). The salvage and the PH pathways begin with the conversion of their precursors into the corresponding mononucleotides; nicotinamide mononucleotide (NMN) and nicotinic acid mononucleotide (NAMN) through the catalytic activity of nicotinamide phosphoribosyltransferase (NAMPT) and nicotinic acid phosphoribosyltransferase (NAPRT) respectively. Thereafter, nicotinamide mononucleotide adenylyl transferase (NMNAT) mediates the formation of NAD from NMN in the salvage pathway and nicotinic acid adenine dinucleotide (NAAD) from NAMN in the PH pathway[10]. Of note, there are three isoforms of NMNAT (NMNAT1, NMNAT2, and NMNAT3) according to their subcellular localization[11,12]. The PH pathway requires an additional third step in which

NAD synthase (NADSYN) amidates NAAD to yield NAD using glutamine to donate nitrogen.

NAD could be also synthesized via the *de novo* pathway starting from the amino acid tryptophan[13]. In this pathway (also known as the kynurenine pathway), tryptophan is transformed into quinolinic acid (QA) via a cascade of five enzymatic reactions[6]. QA is subsequently converted into nicotinic acid mononucleotide through the activity of quinolinic acid phosphoribosyltransferase (QAPRT) enzyme thereby converging with the PH pathway. Afterwards, the last two steps of the *de novo* NAD synthesis from tryptophan proceed in the same manner as those of the PH pathway. Notably, the *de novo* NAD production from tryptophan takes place mainly in the liver and to a lesser extent in the kidneys since these organs express the entire chain of the *de novo* pathway enzymes[14]. The contribution of the *de novo* pathway in the overall cellular NAD pool was thought to be marginal. However, elegant isotope-tracing experiments and NAD flux analysis have recently shown that the liver relies mainly on tryptophan to generate NAD, and then consumes NAD into NAM and finally passes NAM to the circulation so that it could be utilized by the rest of the tissues[14]. This finding raises the possibility that the contribution of the *de novo* pathway to the overall NAD pool could be more relevant than formerly anticipated not so much directly but rather indirectly through multistep inter-tissue cooperation.

In 2004, Bieganowski and Brenner described an alternative salvage pathway (the nucleoside pathway) that uses nicotinamide riboside (NR) as a precursor[15]. In this pathway, NR is phosphorylated by nicotinamide riboside kinase (NMRK1/2) into NMN which, in turn, is transformed into NAD via NMNATs similar to the classical salvage

pathway[16]. Very recently, the reduced forms of nicotinamide riboside (NRH) and nicotinamide mononucleotide (NMNH) were identified as additional NAD precursors that boosted cellular NAD levels through a novel pathway that depends on the kinase activity of adenosine kinase (AK) rather than NMRK[17–19].

NAM, NA, and NR are micronutrients that constitute the three forms of vitamin B3 and could be exogenously obtained from the diet[13]. Likewise, tryptophan is an essential amino acid that needs to be incorporated into mammalian tissues through the intake of high-protein foods. Besides the dietary intake, NAM is a common bi-product that is liberated from the catalytic activity of all NAD-consuming enzymes which can then be recycled to recompose NAD via the classical salvage pathway. Furthermore, NAM feeds the gut microbiome to produce NA since the gut microbial flora can convert NAM into NA taking advantage of their microbial enzyme nicotinamidase (PncA)[20]. The microbial-derived NA can circulate and, in turn, bolster NAD production in body tissues through the PH pathway[20,21]. To avoid NAM accumulation, the nicotinamide N-methyltransferase (NNMT) enzyme catalyzes the transfer of a methyl group to NAM, and methylated NAM is readily cleared from the body[22]. NR, the newest form of vitamin B3, is present in cow milk[23] and can also be generated in mammalian tissues starting from its reduced form, NRH, via NRH: quinone oxidoreductase 2 (NQO2) which uses NRH as an electron donor[24]. Finally, NRH was shown to be endogenously present in the liver[19]. Of note, NAD levels were shown to decline with aging and other aging-related pathological conditions and the exogenous supplementation of NAD precursors (*e.g.* NMN or NR supplements) has demonstrated promising outcomes in ameliorating several aging-associated diseases[7]. The NAD biosynthetic pathways are summarized in Figure 1.1.
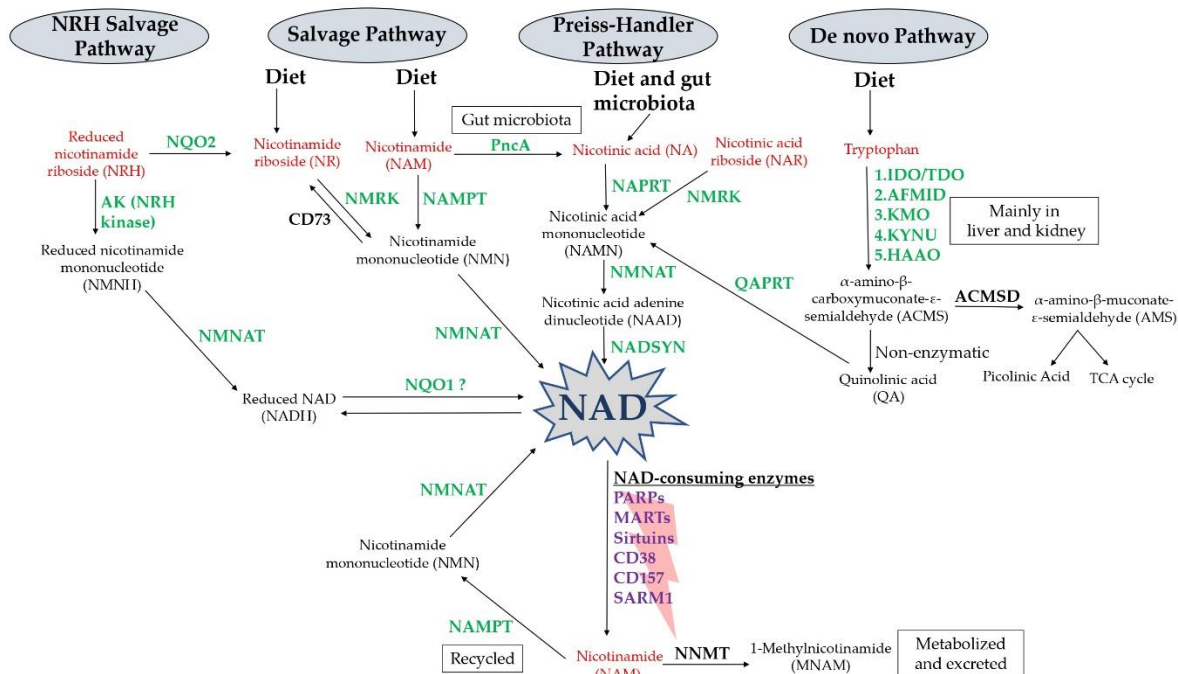
Figure 1.1. Schematic representation of the NAD biosynthetic pathways.

NAD, nicotinamide adenine dinucleotide; NAMPT, nicotinamide phosphoribosyltransferase; NAPRT, nicotinic acid phosphoribosyltransferase; PncA, bacterial nicotinamidase; NMNAT, nicotinamide mononucleotide adenylyltransferase; NMRK, nicotinamide riboside kinase; NADSYN, NAD synthetase; QAPRT, quinolinic acid phosphoribosyltransferase; IDO, indoleamine-2,3-dioxygenase; TDO, tryptophan-2,3-dioxygenase; AFMID, arylformamidase; KMO, kynurenine 3-monooxygenase; KYNU, kynureninase; HAAO, 3-hydroxyanthranilate 3,4-dioxygenase; ACMSD, α-amino-β-carboxymuconate-ε-semialdehyde decarboxylase; MARTs, mono(ADP-ribosyl) transferases; PARPs, poly(ADP-ribose) polymerases; SARM 1, sterile alpha and TIR motif-containing 1; NQO1, NAD(P)H:quinone oxidoreductase; NQO2, NRH:quinone oxidoreductase; AK, adenosine kinase; NNMT, nicotinamide N-methyltransferase; and TCA, tricarboxylic acid

1.3. NAD and cancer

Reprogrammed metabolism has been established as a cancer hallmark[25]. Malignant cells alter their metabolic requirements to drive their growth and proliferation[26]. A central component of these metabolic adaptations is their reliance on glycolysis, even when oxygen is abundant, which mainly guarantees fast, albeit less efficient, energy production and importantly generates metabolites for biomass buildup[26,27]. This process, known as aerobic glycolysis or Warburg effect[28], is closely linked to the propensity of malignant cells to provide a surplus of NAD compared to their normal counterparts. Moreover, NAD homeostasis in tumor cells can be challenged by the elevated expression and/or activity of NAD-consuming enzymes, such as PARPs and sirtuins[27]. For instance, neoplastic response to genomic insults is governed, at least in part, by PARP1 and PARP2 which degrade NAD to generate poly ADP-ribose chains to stimulate DNA repair[29]. To escape the detrimental effects of NAD shortage, tumor cells are requested to enhance NAD production. Thus, interrupting the NAD biosynthetic routes has emerged as a prominent approach for cancer treatment[4,27,30,31].

1.3.1. Targeting the salvage pathway in cancer treatment

Since the classic salvage pathway is widely conceived as the predominant NAD-generating route, most research in this field was focused on developing inhibitors to its rate-limiting enzyme NAMPT. In support of this notion, a large number of studies demonstrated the upregulation of NAMPT expression in various types of cancer including gliomas[32], sarcomas[33], lymphomas[34], melanoma[35], thyroid carcinoma[36], ovarian cancer[37], breast cancer[38,39], pancreatic cancer[40], colorectal cancer[41–43], gastric cancer[44] and prostate cancer[45]. Moreover, NAMPT was found to drive pro-oncogenic and more

aggressive phenotypes and its overexpression has been associated with worsened prognosis in different types of cancer[32,39,41,42,46,47]. Besides being an intracellular enzyme, NAMPT gets secreted outside the cells and this extracellular form (also known as visfatin or eNAMPT) is also implicated in many pro-oncogenic roles[48–50].

1.3.1.1. Regulation of NAMPT in tumors

Several transcriptional and post-transcriptional mechanisms tightly regulate NAMPT expression and activity in tumors. Chowdhry and colleagues recently reported on a putative *NAMPT* enhancer located 65 kb upstream of the *NAMPT* transcription start site, which controls *NAMPT* expression and activity[51]. Chromatin immunoprecipitation and further experiments revealed that this *NAMPT* enhancer is marked by H3K27 acetylation, is bound by the transcription factors c-MYC and MAX that regulate its activity, and that it is required solely by salvage-dependent tumors for their survival[51]. Consistent with a role for c-MYC in NAMPT expression, an earlier study described a c-MYC–NAMPT–SIRT1 positive feedback loop, in which c-MYC directly interacts with the *NAMPT* promoter and induces NAMPT expression, which in turn leads to SIRT1 activation through enhanced NAD provision[52]. SIRT1, in turn, stabilizes c-MYC and enhances its transcriptional activity, and promotes tumorigenesis through the attenuation of p53 activity and the inhibition of c-MYC-induced apoptosis[52]. This c-MYC–NAMPT–SIRT1 positive feedback loop was found to be activated in colorectal carcinoma and its interruption was proposed as a viable therapeutic intervention[53,54]. Additionally, the high-mobility group A (HMGA1) protein was reported to be another protein regulating NAMPT expression through a different enhancer element[55]. The HMGA1–NAMPT–NAD signaling axis was shown to drive the proinflammatory senescence-associated secretory phenotype (SASP) via NAD-

mediated enhancement of nuclear-factor kappa B (NF-κB) activity, to promote an inflammatory environment and to drive tumor progression[55]. Indeed, numerous cancer types overexpress HMGA proteins and their overexpression is often associated with poor prognosis[56]. On the contrary, the transcription factor and tumor suppressor forkhead box O1 (Foxo1) binds to the 5'-flanking region of the *NAMPT* gene and downregulates NAMPT expression in breast cancer cells, an effect that is reversed by the insulin–PI3K–AKT signaling pathway[57]. Additionally, NAMPT-AS "RP11-22N19.2", a new promoter-associated long non-coding RNA (Lnc-RNA), epigenetically regulates NAMPT expression in triple-negative breast cancer (TNBC)[58]. NAMPT-AS activates NAMPT expression at the transcriptional and post-transcriptional levels and promotes tumor progression and invasiveness in TNBC[58]. Similarly, in gliomas, gastric cancer-associated transcript 3 (GACAT3), another long non-coding RNA, regulates NAMPT expression and promotes glioma progression by acting as a molecular sponge to miR-135a, inhibiting its interaction with its target, NAMPT[59]. Several studies report on NAMPT expression being regulated at the post-transcriptional level by microRNAs. Specifically, *NAMPT* mRNA was found to be a target of miR-381[60], miR-206[61], miR-494[62], and miR-154[63] in breast cancer cells, of miR-23b in melanoma[64], of mir-206 in pancreatic cancer[65] and miR-26b[66] in colorectal cancer. Generally, increased expression of these microRNAs was shown to suppress NAMPT expression and it was associated with reduced cancer cell viability, suggesting the potential use of these microRNAs as anti-cancer agents. In this context, we have recently shown that, in addition to being regulated at the gene level, NAMPT enzymatic activity can also be regulated by other enzymes. Specifically, we found that SIRT6 enhances NAMPT enzymatic activity through direct protein deacetylation, protecting

cancer cells against oxidative stress[67]. Similarly, a previous study found that also SIRT1 deacetylates NAMPT, predisposing it to secretion in adipocytes[68]. Mesenchymal glioblastoma stem cells were found to preferentially upregulate NAMPT and NNMT expression through the transcription factor C/EBPβ, which interacts with *NAMPT* and *NNMT* gene regulatory regions. Of note, in these cell subtypes, NNMT induced a state of DNA hypomethylation and downregulated the expression of *DNA* methyltransferases in a methionine-dependent fashion[69]. Whether NNMT epigenetically affects NAMPT expression requires further studies.

### 1.3.1.2.   NAMPT Inhibitors as cancer therapeutic agents

Numerous NAMPT inhibitors have been reported over the past two decades (Figure 1.2). FK866 (also known as (E)-Daporinad, APO866, or WK175) was the first reported NAMPT inhibitor in the early 2000s[70,71]. FK866 was able to gradually blunt NAD levels and induce apoptotic cell death in leukemia and hepatic cancer cells[70,71]. The robust anti-cancer activity observed with FK866 stimulated its testing in clinical trials. Besides FK866, the NAMPT inhibitor CHS-828 and its prodrug GMX1777 were also evaluated in early-phase trials (given their potent antineoplastic efficacy in preclinical models of cancer[72–74]). Regrettably, none of the three NAMPT inhibitors was able to achieve an objective tumor response in cancer patients most likely due to the capability of neoplastic cells to exploit surrogate NAD-production routes to circumvent NAMPT blockade and escape the deleterious effects of NAD deficit. Moreover, patients treated with these agents experienced serious hematological adverse effects and thrombocytopenia was common dose-limiting toxicity[75,76]. Gastrointestinal side effects were also reported with the oral

agents GMX1777 and CHS-828[77–79]. Collectively, these findings reflected an urgent need to refine treatment with NAMPT inhibitors. Nonetheless, additional inhibitors of NAMPT have been reported in the following years such as GNE-617[80] and GNE-618 (Genentech)[81], MV87[82], A-1293201, and A-1326133 (AbbVie)[83], STF-118804[84], LSN3154567 (Eli Lilly)[85], OT-82 [86] as well as the antibody-drug conjugates (ADCs) that incorporate NAMPT inhibitors as their payloads[87–89]. Of note, continuous efforts to optimize the structural-activity relationship of NAMPT inhibitors recently gave rise to the synthesis of remarkably potent NAMPT inhibitors that demonstrated anti-cancer efficacy at picomolar concentrations[90,91]. Significant antitumor efficacy was also attained with dual NAMPT inhibitors which simultaneously target NAMPT and a second enzyme (or a protein) of interest such as the serine/threonine p21-activated kinase 4 (PAK 4)[92], glucose transporter 1 (GLUT1)[93], epidermal growth factor receptor (EGFR)[94], histone deacetylase (HDAC)[95,96] and indoleamine 2,3-dioxygenase 1 (IDO1)[97]. Furthermore, very recent studies succeeded in designing proteolysis-targeting chimeras (PROTACs) or autophagosome-tethering compounds (ATTECs) which target NAMPT and trigger its proteasomal or lysosomal degradation respectively. Interestingly, these NAMPT-degrading chimeras also elicited significant anti-cancer efficacy in several models of cancer[98–101]. Taken together, given the pleiotropic roles of NAMPT in driving tumor progression (recently reviewed by Galli *et al.* and Heske *et al.*[102,103]), the development of NAMPT inhibitors still remains an attractive therapeutic option in oncology[104]. A second wave of NAMPT inhibitors represented by OT-82[86] and the dual NAMPT/PAK inhibitor KPT-9274[92] are being currently tested in clinical trials in patients with hematologic malignancies (Figure 1.3).

FK866

CHS-828

GMX1777

GNE-617

GNE-618

LSN3154567

STF-118804

A-1293201

OT-82

KPT-9274
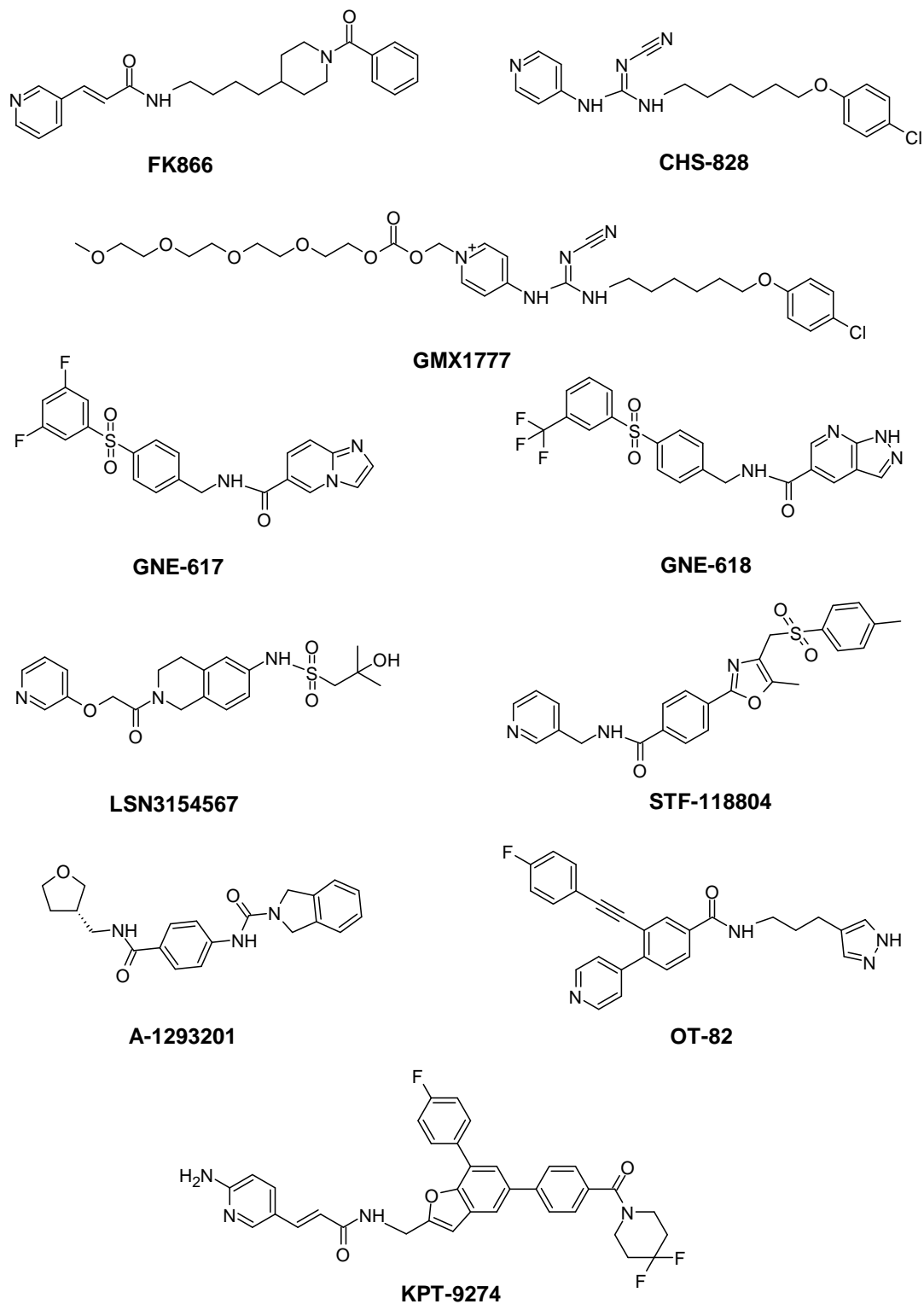
Figure 1.2. The chemical structures of several NAMPT inhibitors identified over the past years.
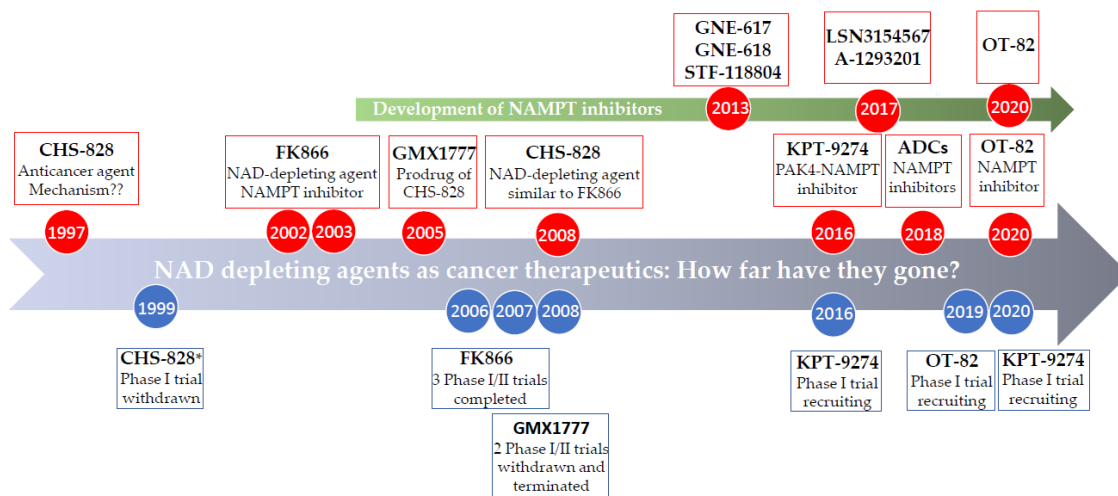
Figure 1.3. Timeline summary for the development of NAMPT inhibitors and their entry for evaluation in clinical studies.

1.3.1.3. Effects of NAD production inhibition in cancer

NAMPT inhibitors and cancer cell death

Several mechanisms were reported to trigger cancer cell death in response to NAD depletion by NAMPT inhibitors. Initially, FK866 was reported to deplete intracellular NAD and to kill cancer cells by inducing apoptosis[70,71]. Similarly, OT-82 and KPT-9274 were also found to induce their antileukemic effect through apoptosis[86,105]. In primary chronic lymphocytic leukemia (CLL) cells, FK866 was demonstrated to induce apoptotic signaling and caspase activation at doses that triggered cell death[106]. However, in the same models, indicators for autophagy induction were also observed at low doses of FK866 and/or at early time points[106]. Several studies linked NAMPT inhibitor-induced cell death to autophagy. In multiple myeloma cells, FK866 triggered autophagic cell death via i) the inhibition of PI3K/mTORC1 activity (a transcription-independent mechanism) and ii) the

inhibition of MAP kinase (MAPK), which permits nuclear translocation of the transcription factor EB (TFEB) that coordinates lysosomal biogenesis and drives the expression of autophagy-related genes[107,108]. Additionally, no evidence of apoptotic cell death was detected in multiple myeloma cells in response to FK866 treatment[107]. Consistent with this observation, autophagy, but not apoptosis, was associated with FK866-induced cytotoxicity in neuroblastoma and hematological cancers[109,110]. In neuroblastoma cells, FK866-induced autophagy was potentiated or antagonized by chloroquine and by 3-methyl adenine (3-MA), respectively, lending support to the notion that aberrant autophagy is involved in FK866-mediated cancer cell demise[111]. Furthermore, NAMPT inhibitor-induced NAD depletion in isocitrate dehydrogenase 1 (*IDH1*)-mutant cancers was associated with inducing AMP kinase (AMPK) and initiating autophagy, and the autophagy inhibitor 3-MA rescued the cells from the cytotoxic effects of NAMPTi-mediated NAD depletion[112]. Intriguingly, FK866 simultaneously activated apoptosis and autophagy and markedly reduced the viability of HTLV-1-infected, adult T-cell leukemia/lymphoma (ATL) cell lines[113]. Furthermore, we showed that autophagy-mediated FK866 antileukemic activity was potentiated by tumor necrosis factor-related apoptosis-inducing ligand (TRAIL)[114]. Another group postulated that oncosis is the critical pathway leading to cancer cell death in response to the NAMPT inhibitor, GNE-617, in several non-hematological cancer cell lines irrespective of the appearance of signs of apoptosis or autophagy[115]. This group also showed that oncosis was driven by dramatic ATP depletion and subsequent loss of plasma membrane integrity, which typically marks the late phases of NAD depletion via NAMPT inhibition[115]. Taken together, the

18

mechanism underlying cancer cell death in response to NAMPT inhibitors might be cancer type-specific and regulated in a dose and time-dependent manner.

NAD depletion and oxidative stress

Oxidative stress is caused by an imbalance between reactive oxygen species (ROS) and the cellular antioxidant capacity in favor of the former. Excessive ROS accumulation is detrimental to cell viability. NADPH is a critical molecule in oxidative homeostasis as it provides the reductive power for glutathione reductase and thioredoxin reductase in glutathione and thioredoxin ROS scavenging systems[3,5]. NADPH is mainly produced via the pentose phosphate pathway (PPP) and accordingly, cancer cells have evolved mechanisms to enhance glucose flux into the PPP to combat oxidative stress[116,117]. As a consequence, building blocks for nucleotide biosynthesis are also more available to cancer cells. Besides, around 10% of the total NAD(H) pool is phosphorylated to NADP(H) by NAD kinases[2,5]. Several studies described a strong link between NAD inhibition and oxidative stress in cancer cells. For instance, enhanced ROS production in MDA-MB-231 breast cancer cells was noted when FK866 was added to ROS-containing plasma-activated medium (PAM)[118]. Also, recently FK866 was reported to exert its antileukemia activity through ROS and reactive nitrogen species generation as a consequence of NAD depletion[119]. Mitochondrial depolarization, ATP loss, and cell death were also reported as downstream effects of FK866-induced oxidative stress in this study[119]. Increased ROS levels were also reported with other NAMPT inhibitors, such as CHS-828 and OT-82[120,121]. In support of the above insights, combining FK866 with β-lapachone, an NQO1 substrate that generates ROS and exerts anti-cancer effects, was shown to cause dramatic NAD depletion and cytotoxic effects in NQO1-expressing

pancreatic ductal adenocarcinoma (PDAC) and non-small cell lung cancer (NSCLC) cells[122–124]. Curiously, in renal and cochlear tissues, β-lapachone was reported to augment NAD levels and to reverse the drop in the NAD/NADH ratio caused by cisplatin treatment[125,126]. This different and apparently contrasting behavior of β-lapachone seems to be attributable to the preferential accumulation of ROS species via this compound in NQO1-overexpressing cancers, but not in normal cells (that are protected by low NQO1 expression and by high catalase levels). In NQO1-overexpressing cancer cells, ROS production in response to β-lapachone causes DNA damage and thereby triggers PARP-mediated NAD degradation to such an extent that it outweighs the possible increase in NAD caused by NQO1, ultimately causing cancer cell demise via NAD and ATP shortage[127,128]. Similarly, paracetamol was found to bind to NQO2 as an off-target effect and NQO2 expression modulated paracetamol-induced ROS production in HeLA cells[129]. Therefore, combining paracetamol with NAD-depleting agents in NQO2-overexpressing cancers might be a promising approach. Last but not least, NAMPT inhibitors augmented oxidative stress induced by temozolomide in glioblastoma cells, and this sensitization effect was reversed by the ROS scavenger tocopherol[130].

NAD depletion and DNA damage and repair

The crosstalk between NAMPT, PARPs, and DNA damage has been thoroughly investigated over the past decades. While NAMPT produces NAD, activated PARPs consume the majority of NAD to support their DNA repair activity in response to DNA-damaging insults[5]. In line with this notion, excision repair cross-complementation group 1 (ERCC1)-deficient NSCLC cells, a DNA-repair defective cancer model, showed reduced basal NAMPT and NAD levels, presumably as a result of chronic PARP1

activation, and FK866 treatment resulted in a catastrophic NAD drop and profound synthetic lethality *in vitro* and *in vivo*[131]. Chemo-potentiation was seen when NAMPT inhibitors were combined with genotoxic agents that cause DNA damage, such as 5-fluorouracil (5-FU) in gastric cancer[44], fludarabine and cytarabine in leukemia[106,121], cisplatin or etoposide in neuroblastoma[111], temozolomide in gliomas[130,132], gemcitabine, paclitaxel and etoposide in pancreatic cancer cells[133,134], pemetrexed in NSCLC[135], and bendamustine and melphalan in Waldenstrom macroglobulinemia (WM)[136]. In addition, NAMPT inhibitors potentiated the efficacy of the radionuclide ^{177}Lu-DOTATATE in neuroendocrine tumors[137], and sensitized head and neck cancer and prostate cancer models to radiotherapy[138,139]. Also, it was hypothesized that combining NAMPT inhibitors with PARP inhibitors would further downregulate PARP activity leading to persistent DNA lesions and ultimately cell death. Indeed, a potentiating effect was shown between NAMPT inhibitors and the PARP inhibitors olaparib or niraparib in triple-negative breast cancer and Ewing sarcoma[140–142]. In opposition, a recent study demonstrated that the FK866 cytotoxic effect against hematological malignant cells is reliant on PARP integrity since PARP1 deletion reversed ROS accumulation, mitochondria depolarization, and ATP loss, and abolished FK866-induced cell death[119]. Similar results were previously reported by our group in human-activated T-cells and T-cell acute lymphoblastic leukemia (ALL) models[143]. The proposed explanation for these findings is that PARP inhibitors, by blocking NAD consumption, elevate NAD levels and this antagonizes NAMPTi-induced NAD depletion and its downstream effects.

NAD depletion and targeted therapy

Owing to their particular mode of action, NAMPT inhibitors lend themselves to be used in combination regimes, enhancing the antitumor activity of immune checkpoint inhibitors [144,145] or targeted therapies such as histone deacetylase inhibitors[146], and tyrosine kinase inhibitors in leukemia[121] and WM[147], proteasome inhibitors in multiple myeloma[148], and mTOR inhibitors in pancreatic neuroendocrine tumors[149]. Finally, we demonstrated that cyclosporin-A and verapamil sensitized leukemia cells to FK866 by inhibiting P-glycoprotein 1 (Pgp), the multidrug resistance transporter, thereby permitting the intracellular accumulation of FK866, which in turn led to ER stress and cell demise[150].

1.3.2. Targeting the Preiss-Handler pathway in cancer treatment.

One of the mechanisms underlying resistance to NAMPT inhibitors is the ability of cancer cells to bypass NAMPT inhibition and the ensuing NAD depletion by exploiting parallel NAD biogenesis routes. In this regard, the Preiss-Handler (PH) pathway has recently gathered growing attention in oncology. The significance of this pathway was highlighted by recent studies, demonstrating that the gene encoding its rate-limiting enzyme nicotinic acid phosphoribosyltransferase (NAPRT) is amplified in a broad subset of solid tumors, including ovarian, pancreatic, prostate, and breast cancers[51,151]. Accumulating evidence emphasizes that NAPRT expression status in neoplastic cells dictates their susceptibility to NAMPT inhibitors. For instance, *NAPRT* silencing restored the anti-cancer activity of NAMPT inhibitors against NAPRT-positive leukemia, ovarian cancer, and pancreatic cancer cell lines[151,152]. Likewise, cancers with genetic mutations that suppress NAPRT activity are found to be extremely vulnerable to NAMPT inhibitors. For example, *IDH1* mutant glioma and sarcoma cell lines tend to downregulate NAPRT levels through

hypermethylation of the *NAPRT* promoter, thereby blocking the NAPRT-dependent pathway, which renders them critically reliant on NAMPT for NAD replenishment[112]. Consequently, NAMPT inhibition led to a metabolic crisis in these types of tumors, blunted NAD pools, and resulted in AMPK-mediated autophagy and cytotoxicity[112]. Consistent with this notion, mutations in the protein phosphatase Mg2+/Mn2+-dependent 1D (PPM1D) gene in pediatric gliomas also drive *NAPRT* gene silencing through the hypermethylation of CpG islands in the NAPRT promoter, thus, again conferring exquisite sensitivity to NAMPT inhibitors[153]. Similar results were also noted with chondrosarcoma cell lines as well as gastric cancer cell lines which show markers of epithelial-to-mesenchymal transition (EMT) where this EMT subtype was particularly associated with loss of NAPRT expression[154,155]. Collectively, these findings reinforce that NAPRT expression could be a useful biomarker of sensitivity to NAMPT inhibitors[112,153–156]. In addition to promoter hypermethylation, other mechanisms that regulate NAPRT gene expression include alternative splicing and mutations in the transcription factor binding sites[157]. Overall, these findings built a strong rationale for evaluating PH pathway obstruction as a means to sensitize tumors to NAMPT inhibitors. It is worth noting that, similar to NAMPT, an extracellular form of NAPRT has been recently detected and shown to play roles in inflammatory signaling[158]. However, whether extracellular NAPRT is involved in malignant transformation needs further investigation.

1.4. Aim of the project

In light of the above insights, the objective of our project was to block the Preiss-Handler NAD-generating pathway as a means to reverse the resistance of tumor cells to NAMPT inhibitors.

1.4.1. Administration of an NA-free diet

Early work from Hara and colleagues demonstrated that several murine tissues such as the heart, liver, kidney, and small intestine express NAPRT in abundant amounts[159]. Similar results were also found in human tissues[157]. Recent extensive analysis unveiled that cancer cells that originate from normal tissues with high NAPRT expression tend to be reliant on the Preiss-Handler pathway for their survival[51]. NA was able to boost NAD production in human embryonic kidney cells via NAPRT and thereby protecting them from oxidative stress-induced cytotoxicity[159]. Accordingly, the intake of NA in the diet can fuel the activation of the PH pathway inside the cells of the human body including malignant cells. As previously mentioned, NA is a form of vitamin B3 that is exogenously supplied from the diet or endogenously provided by the gut microbiota through NAM deamidation via the microbial enzyme nicotinamidase (PncA)[20,152]. Therefore, we proposed a dietary approach that aimed at impairing NAD synthesis via the PH pathway by limiting the availability of its precursor NA. To efficiently eliminate NA sources, the administration of an NA-deficient diet with or without antibiotics (to lower the gut microbiome-derived NA) was adopted. In support of this approach, the concept of integrating dietary modifications to ameliorate the responsiveness to chemotherapeutics has emerged as a promising therapeutic intervention in oncology[160].

1.4.2. Development of NAPRT inhibitors

The most straightforward approach to deactivating the PH pathway of NAD biosynthesis is to design chemical compounds that inhibit NAPRT activity. A limited number of NAPRT inhibitors have been identified so far. Experiments performed in the 1970s on human platelets identified several compounds that inhibited NAPRT activity, including 2-

hydroxynicotinic acid (2-HNA) and several non-steroidal anti-inflammatory drugs (NSAIDs) such as flufenamic acid, mefenamic acid, and phenylbutazone[161–163]. Our group demonstrated that 2-HNA was indeed able to sensitize NAPRT-expressing ovarian and pancreatic cancer cells to NAMPT inhibitors and recapitulated the effect of NAPRT silencing[151]. Galassi *et al.* described a series of endogenous metabolic intermediates that inhibit NAPRT[164]. Among the identified metabolites, coA showed the most potent inhibitory activity[164]. Nevertheless, the relatively low potency and limited aqueous solubility of the currently available NAPRT inhibitors are inherent obstacles to their evaluation in clinical trials. Accordingly, we aimed at identifying new chemical scaffolds with inhibitory activity on the human NAPRT enzyme. To this end, we performed a high-throughput molecular docking screen taking advantage of the crystal structure of NAPRT which had been disclosed by Marletta and colleagues[165]. Hits from the *in silico* screen were subjected to subsequent biological and biochemical characterization. The goals of the project are summarized in Figure 1.4.
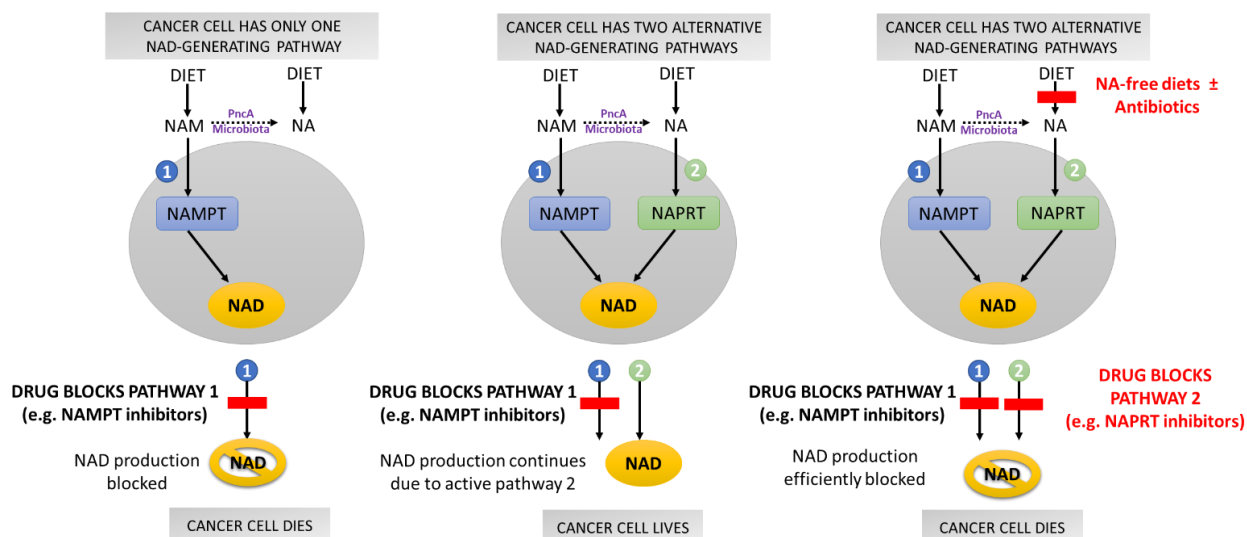
Figure 1.4. A schematic representation of the aim of the project.

2. Materials and methods

2.1. Cell lines and reagents

OVCAR-5, OVCAR-8, SKOV-3, and HCT116 cell lines were provided from the NCI-60 panel. A2780, Capan-1, NCI-N87, and Mia PaCa-2 cell lines were purchased from the ATCC (LGC Standards S.r.l., Milan, Italy). All cell lines were grown RPMI-1640 cell culture medium supplemented with 10% heat-inactivated fetal bovine serum (FBS; Gibco, Waltham, MA, USA) and 1% penicillin (50 units/mL) and streptomycin (50 µg/mL) (Life Technologies Italia, Monza, Italy) and incubated in humidified atmospheric conditions at 5% CO_2 and 37^{0}C. FK866 for *in vitro* experiments was supplied from the NIMH Chemical Synthesis and Drug Supply Program while that used for *in vivo* experiments was purchased from AKos GmbH (Germany). All the antibiotics used for the *in vivo* experiments were provided by the Pharmacy of the IRCCS Ospedale Policlinico San Martino. NA, NAMN, 2-HNA, and pyrazine carbonitrile (PCN) were purchased from Sigma Aldrich S.r.l. 5-hydroxynicotinic acid (5-HNA) and 6-hydroxynicotinic acid (6-HNA) were purchased from Thermo Fischer Scientific. Stock solutions of all the putative NAPRT inhibitors (100 mM), FK866 (100 µM), and 2-HNA (500 mM) were prepared by dissolving the compounds in 100% DMSO.

2.2. Cell growth inhibition assay

Cell viability was determined using the sulforhodamine B (SRB) colorimetric assay as described in [166]. Briefly, cancer cells were seeded in 96-well plates with different seeding densities depending on the cancer cell line and left to attach overnight at 37°C in a humidified atmosphere of 5% CO_2 and 95% air. The following day, the old medium was removed and cells were treated with fresh medium containing the experimental conditions

in triplicates, and the plates were subsequently incubated at 37ºC in a humidified atmosphere of 5% CO_2 and 95% air for 72 hours. To stop the experiment, cold 50% (w/v) trichloroacetic acid (TCA) was then added drop-wise to each well to fix the cells (final concentration, 10% TCA). The plates were incubated at 4ºC for 20 minutes then washed four times with tap water and left to dry in the air. Thereafter, SRB solution (0.057% w/v in 1% acetic acid) was added to stain the fixed cells and the plates were shaken for 10 minutes at room temperature. After staining, the SRB solution was removed and the plates were washed four times with 1% (v/v) acetic acid and left to air-dry. To solubilize the protein-bound dye, 100 µl of 10 mM trizma base was next added and the plates were shaken for 10 minutes at room temperature. Finally, the absorbance was measured at a wavelength of 515 nM by an automated plate reader (Tecan Infinite® 200 PRO instrument)

2.3. *In vivo* experiments

All animal studies were conducted in agreement with the Institutional Animal Care and Use Committee of the Ospedale Policlinico San Martino, I.R.C.C.S. per l'Oncologia. Six- to eight-week-old female BALB/c athymic (nu+/nu+) mice were purchased from Charles Rivers Laboratories. Mice were housed under pathogen-free conditions in air-filtered laminar flow cabinets with a 12-hour light/dark cycle and provided with food and water ad libitum. Mice were allowed to acclimatize for 1 week in their new environment.

The proof-of-concept study of an NA-deficient diet with or without FK866 was evaluated using ovarian cancer (OVCAR-5) xenograft model. Mice were subcutaneously injected in each flank with 5×10^6 OVCAR-5 cells resuspended in 100 µl of 50:50 RPMI-1640: matrigel. When the masses became palpable, the standard ad libitum food was replaced

with a customized control diet (containing the recommended daily NA intake of 30 mg NA /kg diet) or NA-deficient diet (containing the same composition as the control diet but without NA; Mucedola S.r.l.). Nine days after initiating the new diets, mice were randomly assigned to receive either vehicle DMSO or FK866 injection (20 mg/kg i.p. once daily for four consecutive days/week). This resulted in four different experimental groups (*i.e.*, CTR group, NA-free diet group, CTR diet + FK866 group, and NA-free diet + FK866 group). Tumor dimensions and mice weights were routinely recorded and tumor volumes were calculated using the formula: tumor volume $(mm^3) = (w2 \times W) \times \pi/6$, where w (minor side) and W (the major side) are in mm. None of the tumors exceeded the maximum tumor volume of 1500 mm^3 allowed by our Institutional Animal Care and Use Committee (IACUC). At the end of the experiment, mice were sacrificed and tumors were excised and stored at -80 °C for subsequent ex-vivo studies. Mice's whole blood was collected in Eppendorf tubes, left to coagulate for 2 hours at room temperature, and then centrifuged for 20 minutes at 4,000 rpm. After centrifugation, mice serum was then pipetted and then stored at -80 °C, and then shipped to Lausanne for quantification of NAD metabolites.

For the subsequent experiment dedicated to assessing the safety of the NA-deficient diet (with or without FK866), mice were fed with the NA-free diet or control diet three weeks before cell inoculation. After cell injection, FK866 treatment was initiated when the masses became palpable and continued for another three weeks. At the end of the experiment, mice were sacrificed and whole blood was collected and sent to San Raffaelle hospital for evaluation of hematological and biochemical parameters.

2.4. Evaluation of the energy status and oxidative phosphorylation

Tumor masses were washed in phosphate buffer saline (PBS) and homogenized by a Potter–Elvehjem system in 1 mL of PBS plus protease inhibitors. All procedures were performed on ice. Total proteins were estimated by the standard Bradford method[167].

ATP and AMP content inside the tumor samples was evaluated by the enzyme coupling method[168], as previously described in [169]. The ATP/AMP value was calculated as the ratio between the intratumor concentration of ATP and AMP, expressed in mM/mg tissue. The assay of ATP synthesis through FoF1-ATP synthase activity was conducted by measuring formed ATP from added ADP using the highly sensitive luciferin/luciferase method as described in [169].

Oxygen Consumption Rate (OCR) was measured at 25°C in a closed chamber, using an amperometric electrode (Unisense-Microrespiration, Unisense A/S, Denmark). 50 μg of total proteins were used for each experiment. To stimulate the pathways composed by Complexes I, III, and IV, 10 mM pyruvate plus 5 mM malate were added; to activate the Complexes II, III, and IV pathway, 20 mM succinate was employed[169].

The oxidative phosphorylation (OXPHOS) efficiency was calculated as the ratio between the concentration of the produced ATP and the amount of consumed oxygen in the presence of respiring substrate and ADP, obtaining the phosphate/oxygen (P/O) ratio. In coupled conditions, this value is around 2.5 or 1.5 in the presence of pyruvate + malate (P/M) or succinate (Succ), respectively. Conversely, in the uncoupled status, this value decreases proportionally to the grade of the OXPHOS inefficiency[170]. Finally, the enzymatic activities of lactate dehydrogenase (LDH) and glucose 6-phosphate dehydrogenase (G6PD) were assayed according to the protocols described in [170] and [171] respectively.

2.5.   Quantification of NAD levels in cells and tumor masses.

For intratumoral NAD measurements, tumor samples (20-30 mg) were minced and treated with 0.6 M perchloric acid for deproteinization and then they were then neutralized by adding K_2CO_3. For NAD measurements in OVCAR-5 cells, $1x10^5$ OVCAR-5 cells were plated in each well of a 12 wells/plate and let adhere overnight. The day after, cells were treated with combinations of NAPRT inhibitors and FK866 and incubated at 37 °C in a humidified atmosphere of 5% CO_2 and 95% air for 24 hours. The NAPRT inhibitors were used at 100 μM except for 2-HNA which was used at 1 mM, and FK866 at 100 nM. After 24 hours, cells were lysed with 0.6 M perchloric acid (PCA) at 4 °C and manually detached by a scrapper. The cell lysates were subsequently collected, transferred to new tubes, and diluted in 100 mM Na_2HPO_4 at pH 8. Determination of the amount of NAD inside the cells (or the tumors) was carried out using a sensitive enzymatic cyclic assay that takes advantage of the enzymatic activity of alcohol dehydrogenase as previously described in [172]. Briefly, 100 μL of the diluted samples were pipetted into a white 96-well plate followed by the addition of 100 μL of the cycling reaction mixture (100 mM Na_2HPO_4, 90 U/mL alcohol dehydrogenase, 10 μM flavinmononucleotide, 2% ethanol, 130 mU/mL diaphorase, 2.5 μg/mL resazurin, and 10 mM nicotinamide). Fluorescence increase was measured every 60 seconds over 30 minutes using a fluorescence plate reader (544 nm excitation, 590 nm emission). The NAD content was calculated from a standard curve and normalized against the total protein content that was previously quantified for every test sample using the standard Bradford colorimetric assay (Bio-Rad).

2.6.   Detection and quantification of bacterial DNA in murine stools

Murine stool samples were collected from control and antibiotics-treated mice, snap-frozen, and sent to Switzerland for detection and quantification of bacterial DNA. Mouse stools genomic DNA was extracted from a volume of stools equivalent to 30 µL with the Power Fecal PRO kit (ref. 51804) on a QIACube (Qiagen, Germany) and diluted 1000x to avoid PCR inhibition. Two negative controls using DNA-free water (Applichem, Germany) instead of DNA extraction products were analyzed in parallel to the samples. The quantitative PCR was performed with 5 µL DNA, 200 nM of each primer Eubact_27F (AGAGTTTGATCMTGGCTCAG) and Eubact_244R (ACTGCTGCCTCCCGTAG)[152], and 10 µL iTaq Universal SYBR Green Supermix (BioRad, Switzerland, ref. 172-5122) as follows: start 95°C for 5 minutes, denaturation at 95°C for 15 minutes and hybridization at 60°C for 1 minute repeated for 40 cycles. The analyses were performed on the StepOne Plus in MicroAmp Fast Optical 96-Well Reaction Plate (Thermo-Fisher, Switzerland). Ten-fold dilutions of a control plasmid prepared by RDBiotech (France) were used to calibrate the qPCR (1E5/1E4/1E3/1E2/10/5 copies/µL). Negative controls yielded 16S quantification values between 5 and 10 copies/µl.

2.7. Quantification of NAD metabolites using LC-MS/MS

NAD metabolites in the mice serum or cellular supernatants were quantified using an LC-MS/MS method established for the quantification of the NAD intermediates involved in the PH and salvage pathways as described in [152].

2.8. Statistical analysis

All statistical analyses and graphic representations were done with GraphPad Prism version 8.3.0 (GraphPad Software, San Diego, CA). In the animal experiments, adequate study power (>0.80) was verified by PS Power and Sample Size Program

(http://biostat.mc.vanderbilt.edu/wiki/Main/PowerSampleSize). In the tumor growth curves, data of the tumor volumes were presented as mean ± standard error of the mean (SEM). All other data were expressed as means ± standard deviation (SD). Comparisons between experimental groups were performed using an unpaired student's T-test or by ANOVA. P-values less than 0.05 were considered statistically significant.

3. Results

3.1. Administration of an NA-free diet

3.1.1. NA starvation sensitizes NAPRT-proficient cancer cell lines to NAMPT inhibition

NAD formation from NA via the PH pathway starts with NAPRT catalyzing the conversion of NA into NAMN which is then converted into NAAD and finally into NAD. We thus reasoned that reducing NA availability would prevent cancer cells from exploiting this pathway to replenish their NAD pools and thereby render them susceptible to NAMPT inhibitors. To test this hypothesis, the effect of NA deprivation was investigated in a panel of NAPRT-proficient cancer cell lines that represent different types of solid tumors. These cell lines were cultured in standard medium (that lacks NA) and treated with the NAMPT inhibitor FK866, the prototypical NAPRT inhibitor 2-HNA, or their combination. In NA-free conditions, FK866 treatment alone resulted in marked cell growth inhibition of OVCAR-5 (ovarian cancer), CAPAN-1 (pancreatic cancer), and NCI-N87 (gastric cancer). Conversely, all the cancer cell lines were insensitive to 2-HNA, most likely due to the ability of these cells to sustain NAD synthesis via the salvage pathway (since NAMPT is not inhibited by 2-HNA and its substrate, NAM, is present in standard culture medium). Exogenous supplementation with NA prevented FK866 cytotoxicity in the NAPRT-expressing cancer cell lines in a dose-dependent manner indicating that FK866 only exerts its antitumor effects in NAPRT-proficient cancer cells in the absence of NA, which prevents the utilization of the PH pathway (Figure 3.1 A, B, and C). We found that NA concentrations as low as 100 nM were sufficient to completely rescue all the tested cancer cells from FK866-induced cytotoxicity. These results are in agreement with the recent

findings by ElMokh and colleagues in NAPRT-expressing leukemia cells[152]. On the other hand, a 10-fold higher NA concentration ($\approx$ 1 μM) was required to protect them from FK866 in the presence of 2-HNA. These findings could be explained by the fact that 2-HNA is an analog of NA that competitively inhibits NAPRT; therefore higher substrate concentrations were needed to displace 2-HNA and regain NAPRT functionality. To further confirm that the protective effect of NA addition is mediated through activating the PH route, we tested the effect of exogenous NA supplementation in the NAPRT-deficient cancer cell lines A2780 and SKOV3 (ovarian cancer) and Mia PaCa-2 (pancreatic cancer) when exposed to FK866. As expected, FK866 dose-dependently led to cancer cell death which was not rescued by NA addition (Figure 3.1 D, E, and F). Altogether, these results indicate that NA deprivation from culture media, which potentially could be recreated in animal models by removing NA from their diets, is able to overcome the resistance to NAMPT inhibitors that is seen in NAPRT-expressing tumors.

3.1.2. Elimination of microbial-derived NA sensitizes NAPRT-proficient cancer cell lines to NAMPT inhibition

Recent studies revealed that a broad variety of bacterial species including the common cell culture contaminant mycoplasma can significantly contribute to NAD production in mammalians owing to their ability to generate NA from NAM through the catalytic activity of their nicotinamidase enzyme (PncA)[20,152,173]. By contrast, human cells lack this enzyme and thereby can't convert NAM to NA. To address the aforementioned contribution, we took advantage of mycoplasma contamination in several NAPRT-proficient cancer cell lines and monitored their cell viability in baseline conditions and in the presence of FK866.

As shown in Figure 3.1.G, mycoplasma-infected OVCAR-5, Capan-1, and OVCAR-8 cell lines were completely insensitive to FK866 even without external NA addition suggesting that mycoplasma secrete abundant amounts of NA that confer resistance to NAMPT inhibitors. To confirm this mechanism, we measured the concentrations of several NAD metabolites in supernatants of mycoplasma-free OVCAR-5 cells and mycoplasma-contaminated OVCAR-5 and CAPAN-1 cells. Mycoplasma infection resulted in a consistent elevation in NA amounts in supernatants of OVCAR-5 cells: NA concentrations in the supernatant obtained from mycoplasma-free and mycoplasma-infected OVCAR-5 cells were 35 nM and 3.57 µM, respectively. By contrast, NAM concentration was lower in the culture media collected from mycoplasma-contaminated OVCAR-5 cells compared to that of mycoplasma-negative OVCAR-5 cells, which conceivably reflected NAM consumption by mycoplasma. Similar results were also observed with mycoplasma-contaminated CAPAN-1 cells (Figure 3.1 H). In addition, higher levels of NAMN were observed in mycoplasma-contaminated cell supernatants (results not shown). Taken together, these observations confirm the notion that bacteria enable NAPRT-expressing tumor cells to bypass NAMPT inhibition by converting NAM into NA, which is the key precursor of the PH NAD biosynthesis pathway. To further verify this hypothesis, we evaluated whether pharmacological PncA inhibition in mycoplasma-contaminated, NAPRT-proficient cell lines would restore FK866 activity. To this end, we made use of the irreversible PncA inactivator, pyrazine carbonitrile (PCN; reported Ki ≈ 61 µM)[174]. PCN, which by itself showed no cytotoxic activity in the tested cancer cell lines, effectively sensitized NAPRT-expressing ovarian and pancreatic cancer cells to FK866 (Figure 3.1 I, J, and K). Consistent with the notion that the enhancement of FK866 activity through

PCN was due to PncA obstruction (and to the consequent elimination of mycoplasma derived-NA), exogenous NA addition (10 μM) fully abolished the anti-proliferative activity of combined FK866 and PCN in mycoplasma-infected NAPRT-expressing cancer cell lines (i.e, OVCAR-5, Capan-1, and OVCAR-8) (Figure 3.1 I, J, and K). To rule out the possibility that PCN might exert its effect through NAPRT inhibition (given the structural analogy between NA and PCN), we treated mycoplasma-free OVCAR-5 with FK866 with or without 1 mM PCN in the presence or absence of 100 nM NA (since this NA concentration was found to be sufficient to rescue OVCAR-5 cells from FK866 alone but not from FK866 plus 2-HNA; Figure 3.1 A). The prototypical NAPRT inhibitor 2-HNA was used as a positive control. As expected, NA (at 100 nM) was able to rescue mycoplasma-free OVCAR-5 cells from FK866 and from FK866 plus PCN, but not from combined FK866 and 2-HNA treatment. Thus, these results are consistent with PCN not acting as a direct NAPRT inhibitor (Figure 3.1 L). Of note, we failed to detect a similar sensitization effect with the nicotinamidase inhibitor nicotinaldehyde despite its K_i values which were reported to lie within the low micromolar to low nanomolar range[174,175]. This observation could be explained by a recent report that shows that nicotinaldehyde, by itself, is also a NAD precursor that was able to activate the PH pathway and abolish the cytotoxic activity of FK866 in leukemia cells[176]. Taken together, our results confirm that PCN restored FK866 cytotoxic effects against mycoplasma-infected cancer cells by blocking the conversion of NAM into NA through PncA. Notably, PcnA-catalysed NA production also takes place at the level of gut microbiota, jeopardizing the efficacy of NAMPT inhibitors against different types of cancer, as we and others recently found[152]. Therefore, to effectively diminish NA stores *in vivo*, both dietary and microbial-derived NA should be taken into consideration.
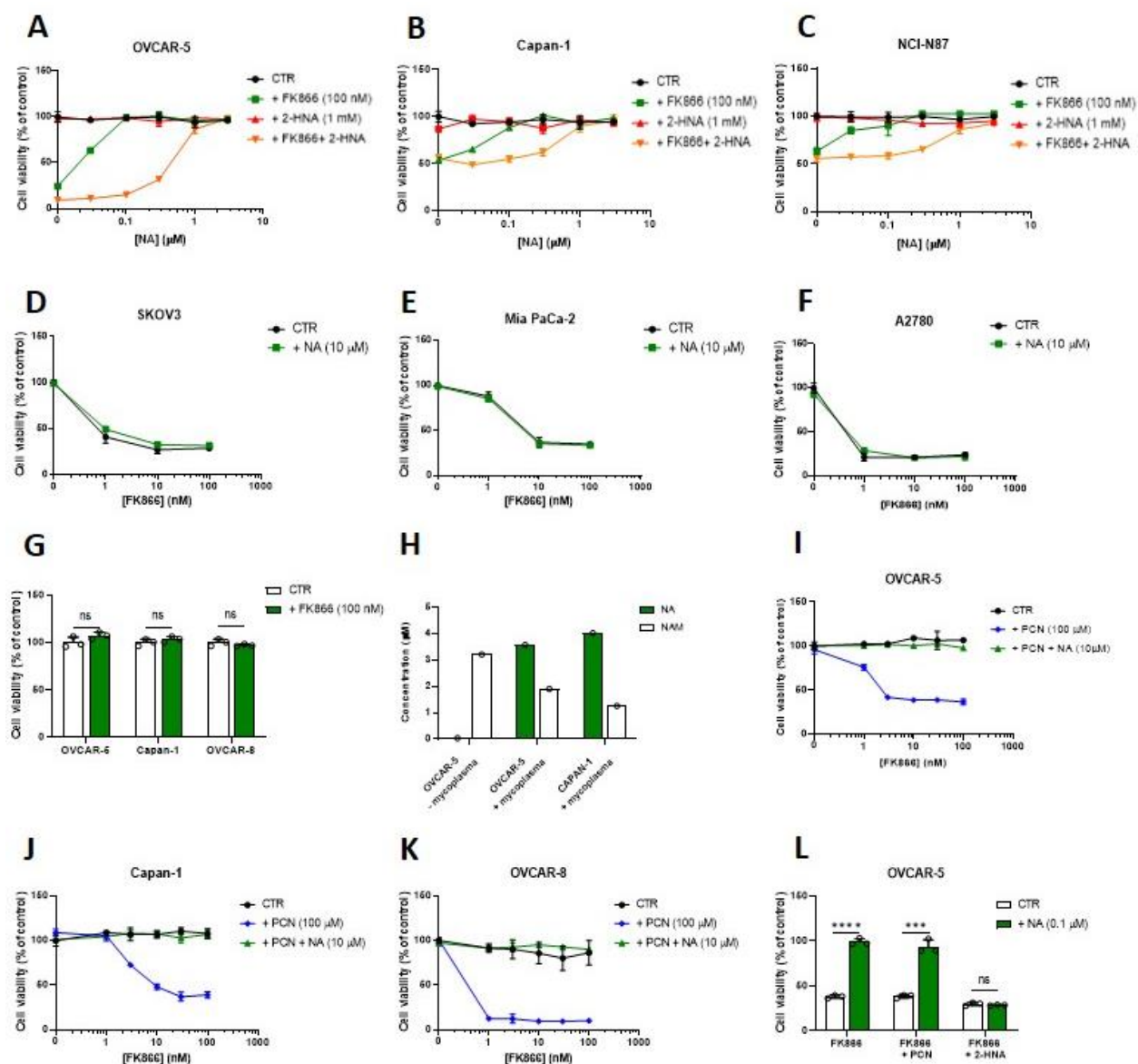
Figure 3.1. NA depletion sensitizes NAPRT-expressing cancer cell lines to FK866. Mycoplasma-free OVCAR-5 (**A**), CAPAN-1 (**B**), or NCI-N87 (**C**) cells were seeded in 96-well plates ($2x10^3$ to $3x10^3$ cells per well in case of OVCAR-5 or CAPAN-1 and 10^4 cells per well in case of NCI-N87) and left to adhere overnight. The following day, the old media were replaced with new media containing FK866 (100 nM), 2-HNA (1 mM), or both. NA was subsequently added at increasing concentrations from 30 nM to 3 µM and cells were incubated for 72 h. Cell viability was determined using the SRB assay. (**D-F**) SKOV3 (**D**), Mia-PaCa-2 (**E**), or A2780 (**F**) cells were seeded in 96-well plates ($1x10^3$ to $4x10^3$ cells

per well) and left to adhere overnight. The following day, the old media were replaced with fresh media with or without the addition of NA (10 µM). FK866 was subsequently added at increasing concentrations from 1 nM to 100 nM and cells were incubated for 72 h. Cell viability was determined using the SRB assay. Data are presented as mean ± SD. (**G**) Mycoplasma-infected OVCAR-5, CAPAN-1, or OVCAR-8 cells were seeded in 96-well plates ($2x10^3$ to $3x10^3$ cells per well) and left to adhere overnight. The following day, the old media were replaced with new media containing FK866 (100 nM) and cells were incubated for 72 h. Cell viability was determined using the SRB assay. (**H**) NA and NAM concentrations in the supernatants collected from uninfected OVCAR-5 cells or mycoplasma-infected OVCAR-5 and Capan-1 cells were quantified using LC-MS/MS.(**I-K**) Mycoplasma-infected OVCAR-5 (**I**), CAPAN-1 (**J**) or OVCAR-8 (**K**) cells were seeded in 96-well plates ($2x10^3$ to $3x10^3$ cells per well) and left to adhere overnight. The following day, the old media were replaced with fresh media containing pyrazine carbonitrile (PCN) at 100 µM in the presence or absence of NA (10 µM). FK866 was subsequently added at increasing concentrations from 1 nM to 100 nM and cells were incubated for 72 h. Cell viability was determined using the SRB assay. (**L**) Mycoplasma-free OVCAR-5 were seeded in 96-well plates ($3x10^3$ cells per well) and left to adhere overnight. The following day, cells were treated with FK866 (100 nM) alone or combined with 2-HNA or with PCN (both at 1 mM) in the presence or absence of low concentration of NA (100 nM) and cells were incubated for 72 h. Cell viability was determined using the SRB assay. Data are presented as mean ± SD. ns, non-significant; ***, $P<0.001$; ****, $P<0.0001$.

3.1.3. NA-free diet sensitizes NAPRT-proficient cancer xenografts to NAMPT inhibition

Our *in vitro* results demonstrated that NAPRT-proficient cancer cell lines were only sensitive to FK866 in the absence of NA, whereas the add-back of NA fully abrogated FK866-induced cytotoxicity. Thereafter we evaluated whether NA deficiency would also sensitize NAPRT-expressing tumors to NAMPT inhibition *in vivo*. Since NA is an essential nutrient that is supplemented in rodents' diets[177], we attempted to simulate *in vitro* NA-

free cell culture conditions by removing NA from the mouse diet. To this end, we established subcutaneous OVCAR-5 xenografts in nude mice, fed the animals with NA-free (0 mg NA/kg diet) or a matched control "CTR" (30 mg NA/kg) diet and, when tumors were palpable, subjected the animals to FK866 treatment (or vehicle DMSO) (Figure 3.2 A). Mice receiving both the NA-free diet and FK866 treatment demonstrated a significant reduction in tumor growth relative to control and to the single-treatment groups (Figure 3.2 B, C, and D). Both the NA-free diet and FK866 failed to reduce the growth of OVCAR-5 tumors when not combined with one another (Figure 3.2 B, C, and D). Overall, these results indicated that, at least in this *in vivo* model, simultaneous obstruction of the salvage and the PH NAD production routes is crucial to achieving antitumor effects. Next, to confirm that the anti-cancer activity we observed with the combined intervention (*i.e.*, FK866 and NA-free diet) was mediated by NAD depletion, we quantified NAD content inside the tumors. Tumors that were isolated from mice fed with the NA-free diet showed lower NAD levels as compared to animals receiving the control diet. Likewise, in mice fed with the control diet, FK866 treatment significantly reduced intratumor NAD levels compared to vehicle treatment. However, the most pronounced reduction in intratumor NAD we observed in tumors that were isolated from the mice receiving both the NA-free diet and FK866. (Figure 3.2 F) We also evaluated the circulating levels of NA in the serum of mice from the different groups. We found these NA concentrations to be typically low (*i.e.* NA was detected at low nanomolar concentrations), implying that dietary NA is rapidly internalized and stored in cells. However, circulating NA levels also declined with a trend similar to that observed in tumors among the experimental groups (data not shown). Collectively, these data are in line with a previous study by O'Brien *et al.* which suggested

that NAD levels need to be sufficiently depleted to significantly inhibit tumor growth *in vivo*[178].

Previous studies suggested that cellular bioenergetic processes could be impaired as a result of NAD depletion[70,151,178]. Therefore, we investigated the impact of our dietary interventions (in the presence or absence of FK866) on energy status and oxidative phosphorylation of OVCAR-5 tumors. Tumor masses isolated from FK866-treated mice or from mice fed with the NA-free diet alone exhibited considerable reductions in the oxygen consumption rate and ATP synthase activity compared to the control animals (Figure 3.3 A and B). In line with these results, we detected lower ATP and higher AMP levels in the tumors, which ultimately translated into a lower ATP/AMP ratio (Figure 3.3 C, D, and E). We observed the sharpest reductions in the oxygen consumption rate, ATP synthase activity, ATP levels, and ATP/AMP ratio in tumors treated with both the NA-free diet and FK866 (Figure 3.3 A-E), which is again consistent with the marked drop in NAD levels observed with this combined intervention. Ultimately, we investigated the effect of our combined intervention on the activity of two NAD(P)- dependent dehydrogenases, namely lactate dehydrogenase (LDH) and glucose 6-phosphate dehydrogenase (G6PDH) that use NAD and NADP as a co-factor, respectively. Again, we found the sharpest reduction in LDH and G6PD enzymatic activities to occur in tumors treated with an NA-free diet and FK866 (Figure 3.3 F and G). Reduced LDH activity is indicative of compromised aerobic glycolysis, while the drop in G6PD activity could impair nucleotide
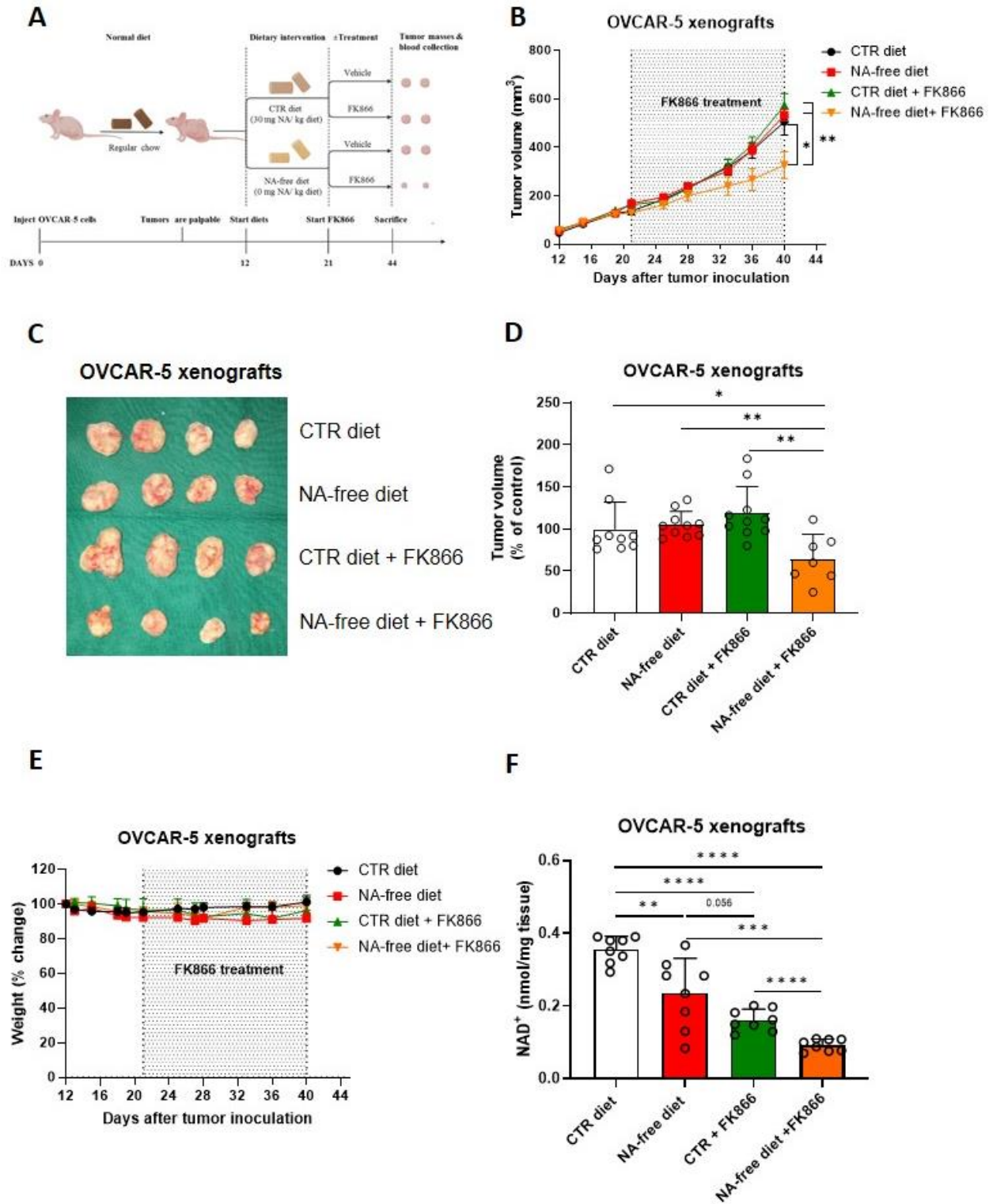
Figure 3.2. NA-free diet sensitizes NAPRT-expressing cancer xenografts to FK866.
(**A**) 8-week-old female nude mice were injected subcutaneously with 5x10^6 OVCAR-5

cells in both flanks. When tumors became palpable, mice (n=5 per group) were randomized to receive the different diets and after 9 days were randomized again to receive FK866 (20 mg/kg i.p once daily for four consecutive days per week) or vehicle treatment for 3 weeks. Tumor volumes (**B**) and mice weights (**E**) were measured every 3-4 days. On the last day, tumor volumes were recorded (**D**), mice were then sacrificed, tumors were excised, imaged (**C**), and stored at -80 ºC. Tumor masses were subsequently used for the determination of intratumor NAD levels (**F**). Data are presented as mean ± SEM in (**B**) and mean ± SD in (**D**) and (**F**) *, $P<0.05$; **, $P<0.01$; ***, $P<0.001$; ****, $P<0.0001$.

synthesis and also allow high rates of reactive oxygen species (ROS) to accumulate in cancer cells given that G6PD plays a key role in regulating the pentose phosphate pathway and in counteracting oxidative damage. Taken together, our analysis confirmed that depleting intratumor NAD levels via a combined NA-free diet and NAMPT inhibition markedly reduced NAD-dependent metabolic bioenergetic processes, which could likely contribute to reducing tumor growth.

As highlighted earlier, NAMPT inhibitors were reported to cause adverse effects such as lymphopenia and thrombocytopenia in clinical trials[77]. Gastrointestinal toxicities were also reported, particularly with the orally administered NAMPT inhibitors CHS-828 GMX1777[79]. On the other hand, severe NA deficiency may lead to the condition called pellagra (which typically includes, dermatitis, diarrhea, and mental confusion)[179]. Thus, to rule out potential side effects of the NA-free diet, FK866, and their combination, we monitored mice for clinical signs of toxicity (*e.g.* weight loss), as well as for their blood cell counts and biochemical markers of organ damage. In no treatment group did we detect clinical signs of toxicity, including weight loss (Figure 3.2 E). We also failed to detect signs of haematologic toxicity (Table 3.1), liver, kidney, or muscle damage, or detrimental

changes in lipid profile (Table 3.2). Altogether, the results of these tests show that coupling an NA-free diet to NAMPT inhibitors is an effective and safe antineoplastic approach against PH-dependant tumors.
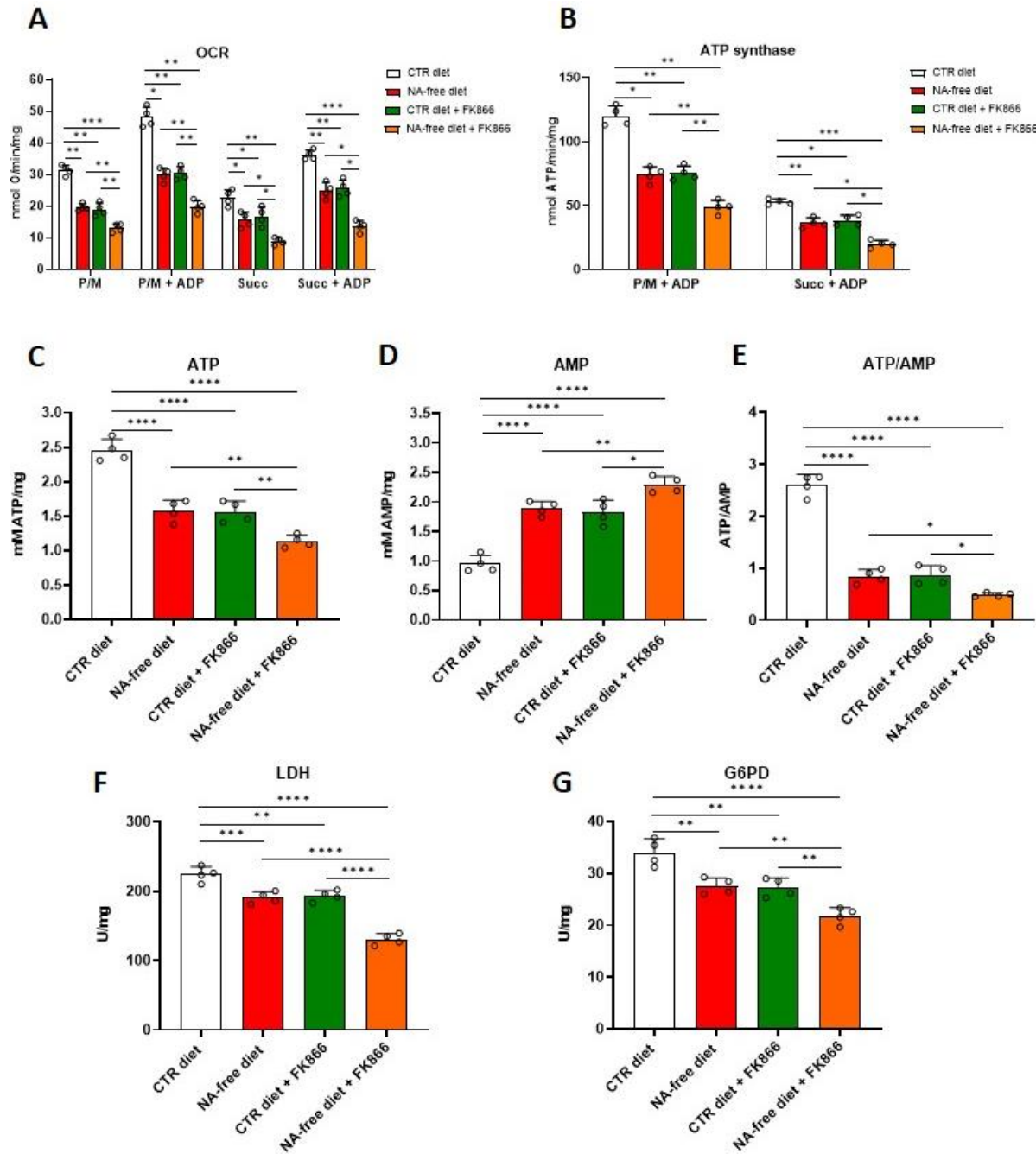
Figure 3.3. Combining an NA-free diet with FK866 severely impairs the energy status, OXPHOS, and the activity of NAD(P)-utilizing enzymes in NAPRT-expressing cancer xenografts. (**A-G**) 8-week-old nude mice were injected subcutaneously with $5x10^6$ OVCAR-5 cells in both flanks. When tumors became palpable, mice (n=5 per group) were randomized to receive the different diets and after 9 days were randomized again to receive FK866 (20 mg/kg i.p once daily for four consecutive days per week) or vehicle for 3 weeks. On the last day, mice were sacrificed, tumors were excised and subsequently used to determine the oxygen consumption rate (**A**), ATP synthase activity (**B**), ATP levels (**C**), AMP levels (**D**), ATP/AMP ratio (**E**), LDH activity (**F**), and G6PD activity (**G**).Data are represented as mean ± SD *, $P<0.05$; **, $P<0.01$; ***, $P<0.001$; ****, $P<0.0001$

Table 3.1. Hematological parameters of the study assessing the safety of NA-free diet with or without FK866 in mice (n=3-4 mice per group)

Parameters	CTR diet (Mean ± SD)	NA-free diet (Mean ± SD)	CTR diet + FK866 (Mean ± SD)	NA-free diet + FK866 (Mean ± SD)
RBC (10^6/µL)	9.64 ± 0.76	10.28 ± 0.38	9.19 ± 0.69	9.22 ± 0.78
HGB (g/dL)	14.80 ± 1.20	16.33 ± 0.47	14.15 ± 1.28	13.97 ± 1.27
HCT (%)	51.63 ± 4.84	55.87 ± 2.32	47.85 ± 4.42	47.07 ± 3.29
MCV (fL)	53.60 ± 2.96	54.37 ± 2.44	52.03 ± 2.30	51.10 ± 1.56
MCH (pg)	15.40 ± 0.26	15.90 ± 0.52	15.43 ± 0.83	15.13 ± 0.75
MCHC (g/dL)	28.70 ± 1.13	29.23 ± 0.42	29.58 ± 0.57	29.67 ± 0.81
RDW-SD (fL)	33.03 ± 1.33	34.37 ± 3.74	31.83 ± 0.74	30.53 ± 1.55
Reticulocyte# (10^3/ µL)	488.53 ± 139.37	462.07 ± 18.01	405.25 ± 99.71	388.23 ± 74.64
Reticulocyte% (%)	5.17 ± 1.92	4.50 ± 0.18	4.42 ± 1.04	4.25 ± 0.99
Platelets (10^3/µL)	1400 ± 31.58	1166 ± 158.08	1412.25 ± 192.31	1161 ± 91.11
WBC (10^3/µL)	11.86 ± 2.90	11.62 ± 1.32	9.76 ± 0.75	11.79 ± 4.68
Neutrophils# (10^3/µL)	4.48 ± 1.03	3.87 ± 1.26	3.65 ± 0.51	3.31 ± 1.06

Lymphocytes# (10^3/μL)	6.27 ± 2.04	7.03 ± 0.17	4.98 ± 1.01	7.68 ± 4.19
Monocytes# (10^3/μL)	0.93 ± 0.44	0.58 ± 0.30	1.01 ± 0.39	0.65 ± 0.13
Eosinophils# (10^3/μL)	0.17 ± 0.05	0.13 ± 0.02	0.10 ± 0.06	0.13 ± 0.02
Basophils# (10^3/μL)	0.01 ± 0.01	0.01 ± 0.00	0.01 ± 0.01	0.03 ± 0.02
Neutrophils% (%)	37.87 ± 2.40	32.80 ± 7.86	37.55 ± 5.50	29.87 ± 12.45
Lymphocytes% (%)	52.27 ± 7.07	61.10 ± 8.23	50.95 ± 8.95	62.80 ± 14.99
Monocytes% (%)	8.20 ± 4.93	4.90 ± 2.09	10.40 ± 4.07	5.87 ± 1.97
Eosinophils% (%)	1.53 ± 0.59	1.10 ± 0.20	0.98 ± 0.56	1.17 ± 0.40
Basophils% (%)	0.13 ± 0.06	0.10 ± 0.00	0.13 ± 0.05	0.30 ± 0.26

RBC, red blood cells; HGB, hemoglobin; HCT, hematocrit; MCV, mean corpuscular volume; MCH, mean corpuscular hemoglobin; MCHC, mean corpuscular hemoglobin concentration; RDW, red cell distribution width; WBC, white blood cells.

Table 3.2. Biochemical parameters of the study assessing the safety of NA-free diet with or without FK866 in mice (n=3-4 mice per group)

Parameters	CTR diet (Mean ± SD)	NA-free diet (Mean ± SD)	CTR diet + FK866 (Mean ± SD)	NA-free diet + FK866 (Mean ± SD)
Albumin (g/dL)	3.63 ± 0.21	3.70 ± 0.10	3.53 ± 0.43	3.80 ± 0.22
Urea (mg/dL)	35.33 ± 2.08	33.33 ± 5.77	27.00 ± 5.23	34.00 ± 9.90
Creatinine (mg/dL)	0.46 ± 0.04	0.45 ± 0.02	0.43 ± 0.03	0.41 ± 0.02
Triglycerides (mg/dL)	121.67 ± 45.01	132.67 ± 41.96	98.50 ± 28.49	145.50 ± 24.69
Cholesterol (mg/dL)	158.00 ± 15.62	130.67 ± 31.26	146.00 ± 21.43	140.50 ± 20.40
ALT (U/L)	32.00 ± 1.00	32.00 ± 2.65	34.00 ± 7.75	37.25 ± 9.84
HDL (mg/dL)	75.27 ± 3.27	66.42 ± 11.83	75.58 ± 8.87	71.99 ± 9.40
LDL (mg/dL)	42.67 ± 20.21	27.67 ± 15.63	36.00 ± 3.37	27.25 ± 5.74

ALT, alanine transaminase; HDL, high-density lipoprotein; LDL, low-density lipoprotein

3.1.4. Combining an NA-deficient diet and antibiotics delays the tumor progression *in vivo*

As mentioned previously, besides dietary NA, the gut flora also generates NA from NAM through the PncA enzyme. Thus, we aimed to eliminate microbiota-derived NA in the body by administering an antibiotics cocktail that depletes the gut microbiota (*i.e.* vancomycin, ampicillin, gentamycin, and metronidazole)[180]. We confirmed that this antibiotic treatment successfully depleted the gut flora by quantitative PCR analysis, showing that bacterial DNA became undetectable in the stools of antibiotics-treated mice (Figure 3.4 A). Depletion of the gut microbiome also caused mouse caeca to become enlarged, which is characteristic of mice with depleted intestinal microbiota[180] (Figure 3.4 B). The effect of combining antibiotics with an NA-free diet was then assessed in OVCAR-5 xenografts. As expected, mice receiving either the NA-free diet or antibiotics alone did not demonstrate any significant difference in tumor volumes. However, mice receiving both the NA-free diet and antibiotics exhibited a mild, but significant reduction in tumor growth as compared to the control group (mice fed with the control diet without antibiotics) (Figure 3.4 C, D, and E). Of note, since in this experiment, we did not make use of a NAMPT inhibitor, these results suggest that simultaneous depletion of NA through intestinal antibiotics and an NA-free diet is sufficient to exert some antitumor activity in this NAPRT-proficient tumor model. Next, we investigated whether this effect is mediated, at least in part, by blunting intratumor NAD pools. To answer this question, we quantified NAD content inside tumor masses and found that indeed only the combined intervention

reduced intratumor NAD in comparison to the NAD levels found in tumors from the control

group (Figure 3.4 F).
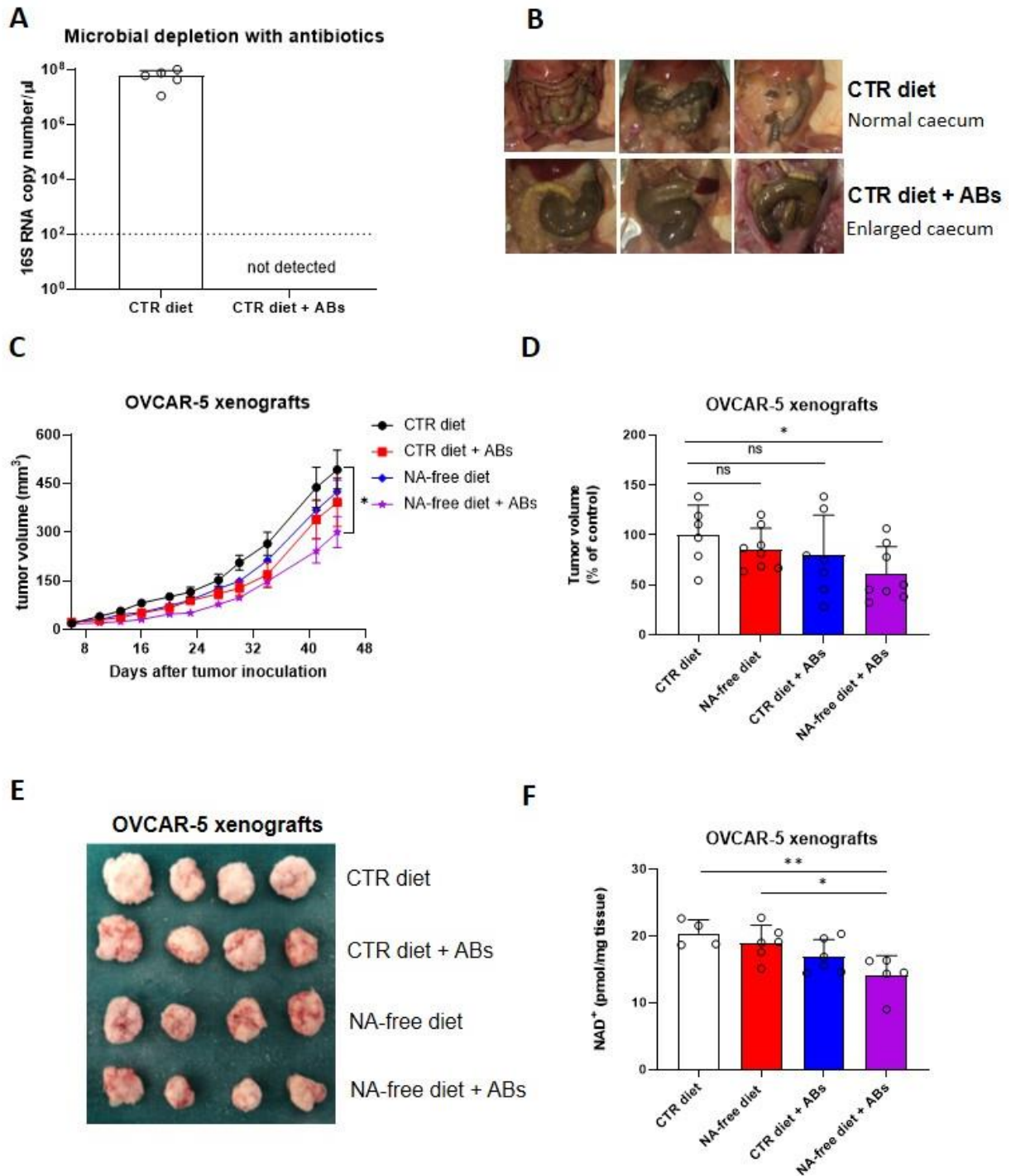
Figure 3.4. Combining an NA-free diet with antibiotics slows tumor progression *in vivo*. Results from a previous preliminary experiment showed that treating mice with an

antibiotics cocktail (vancomycin, ampicillin, metronidazole, and gentamycin) successfully depleted the gut microbial flora as seen by 16S rRNA PCR analysis on murine stool samples (**A**) and the enlarged caeca (**B**) in the antibiotics-treated animals. (**C-D**) In the proof-of-concept experiment, 8-week-old nude female mice were fed with CTR or NA-free diets with or without antibiotics cocktail (administered by oral gavage for 4 consecutive days/week) for two weeks and then injected subcutaneously with 5×10^6 OVCAR-5 cells in both flanks. When tumors became palpable, tumor growth was monitored (**C**). Diets with or without antibiotics were provided until the end of the experiment. On the last day, tumor volumes were measured (**D**). Mice were then sacrificed, tumors were excised, imaged (**E**), and stored at -80 ºC. Tumor masses were subsequently used for the determination of intratumor NAD levels (**F**). Data are presented as mean ± SEM in (**C**) and mean ± SD in (**D**) and (**F**) ns, non-significant; *, P<0.05; **, P<0.01.
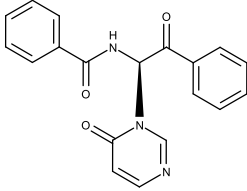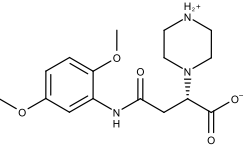
3.2. Development of NAPRT inhibitors

3.2.1. *In silico* compounds screening

In the second part of the project, we aimed to identify novel NAPRT inhibitors starting from a virtual screening of the HTS Compound Collection from Life Chemicals (http://www.lifechemicals.com/) which consists of 537,009 drug-like compounds. The crystal structure of NAPRT was used as a template for the *in silico* docking study[165]. Results were ranked based on the score and the first 500 hits were visually inspected to prioritize compounds that reproduced, at least in part, the putative binding mode of the NAPRT substrates. This evaluation led to a final list of 35 purchasable compounds to be tested *in vitro* as putative NAPRT inhibitors. In addition, from the same Life Chemicals compound collection, a set of 2-hydroxynicotinic acid (2-HNA) analogs was manually selected as 2-HNA is known to inhibit NAPRT in the micro/millimolar range of concentration. A brief description of the compounds selected for *in vitro* characterization can be found in Table 3.3.

Table 3.3. Selected structurally diverse compounds and 2-HNA analogs for *in vitro* characterization as putative NAPRT inhibitors.

Compound ID	Structure	Vendor ID	M.W.*	Compound ID	Structure	Vendor ID	M.W.
1		F0020-0171	333.3407	26		F2721-0386	337.3709
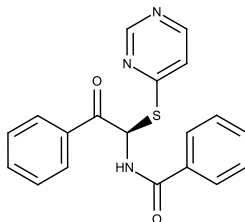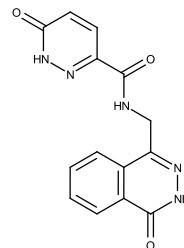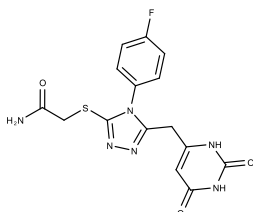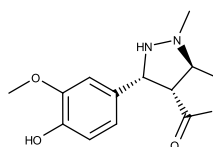
No.	Structure	ID	Value	Structure	ID	Value	No.
2		F0173-0133	349.4063		F2758-0213	297.2688	27
3		F0648-0699	376.3655		F3188-0088	277.2759	28
4		F0648-0785	391.3769		F3226-2226	397.4427	29
5		F1199-0146	358.7757		F3229-0191	283.7076	30
6		F1260-1693	421.4889		F3295-0007	355.3927	31
7		F1299-0156	462.6037		F3311-0032	471.9565	32
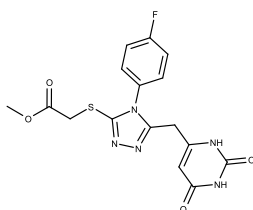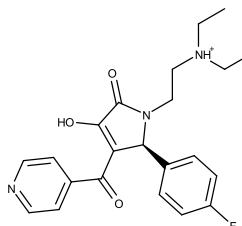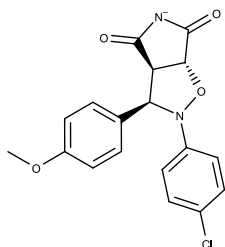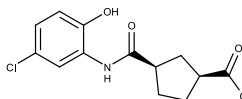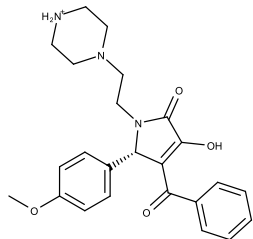
8		F1371-0219	139.1088	33	F3371-0859	414.4268
9		F1566-0988	333.3192	34	F3385-4161	440.9226
10		F1710-0049	460.429	35	F5008-0290	369.3977
11		F1811-0048	282.2957	36	F5857-5354	311.3319
12		F1907-0958	230.2194	37	F6127-0104	303.2769
13		F1967s-1157	180.1607	38	F6127-0210	333.3574
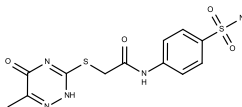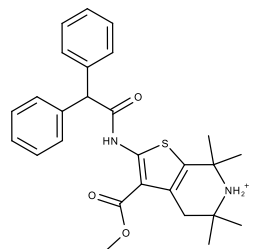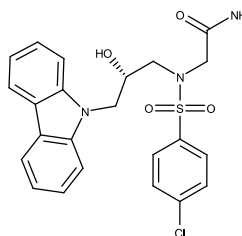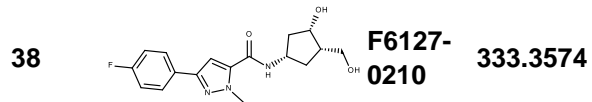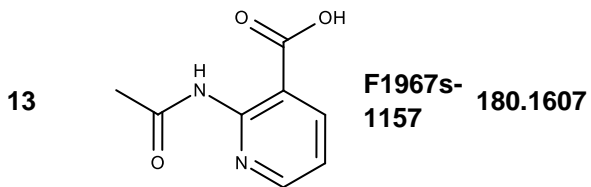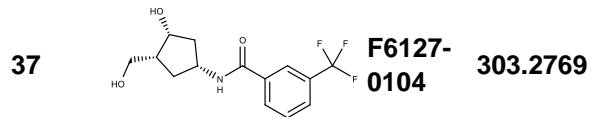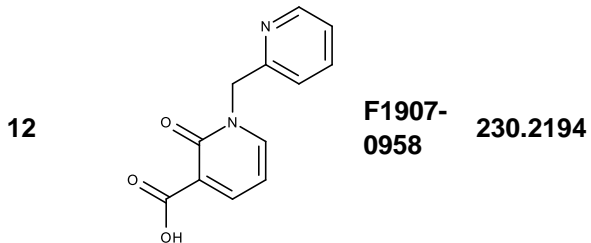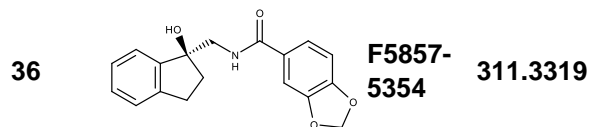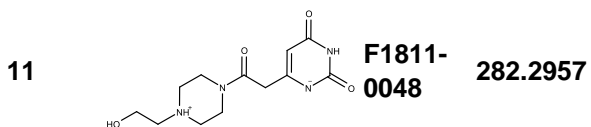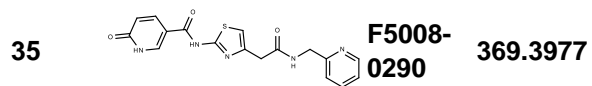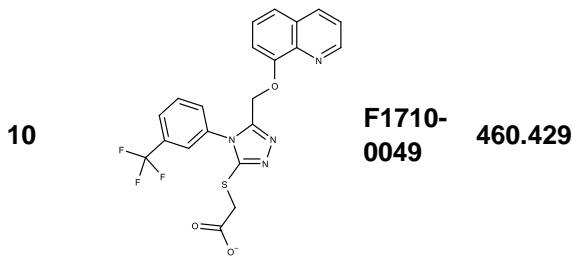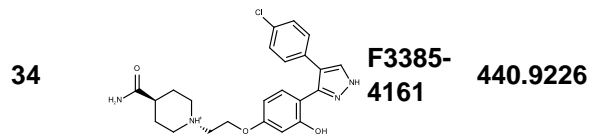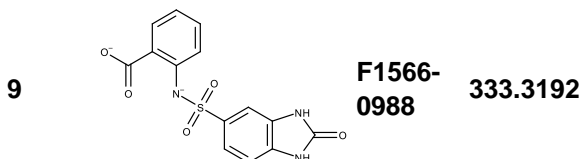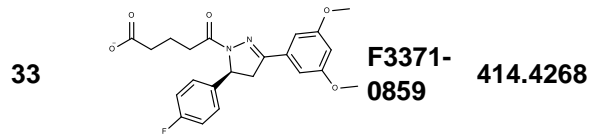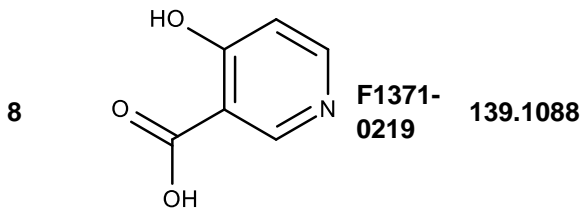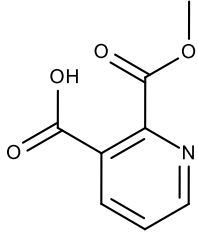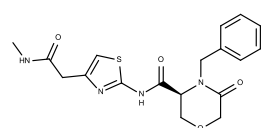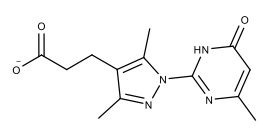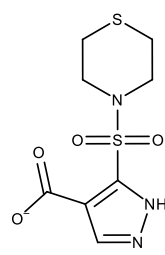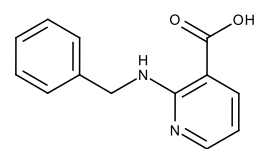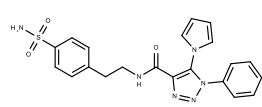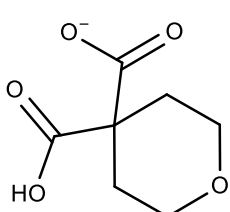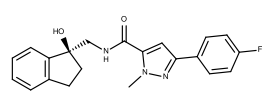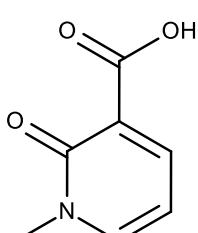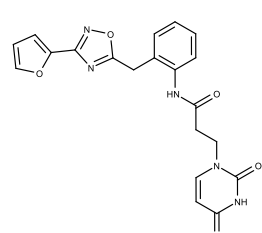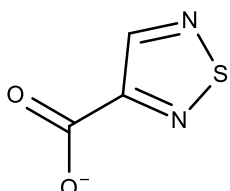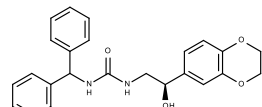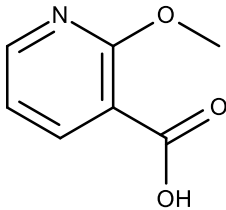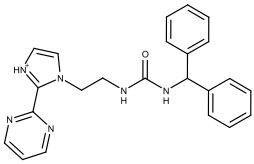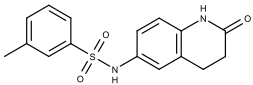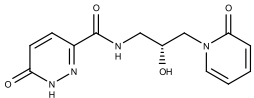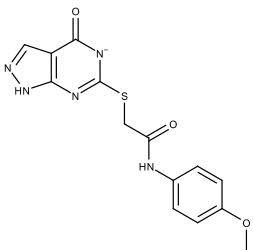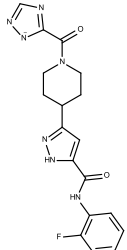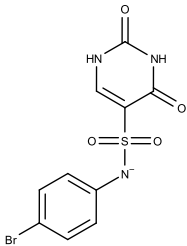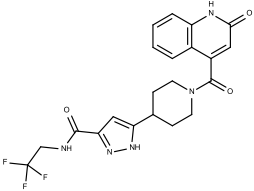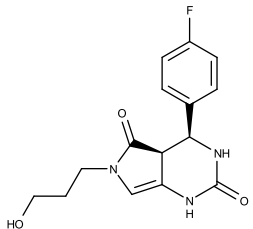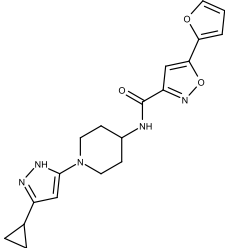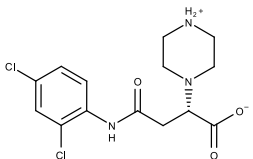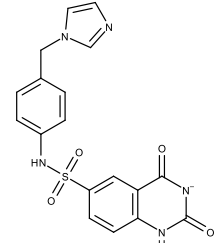
14		F2135-0162	181.1455	39		F6241-0336	388.4408
15		F2135-0875	276.2911	40		F6252-1248	277.3206
16		F2135-0897	228.2466	41		F6252-5764	436.4869
17		F2147-0724	174.1513	42		F6279-0434	365.4008
18		F2168-0001	153.1354	43		F6372-1828	407.3795
19		F2169-0490	130.1252	44		F6414-0992	404.4584

20	F2191-0003	153.1354	45	F6439-7266	398.4604
21	F2278-0232	316.3748	46	F6465-0031	290.2747
22	F2503-0045	331.3497	47	F6497-7775	383.3796
23	F2526-0046	346.1572	48	F6497-8054	447.4104
24	F2711-0182	305.3042	49	F6523-1712	367.4017
25	F2721-0331	346.2091	50	F9994-0201	397.4078

M.W., molecular weight.

3.2.2. *In vitro* compounds screening

To rapidly screen the 50 selected compounds for their ability to inhibit NAPRT, we used their capacity to sensitize the NAPRT-proficient ovarian cancer cell line, OVCAR-5, to FK866 as a reading frame (since this cell line is normally resistant to the NAMPT inhibitor, but becomes sensitized to it through either NAPRT silencing or inhibition). By itself, the addition of putative NAPRT inhibitors is postulated to show minimal anti-proliferative activity due to the ability of the cells to use the NAM that is present in the cell culture media to synthesize NAD[151]. OVCAR-5 cells were treated with the putative NAPRT inhibitors at 100 µM concentration with or without 100 nM FK866. As depicted in Figures 3.5 A and 3.5 B, five compounds out of the 50 that were tested (*i.e.*, compounds **1**, **2**, **8**, **16**, and **19**) led to significant cancer cell growth inhibition when coupled with FK866, while being minimally active when used alone. The remaining compounds were discarded since they were either completely inactive or caused remarkable anti-proliferative without FK866 (as observed in Figure 3.5 A with compound **5** and compound **7**). The complete inactivity of some compounds could be ascribed to their inability to bind NAPRT or to poor cell membrane permeability. The intrinsic anti-cancer effect of some of the compounds (*i.e.*, without FK866) was considered to be indicative of non-specific toxicity that would possibly also affect healthy cells.

Afterwards, we aimed at assessing the downstream effects of inhibiting both enzymes in cancer cells, particularly in terms of intracellular NAD concentration. In line with our previous observations with NAPRT silencing, by themselves, 2-HNA and the new 5 putative NAPRT inhibitors failed to reduce intracellular NAD levels[151]. However, 2-HNA and the new putative inhibitors did cooperate with the NAMPT inhibitor, FK866, to blunt

intracellular NAD concentrations (Figure 3.5 C). We next evaluated the ability of these compounds to sensitize OVCAR-5 cells to lower concentrations of FK866. Four out of the five compounds (*i.e.*, compounds **1**, **2**, **8,** and **19**) were indeed able to sensitize OVCAR-5 cells when incubated (at 200 µM) with increasing concentrations of FK866 (Figure 3.5 D). The degree of sensitization varied among the putative inhibitors with compound **8** exhibiting the most potent sensitization effect. Notably, the sensitizing activity of compound **8** was even more pronounced than that of the classical NAPRT inhibitor, 2-HNA (Figure 3.5 D). On the other hand, compound **16** was the only compound that completely failed to sensitize the ovarian cancer cells to FK866 and thus it was not further investigated. To further confirm the observed sensitization effect of our putative inhibitors on the antitumor activity of NAMPT inhibitors, we extended our experiments in two additional NAPRT-expressing cancer cell lines (*i.e.*, HCT116 and OVCAR-8). Consistent with our previous observations in OVCAR-5 cells, compound **8** and compound **19** also
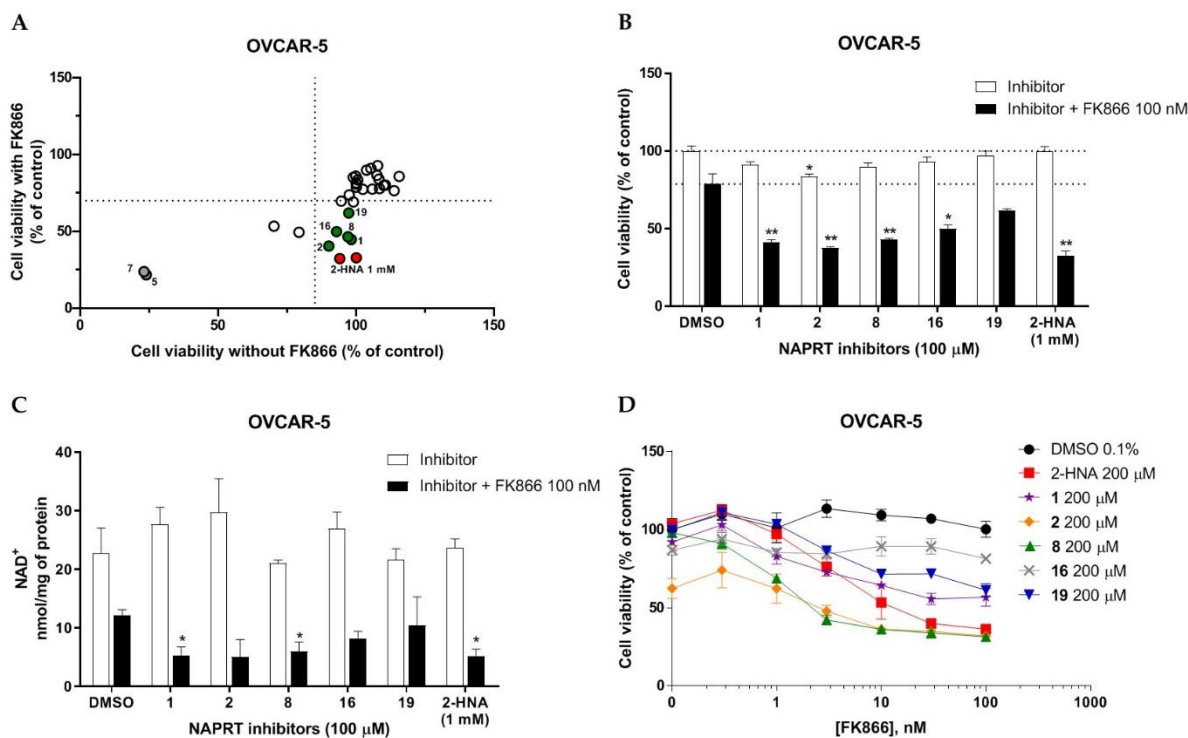
Figure 3.5. *In vitro* screening of the putative NAPRT inhibitors identifies several promising candidates. (A) Graphical representation of the cell viability results obtained from screening our selected compounds in ovarian cancer cells. OVCAR-5 cells were plated in 96-well plates ($2x10^3$ cells/well) and left to adhere overnight. The following day, the culture media were replaced with new media containing the respective treatments (*i.e.*, with or without 100 nM FK866 and the putative NAPRT inhibitors, all at 100 μM final concentration, except for 2-HNA which was used at 1 mM). Each point is the mean of three experimental replicates normalized to the control. The green circles indicate the five most promising putative inhibitors and the red circles represent 2-HNA as the control NAPRT inhibitor. **(B)** The viability results for the five most promising NAPRT inhibitors from **(A)** are also represented in a bar graph. *, $P< 0.05$; **, $P< 0.01$ **(C)** OVCAR-5 cells were plated in 12-well plates ($1x10^5$ cells/well) and allowed to adhere overnight. The following day, the culture media were replaced with new media containing the respective treatments (*i.e.*, with or without 100 nM FK866 and the putative NAPRT inhibitors, all at 100 μM final concentration, except for 2-HNA which was used at 1 mM). *, $P< 0.05$ **(D)** OVCAR-5 were plated in 96-well plates ($2x10^3$ cells/well) and allowed to adhere overnight. The following day, the culture media were replaced with new media that contain the respective treatments (*i.e.*, with or without FK866 at increasing concentrations from 1 to 100 nM and the putative NAPRT inhibitors, added at 200 μM final concentration), and the plates were then incubated for 72 hours. Afterwards, the cell viability was determined using the SRB assay.

sensitized these other two cell models to FK866 when they were used at 100 μM concentration (Figure 3.6 A, B, and C). By contrast, compound **1** and compound **2**, when used at the same concentration, failed to sensitize these two cancer cell lines to FK866, with compound **2** even showing unspecific anti-proliferative activity in these models (Figure 3.6 D and E). Since compound **8** (4-hydroxynicotinic acid) and 2-HNA are structural isomers, we decided to evaluate whether the remaining 2-HNA analogs [*i.e.*, 5-hydroxynicotinic acid (5-HNA) and 6-hydroxynicotinic acid (6-HNA)] are also capable of

inhibiting NAPRT. We tested this hypothesis in OVCAR-8 cells. Neither 5-HNA nor 6-HNA could recreate the effects of compounds **8** and 2-HNA in terms of cell sensitization to FK866 (Figure 3.6 F). We hypothesize this to reflect the inability of these compounds to bind within the NAPRT enzymatic pocket. Overall, these findings highlight the specificity of compound **8**, since shifting the position of the -OH group from position 4 to position 5 or 6 entirely abolished their ability to sensitize cancer cells to FK866 (and thus, arguably, to inhibit NAPRT). Ultimately, these experiments indicate that the NAPRT inhibitory activity of these hydroxylated analogs of nicotinic acid strictly relies on the -OH substitution at position 2 or 4 of the pyridine ring. In order to confirm that the ability of our new inhibitors to sensitize NAPRT-proficient cancer cells to FK866 is on-target, *i.e.*, due to NAPRT obstruction, we supplemented HCT116 and OVCAR-8 cells with NA or NAMN (at 10 µM) while treating them with our putative NAPRT inhibitors, in the presence or absence of FK866. Both NA and NAMN fully rescued these cells from the marked anti-proliferative effect that was achieved by combining FK866 with 2-HNA, compound **8**, or compound **19** (Figure 3.6 G and H). Taken together, these observations are in line with compound **8** and compound **19** being NAPRT inhibitors.
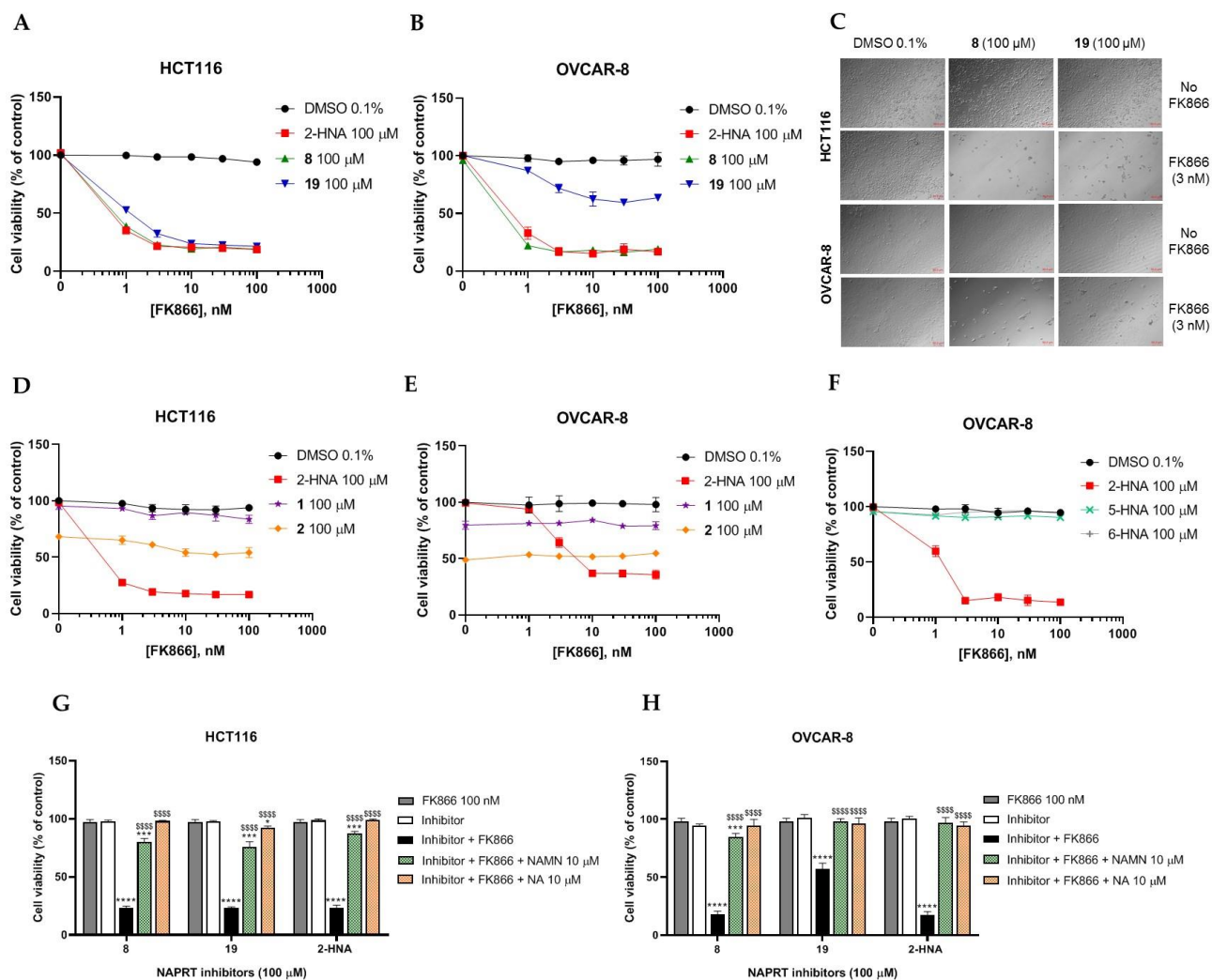
Figure 3.6. Compound 8 and compound 19 sensitize ovarian and colon cancer cells to FK866 via NAPRT inhibition. (A-F) HCT116 and OVCAR-8 were plated in 96-well plates (2×10^3 cells/well) and allowed to adhere overnight. The following day, culture media were replaced with new media containing the respective treatments (i.e., with or without FK866 at increasing concentrations from 1 to 100 nM and the putative NAPRT inhibitors, added at 100 μM final concentration), and the plates were then incubated for 72 hours. Afterwards, the cells were imaged using light microscopy as in **(C)** and cell viability was determined using the Sulforhodamine B assay. Data are mean ± SD of three experimental replicates. **(G-H),** the same experimental procedure was employed as in **(A-F)**. Single concentrations of the NAPRT inhibitors (100 μM), 100 nM FK866, 10 μM NA, and 10 μM NAMN were added. Data are mean ± SD of 4 experimental replicates. One

representative experiment is shown. *, P< 0.05; ***, P< 0.001; ****, P< 0.0001; $$$$, P< 0.0001. The * symbols refer to the statistical significance compared to the treatment with FK866 alone, whereas the $ symbols refer to the statistical significance compared to the combined treatment with FK866 and the NAPRT inhibitors.

3.2.3. *In silico* solubility prediction and pharmacokinetic characterization

In a previous study involving animal experiments, we were unable to dissolve 2-HNA in saline at the desired concentration for intraperitoneal injections and thus, we used its sodium salt as an alternative[151]. Indeed, poor water solubility is a major hurdle during the drug development process, especially when a drug is meant to be administered orally or parenterally[181]. It was estimated that approximately 40% of the new chemical entities demonstrate modest solubility in water[181]. Given the promising pharmacological results of our drug candidates compound **8** and compound **19**, we addressed their physicochemical and pharmacokinetic parameters. In order to predict their solubility, we made use of the SwissADME website, a publicly available online computational tool that characterizes physicochemical parameters, ADME properties, and drug-likeliness of a molecule[182]. Compound **8** and compound **19** possess favorable drug-like properties since they don't violate Lipinski's rule of five. Based on 2 out of the 3 predictive models employed by the software to calculate water solubility, we found a 1.64 and a 2.25-fold improvement in the predicted molar solubrity of compound **8** compared to 2-HNA (reported as Log(S) in Table 3.4). Likewise, the molar solubility of compound **19** was higher than that of 2-HNA according to all 3 estimating methods (Table 3.4). Moreover, compound **8** and compound **19** had high predicted GI absorption. Compound **8** had the same bioavailability score compared to 2-HNA and a higher bioavailability score than compound **19** (Table 3.4). Neither of the two chemical entities seemed to be able to cross

the blood-brain barrier (BBB). Finally, neither compound **8** nor compound **19** was predicted to be a substrate of the efflux transporter P-glycoprotein (Pgp), which is frequently associated with cancer resistance against chemotherapeutics[183]. Collectively, these results indicate promising pharmacokinetic features for compound **8** and compound **19**.

Table 3.4. Predicted water solubility and additional pharmacokinetic properties of the two most promising putative NAPRT inhibitors.

Compound ID	Log S (ESOL)	Log *S* (Ali)	Log *S* (SILICOS-IT)	GI absorption	Pgp Substrate	BBB permeant	Bioavailability score
2-HNA	-1.65	-1.97	-0.8	High	No	No	0.85
8	-1.44	-1.62	-0.8	High	No	No	0.85
19	-1.18	-1.77	-0.26	High	No	No	0.56

4.   Discussion

NAMPT inhibitors are NAD-lowering agents that elicited potent anti-cancer activities in different preclinical cancer models but their limited efficacy in clinical trials prompted subsequent efforts to optimize their use as cancer therapeutics. Resistance to NAMPT inhibitors arises in a wide spectrum of solid tumors that retain an intact NAD-generating PH route which enables them to circumvent NAMPT-inhibitor-mediated NAD depletion. On this basis, simultaneous obstruction of the salvage and the PH pathways could result in more pronounced NAD reduction and, as a consequence, more robust anti-cancer activity. Herein, we describe a novel dietary approach that interrupts the PH pathway which, in turn, offers the possibility to broaden the efficacy of the prototypical NAMPT inhibitor FK866 *in vivo*. In addition, we report on the identification of two chemical NAPRT inhibitors that sensitized NAPRT-expressing cancer cell lines to FK866.

We demonstrate that restricting the nutritional intake of NA via an NA-free diet restores susceptibility to FK866 in a mouse model of ovarian cancer harboring an active NAD-generating PH route. The interaction between the NA-free diet and FK866 translated into a dramatic intratumor NAD depletion that was not attained by FK866 treatment alone and, subsequently, into reduced tumor volumes. A recent study showed that the therapeutic index of the novel NAMPT inhibitor OT-82 was compromised in animals that were fed diets containing NA amounts exceeding the recommended daily intake[121]. However, to our best knowledge, this is the first study that reports on a synergetic combination between NAMPT inhibitors and a specific dietary intervention, *i.e.*, an NA-free diet, against NAPRT-expressing solid tumors. This dietary modification proved safe since the NA-free diet failed to cause haematologic or organ toxicities. Importantly, no symptoms of pellagra were noted with dietary nicotinic acid deprivation likely due to the presence of

tryptophan in the diet, which is a pellagra-preventing factor[179]. Although NAD could be generated *de novo* starting from tryptophan (which could potentially compromise intratumor NAD depletion with our intervention), we previously found that the addition of tryptophan was not able to rescue NAPRT-silenced OVCAR-5 cells from NAMPT inhibition (results not shown), most likely due the lack of expression of one or more of the *de novo* pathway enzymes. In line with these results, Liu *et al.* elegantly demonstrated that NAD generation from tryptophan principally occurs in the liver[14].

Using the same *in vivo* model, we showed that combining an NA-free diet with an oral antibiotic regimen that depletes gut microbiota (and thereby eliminates microbial endogenous NA generation) also slows down tumor progression. Notably, this effect was observed in the absence of NAMPT inhibitors treatment, suggesting that blocking the PH route *per se* could provide some anti-cancer effects, particularly in tumors with high NAPRT expression. In keeping with this observation, we previously demonstrated that NAPRT-silenced OVCAR-5 cells and spheroids were smaller than those of the control cells, presumably as a consequence of impaired energy status and protein synthesis[151]. Again consistent with our these results, in the OV4 tumor model (another ovarian adenocarcinoma cell line that shows amplification of PH pathway enzymes) inducible *NAPRT* or *NADSYN* depletion reduced NAD levels inside the tumors and resulted in their complete regression[51]. Furthermore, we provide evidence that the nicotinamidase inhibitor pyrazine carbonitrile (PCN) is effective in sensitizing mycoplasma-contaminated, NAPRT-proficient cancer cells towards FK866, suggesting that this agent could be used instead of an antibiotics cocktail therapy (that completely deplete gut flora) in combination with an NA-free diet and/or with a NAMPT inhibitor.

Given the serious toxicities that accompanied treatment with NAMPT inhibitors in clinical trials, the role of NA in improving the NAMPT inhibitors therapy has been subsequently introduced by its administration rather than its deprivation: concomitant administration of NA and a NAMPT inhibitor was proven to mitigate the side effects of NAMPT inhibitors while allowing higher doses of NAMPT inhibitors to be administered in several *in vivo* cancer models[85,184,185]. However, this intervention mainly applies to NAPRT-deficient tumors. Our study enhances the usefulness to modulate NA dietary intake, specifically to deplete NA intake, in combination with NAMPT inhibitors: we show for the first time that NA-depletion effectively sensitizes NAPRT-proficient tumors to FK866 and to an antibiotics combination that depletes intestinal bacteria, and that these effects are not associated with significant toxicities. Last but not least, our *in vivo* results provide further support to the notion of applying diet modifications as a complementary strategy to enhance the responsiveness of therapeutic agents in cancer[186].

On the other side, we took advantage of *in silico* drug design techniques to identify two small molecules that selectively inhibit NAPRT. Our best candidates, compound **8** and compound **19**, were able to restore the sensitivity of NAPRT-expressing cancer cells to NAMPT inhibitors through NAPRT inhibition. Our cell growth inhibition assays demonstrated that our best NAPRT inhibitor, compound **8** (4-hydroxynicotinic acid), but not 5-hydroxy or 6-hydroxynicotinic acid, exhibited marked anti-cancer activity when combined with FK866 while showing no significant growth inhibition when used alone. These results are in line with our previous work, showing that NAPRT inhibition by 2-HNA does strongly sensitize NAPRT-expressing cancer cells (such as OVCAR-5 and OVCAR-8) to NAMPT inhibitors but by themselves have minor anti-proliferative activity[151]. Similar

to 2-HNA, compounds **8** and **19** displayed anti-cancer activity in the micromolar range. The specificity of the two inhibitors was emphasized by experiments demonstrating that their chemo-sensitizing activity was abolished upon supplementing cancer cells with sufficient amounts of the substrate (NA) or the downstream product (NAMN) of the NAPRT enzyme. However, similar to the analyses conducted in the case of NAMPT inhibitors[187,188], additional crystallographic studies of the NAPRT enzyme in complex with one or more of our identified inhibitors are warranted to precisely disclose the binding mode of these compounds and describe their interactions within the enzymatic pocket. Interestingly, computational analysis supported desirable drug-like and pharmacokinetic features of these agents.

Although a substantial improvement in the potency of NAPRT inhibitors has not been achieved yet, the structural backbones of these two inhibitors lend themselves to future optimization efforts. The hit rate observed with our virtual screening procedure is essentially consistent with the hit rate obtained in our previous *in silico* screenings, including work that led us to discover the first selective SIRT6 inhibitors[189]. In keeping with this approach, Franco and colleagues adopted a similar high-throughput virtual screening strategy to discover novel NAPRT inhibitors[190]. Collectively, these studies further underscore the advantage of *in silico* screening techniques for drug discovery when compared to the traditional high throughput screening procedures that are time and resource-intensive and typically achieve lower hit rates[191].

Very recently, we demonstrated that gut microbiota caused leukemia-bearing mice which were fed with a NAM-enriched diet to become resistant to FK866 treatment (through gut-microbiota-derived NA and the consequent activation of the PH pathway) and that this

resistance was reversed when their gut microbiota was depleted by an antibiotics cocktail[20,152]. Accordingly, coupling FK866 to our NAPRT inhibitors would presumably reverse the protective effect of the intestinal bacteria and restore the antitumor effect of NAMPT inhibitors *in vivo*. Since the *in vitro* anti-cancer activity observed upon combining NAMPT and NAPRT inhibitors was abrogated when NA was exogenously added in excess to the culture media, it could be argued that the *in vivo* activity of this combination therapy might be compromised when NA levels rise considerably in the body, as could happen in response to NA- or NAM-rich diets or to NA supplements (*e.g.*, NA is used in gram doses in cases of dyslipidemia due to its lipid-modifying effects). Indeed, the anti-leukemic effect of FK866 was abrogated when animals received an NA-enriched diet, even if their gut microbiota was depleted by antibiotics[152]. Future studies should address whether the compounds we identified as NAPRT inhibitors actually show antitumor activity *in vivo* and whether conditions characterized by high circulating NA levels actually hamper their efficacy. By contrast, combining an NA-free diet with NAMPT inhibitors and NAPRT inhibitors might further increase the susceptibility of NAPRT-expressing tumors to NAMPT inhibition. Further improvements in the affinity of these NAPRT inhibitors will increase their therapeutic potential and also reduce the risk of reduced activity in the presence of high systemic NA availability.

In conclusion, our work paves the way for clinical studies of NA-deficient diets in combination with NAMPT inhibitors and/or with antibiotics (or alternatively the nicotinamidase inhibitor PCN) against NAPRT-expressing malignancies. Lastly, it lays the foundation for further studies of these new NAPRT inhibitors, including *in vivo* testing in mouse tumor models and further drug optimization steps.

5. Acknowledgments

6. References

(1) Harden, A.; Young, W. J. The Alcoholic Ferment of Yeast-Juice. *Proc. R. Soc. Lond. Ser. B* **1906**, *77*, 405–420.

(2) Katsyuba, E.; Romani, M.; Hofer, D.; Auwerx, J. NAD+ Homeostasis in Health and Disease. *Nat. Metab.* **2020**, *2* (1), 9–31. https://doi.org/10.1038/s42255-019-0161-5.

(3) Yang, Y.; Sauve, A. A. NAD+ Metabolism: Bioenergetics, Signaling and Manipulation for Therapy. *Biochim. Biophys. Acta BBA - Proteins Proteomics* **2016**, *1864* (12), 1787–1800. https://doi.org/10.1016/j.bbapap.2016.06.014.

(4) Navas, L. E.; Carnero, A. NAD+ Metabolism, Stemness, the Immune Response, and Cancer. *Signal Transduct. Target. Ther.* **2021**, *6* (1), 2. https://doi.org/10.1038/s41392-020-00354-w.

(5) Xie, N.; Zhang, L.; Gao, W.; Huang, C.; Huber, P. E.; Zhou, X.; Li, C.; Shen, G.; Zou, B. NAD+ Metabolism: Pathophysiologic Mechanisms and Therapeutic Potential. *Signal Transduct. Target. Ther.* **2020**, *5* (1), 1–37. https://doi.org/10.1038/s41392-020-00311-7.

(6) Houtkooper, R. H.; Cantó, C.; Wanders, R. J.; Auwerx, J. The Secret Life of NAD+: An Old Metabolite Controlling New Metabolic Signaling Pathways. *Endocr. Rev.* **2010**, *31* (2), 194–223. https://doi.org/10.1210/er.2009-0026.

(7) Covarrubias, A. J.; Perrone, R.; Grozio, A.; Verdin, E. NAD+ Metabolism and Its Roles in Cellular Processes during Ageing. *Nat. Rev. Mol. Cell Biol.* **2021**, *22* (2), 119–141. https://doi.org/10.1038/s41580-020-00313-x.

(8) Preiss, J.; Handler, P. Biosynthesis of Diphosphopyridine Nucleotide. I. Identification of Intermediates. *J. Biol. Chem.* **1958**, *233* (2), 488–492.

(9) Preiss, J.; Handler, P. Biosynthesis of Diphosphopyridine Nucleotide. II. Enzymatic Aspects. *J. Biol. Chem.* **1958**, *233* (2), 493–500.

(10) Magni, G.; Amici, A.; Emanuelli, M.; Orsomando, G.; Raffaelli, N.; Ruggieri, S. Structure and Function of Nicotinamide Mononucleotide Adenylyltransferase. *Curr. Med. Chem.* **2004**, *11* (7), 873–885. https://doi.org/10.2174/0929867043455666.

(11) Lau, C.; Niere, M.; Ziegler, M. The NMN/NaMN Adenylyltransferase (NMNAT) Protein Family. *Front. Biosci. Landmark Ed.* **2009**, *14* (2), 410–431. https://doi.org/10.2741/3252.

(12) Berger, F.; Lau, C.; Dahlmann, M.; Ziegler, M. Subcellular Compartmentation and Differential Catalytic Properties of the Three Human Nicotinamide Mononucleotide Adenylyltransferase Isoforms. *J. Biol. Chem.* **2005**, *280* (43), 36334–36341. https://doi.org/10.1074/jbc.M508660200.

(13) Bogan, K. L.; Brenner, C. Nicotinic Acid, Nicotinamide, and Nicotinamide Riboside: A Molecular Evaluation of NAD+ Precursor Vitamins in Human Nutrition. *Annu. Rev. Nutr.* **2008**, *28*, 115–130. https://doi.org/10.1146/annurev.nutr.28.061807.155443.

(14) Liu, L.; Su, X.; Quinn, W. J.; Hui, S.; Krukenberg, K.; Frederick, D. W.; Redpath, P.; Zhan, L.; Chellappa, K.; White, E.; Migaud, M.; Mitchison, T. J.; Baur, J. A.; Rabinowitz, J. D. Quantitative Analysis of NAD Synthesis-Breakdown Fluxes. *Cell Metab.* **2018**, *27* (5), 1067-1080.e5. https://doi.org/10.1016/j.cmet.2018.03.018.

(15) Bieganowski, P.; Brenner, C. Discoveries of Nicotinamide Riboside as a Nutrient and Conserved NRK Genes Establish a Preiss-Handler Independent Route to NAD+ in Fungi and Humans. *Cell* **2004**, *117* (4), 495–502. https://doi.org/10.1016/s0092-8674(04)00416-7.

(16) Tempel, W.; Rabeh, W. M.; Bogan, K. L.; Belenky, P.; Wojcik, M.; Seidle, H. F.; Nedyalkova, L.; Yang, T.; Sauve, A. A.; Park, H.-W.; Brenner, C. Nicotinamide Riboside Kinase Structures Reveal New Pathways to NAD+. *PLoS Biol.* **2007**, *5* (10), e263. https://doi.org/10.1371/journal.pbio.0050263.

(17) Zapata-Pérez, R.; Tammaro, A.; Schomakers, B. V.; Scantlebery, A. M. L.; Denis, S.; Elfrink, H. L.; Giroud-Gerbetant, J.; Cantó, C.; López-Leonardo, C.; McIntyre, R. L.; van Weeghel, M.; Sánchez-Ferrer, Á.; Houtkooper, R. H. Reduced Nicotinamide Mononucleotide Is a New and Potent NAD+ Precursor in Mammalian Cells and Mice. *FASEB J. Off. Publ. Fed. Am. Soc. Exp. Biol.* **2021**, *35* (4), e21456. https://doi.org/10.1096/fj.202001826R.

(18) Yang, Y.; Mohammed, F. S.; Zhang, N.; Sauve, A. A. Dihydronicotinamide Riboside Is a Potent NAD+ Concentration Enhancer in Vitro and in Vivo. *J. Biol. Chem.* **2019**, *294* (23), 9295–9307. https://doi.org/10.1074/jbc.RA118.005772.

(19) Yang, Y.; Zhang, N.; Zhang, G.; Sauve, A. A. NRH Salvage and Conversion to NAD+ Requires NRH Kinase Activity by Adenosine Kinase. *Nat. Metab.* **2020**, *2* (4), 364–379. https://doi.org/10.1038/s42255-020-0194-9.

(20) Shats, I.; Williams, J. G.; Liu, J.; Makarov, M. V.; Wu, X.; Lih, F. B.; Deterding, L. J.; Lim, C.; Xu, X.; Randall, T. A.; Lee, E.; Li, W.; Fan, W.; Li, J.-L.; Sokolsky, M.; Kabanov, A. V.; Li, L.; Migaud, M. E.; Locasale, J. W.; Li, X. Bacteria Boost Mammalian Host NAD Metabolism by Engaging the Deamidated Biosynthesis Pathway. *Cell Metab.* **2020**, *31* (3), 564-579.e7. https://doi.org/10.1016/j.cmet.2020.02.001.

(21) Chellappa, K.; McReynolds, M. R.; Lu, W.; Zeng, X.; Makarov, M.; Hayat, F.; Mukherjee, S.; Bhat, Y. R.; Lingala, S. R.; Shima, R. T.; Descamps, H. C.; Cox, T.; Ji, L.; Jankowski, C.; Chu, Q.; Davidson, S. M.; Thaiss, C. A.; Migaud, M. E.; Rabinowitz, J. D.; Baur, J. A. NAD Precursors Cycle between Host Tissues and the Gut Microbiome. *Cell Metab.* **2022**, *34* (12), 1947-1959.e5. https://doi.org/10.1016/j.cmet.2022.11.004.

(22) Pissios, P. Nicotinamide N-Methyltransferase: More than a Vitamin B3 Clearance Enzyme. *Trends Endocrinol. Metab. TEM* **2017**, *28* (5), 340–353. https://doi.org/10.1016/j.tem.2017.02.004.

(23) Trammell, S. A.; Yu, L.; Redpath, P.; Migaud, M. E.; Brenner, C. Nicotinamide Riboside Is a Major NAD+ Precursor Vitamin in Cow Milk. *J. Nutr.* **2016**, *146* (5), 957–963. https://doi.org/10.3945/jn.116.230078.

(24) Long, D. J.; Jaiswal, A. K. NRH:Quinone Oxidoreductase2 (NQO2). *Chem. Biol. Interact.* **2000**, *129* (1–2), 99–112. https://doi.org/10.1016/s0009-2797(00)00200-3.

(25) Hanahan, D.; Weinberg, R. A. Hallmarks of Cancer: The next Generation. *Cell* **2011**, *144* (5), 646–674. https://doi.org/10.1016/j.cell.2011.02.013.

(26) Pavlova, N. N.; Thompson, C. B. The Emerging Hallmarks of Cancer Metabolism. *Cell Metab.* **2016**, *23* (1), 27–47. https://doi.org/10.1016/j.cmet.2015.12.006.

(27) Chiarugi, A.; Dölle, C.; Felici, R.; Ziegler, M. The NAD Metabolome — a Key Determinant of Cancer Cell Biology. *Nat. Rev. Cancer* **2012**, *12* (11), 741–752. https://doi.org/10.1038/nrc3340.

(28) Warburg, O. On Respiratory Impairment in Cancer Cells. *Science* **1956**, *124* (3215), 269–270.

(29) Yelamos, J.; Farres, J.; Llacuna, L.; Ampurdanes, C.; Martin-Caballero, J. PARP-1 and PARP-2: New Players in Tumour Development. *Am. J. Cancer Res.* **2011**, *1* (3), 328–346.

(30) Navas, L. E.; Carnero, A. Nicotinamide Adenine Dinucleotide (NAD) Metabolism as a Relevant Target in Cancer. *Cells* **2022**, *11* (17), 2627. https://doi.org/10.3390/cells11172627.

(31) Pramono, A. A.; Rather, G. M.; Herman, H.; Lestari, K.; Bertino, J. R. NAD- and NADPH-Contributing Enzymes as Therapeutic Targets in Cancer: An Overview. *Biomolecules* **2020**, *10* (3), 358. https://doi.org/10.3390/biom10030358.

(32) Lucena-Cacace, A.; Otero-Albiol, D.; Jiménez-García, M. P.; Peinado-Serrano, J.; Carnero, A. NAMPT Overexpression Induces Cancer Stemness and Defines a Novel Tumor Signature for Glioma Prognosis. *Oncotarget* **2017**, *8* (59), 99514–99530. https://doi.org/10.18632/oncotarget.20577.

(33) Vora, M.; Ansari, J.; Shanti, R. M.; Veillon, D.; Cotelingam, J.; Coppola, D.; Shackelford, R. E. Increased Nicotinamide Phosphoribosyltransferase in Rhabdomyosarcomas and Leiomyosarcomas Compared to Skeletal and Smooth Muscle Tissue. *Anticancer Res.* **2016**, *36* (2), 503–507.

(34) Olesen, U. H.; Hastrup, N.; Sehested, M. Expression Patterns of Nicotinamide Phosphoribosyltransferase and Nicotinic Acid Phosphoribosyltransferase in Human Malignant Lymphomas. *APMIS Acta Pathol. Microbiol. Immunol. Scand.* **2011**, *119* (4–5), 296–303. https://doi.org/10.1111/j.1600-0463.2011.02733.x.

(35) Maldi, E.; Travelli, C.; Caldarelli, A.; Agazzone, N.; Cintura, S.; Galli, U.; Scatolini, M.; Ostano, P.; Miglino, B.; Chiorino, G.; Boldorini, R.; Genazzani, A. A. Nicotinamide Phosphoribosyltransferase (NAMPT) Is over-Expressed in Melanoma Lesions. *Pigment Cell Melanoma Res.* **2013**, *26* (1), 144–146. https://doi.org/10.1111/pcmr.12037.

(36) Sawicka-Gutaj, N.; Waligórska-Stachura, J.; Andrusiewicz, M.; Biczysko, M.; Sowiński, J.; Skrobisz, J.; Ruchała, M. Nicotinamide Phosphorybosiltransferase Overexpression in Thyroid Malignancies and Its Correlation with Tumor Stage and with Survivin/Survivin DEx3 Expression. *Tumour Biol. J. Int. Soc. Oncodevelopmental Biol. Med.* **2015**, *36* (10), 7859–7863. https://doi.org/10.1007/s13277-015-3506-z.

(37) Shackelford, R. E.; Bui, M. M.; Coppola, D.; Hakam, A. Over-Expression of Nicotinamide Phosphoribosyltransferase in Ovarian Cancers. *Int. J. Clin. Exp. Pathol.* **2010**, *3* (5), 522–527.

(38) Zhu, Y.; Guo, M.; Zhang, L.; Xu, T.; Wang, L.; Xu, G. Biomarker Triplet NAMPT/VEGF/HER2 as a de Novo Detection Panel for the Diagnosis and Prognosis of Human Breast Cancer. *Oncol. Rep.* **2016**, *35* (1), 454–462. https://doi.org/10.3892/or.2015.4391.

(39) Zhou, S.-J.; Bi, T.-Q.; Qin, C.-X.; Yang, X.-Q.; Pang, K. Expression of NAMPT Is Associated with Breast Invasive Ductal Carcinoma Development and Prognosis. *Oncol. Lett.* **2018**, *15* (5), 6648–6654. https://doi.org/10.3892/ol.2018.8164.

(40) Ju, H.-Q.; Zhuang, Z.-N.; Li, H.; Tian, T.; Lu, Y.-X.; Fan, X.-Q.; Zhou, H.-J.; Mo, H.-Y.; Sheng, H.; Chiao, P. J.; Xu, R.-H. Regulation of the Nampt-Mediated NAD Salvage Pathway and Its Therapeutic Implications in Pancreatic Cancer. *Cancer Lett.* **2016**, *379* (1), 1–11. https://doi.org/10.1016/j.canlet.2016.05.024.

(41) Li, X.; Lei, J.; Mao, L.; Wang, Q.; Xu, F.; Ran, T.; Zhou, Z.; He, S. NAMPT and NAPRT, Key Enzymes in NAD Salvage Synthesis Pathway, Are of Negative Prognostic Value in Colorectal Cancer. *Front. Oncol.* **2019**, *9*, 736. https://doi.org/10.3389/fonc.2019.00736.

(42) Ye, C.; Qi, L.; Li, X.; Wang, J.; Yu, J.; Zhou, B.; Guo, C.; Chen, J.; Zheng, S. Targeting the NAD+ Salvage Pathway Suppresses APC Mutation-Driven Colorectal Cancer Growth and Wnt/β-Catenin Signaling via Increasing Axin Level. *Cell Commun. Signal. CCS* **2020**, *18* (1), 16. https://doi.org/10.1186/s12964-020-0513-5.

(43) Van Beijnum, J. R.; Moerkerk, P. T. M.; Gerbers, A. J.; De Bruïne, A. P.; Arends, J.-W.; Hoogenboom, H. R.; Hufton, S. E. Target Validation for Genomics Using Peptide-Specific Phage Antibodies: A Study of Five Gene Products Overexpressed in Colorectal Cancer. *Int. J. Cancer* **2002**, *101* (2), 118–127. https://doi.org/10.1002/ijc.10584.

(44) Bi, T.-Q.; Che, X.-M.; Liao, X.-H.; Zhang, D.-J.; Long, H.-L.; Li, H.-J.; Zhao, W. Overexpression of Nampt in Gastric Cancer and Chemopotentiating Effects of the Nampt Inhibitor FK866 in Combination with Fluorouracil. *Oncol. Rep.* **2011**, *26* (5), 1251–1257. https://doi.org/10.3892/or.2011.1378.

(45) Wang, B.; Hasan, M. K.; Alvarado, E.; Yuan, H.; Wu, H.; Chen, W. Y. NAMPT Overexpression in Prostate Cancer and Its Contribution to Tumor Cell Survival and Stress Response. *Oncogene* **2011**, *30* (8), 907–921. https://doi.org/10.1038/onc.2010.468.

(46) Audrito, V.; Messana, V. G.; Moiso, E.; Vitale, N.; Arruga, F.; Brandimarte, L.; Gaudino, F.; Pellegrino, E.; Vaisitti, T.; Riganti, C.; Piva, R.; Deaglio, S. NAMPT Over-Expression Recapitulates the BRAF Inhibitor Resistant Phenotype Plasticity in Melanoma. *Cancers* **2020**, *12* (12). https://doi.org/10.3390/cancers12123855.

(47) Lucena-Cacace, A.; Otero-Albiol, D.; Jiménez-García, M. P.; Muñoz-Galvan, S.; Carnero, A. NAMPT Is a Potent Oncogene in Colon Cancer Progression That Modulates Cancer Stem Cell Properties and Resistance to Therapy through Sirt1 and PARP. *Clin. Cancer Res.* **2018**, *24* (5), 1202–1215. https://doi.org/10.1158/1078-0432.CCR-17-2575.

(48) Grolla, A. A.; Travelli, C.; Genazzani, A. A.; Sethi, J. K. Extracellular Nicotinamide Phosphoribosyltransferase, a New Cancer Metabokine. *Br. J. Pharmacol.* **2016**, *173* (14), 2182–2194. https://doi.org/10.1111/bph.13505.

(49) Gholinejad, Z.; kheiripour, N.; Nourbakhsh, M.; Ilbeigi, D.; Behroozfar, K.; Hesari, Z.; Golestani, A.; Shabani, M.; Einollahi, N. Extracellular NAMPT/Visfatin Induces Proliferation through ERK1/2 and AKT and Inhibits Apoptosis in Breast Cancer Cells. *Peptides* **2017**, *92*, 9–15. https://doi.org/10.1016/j.peptides.2017.04.007.

(50) Soncini, D.; Caffa, I.; Zoppoli, G.; Cea, M.; Cagnetta, A.; Passalacqua, M.; Mastracci, L.; Boero, S.; Montecucco, F.; Sociali, G.; Lasigliè, D.; Damonte, P.; Grozio, A.; Mannino, E.; Poggi, A.; D'Agostino, V. G.; Monacelli, F.; Provenzani, A.; Odetti, P.; Ballestrero, A.; Bruzzone, S.; Nencioni, A. Nicotinamide Phosphoribosyltransferase Promotes Epithelial-to-Mesenchymal Transition as a Soluble Factor Independent of Its Enzymatic Activity. *J. Biol. Chem.* **2014**, *289* (49), 34189–34204. https://doi.org/10.1074/jbc.M114.594721.

(51) Chowdhry, S.; Zanca, C.; Rajkumar, U.; Koga, T.; Diao, Y.; Raviram, R.; Liu, F.; Turner, K.; Yang, H.; Brunk, E.; Bi, J.; Furnari, F.; Bafna, V.; Ren, B.; Mischel, P. S. NAD Metabolic Dependency in Cancer Is Shaped by Gene Amplification and Enhancer Remodelling. *Nature* **2019**, *569* (7757), 570–575. https://doi.org/10.1038/s41586-019-1150-2.

(52) Menssen, A.; Hydbring, P.; Kapelle, K.; Vervoorts, J.; Diebold, J.; Luscher, B.; Larsson, L.-G.; Hermeking, H. The C-MYC Oncoprotein, the NAMPT Enzyme, the SIRT1-Inhibitor DBC1, and the SIRT1 Deacetylase Form a Positive Feedback Loop. *Proc. Natl. Acad. Sci.* **2012**, *109* (4), E187–E196. https://doi.org/10.1073/pnas.1105304109.

(53) Brandl, L.; Kirstein, N.; Neumann, J.; Sendelhofert, A.; Vieth, M.; Kirchner, T.; Menssen, A. The C-MYC/NAMPT/SIRT1 Feedback Loop Is Activated in Early Classical and Serrated Route Colorectal Cancer and Represents a Therapeutic Target. *Med. Oncol.* **2018**, *36* (1), 5. https://doi.org/10.1007/s12032-018-1225-1.

(54) Brandl, L.; Zhang, Y.; Kirstein, N.; Sendelhofert, A.; Boos, S. L.; Jung, P.; Greten, F.; Rad, R.; Menssen, A. Targeting C-MYC through Interference with NAMPT and SIRT1 and Their Association to Oncogenic Drivers in Murine Serrated Intestinal Tumorigenesis. *Neoplasia N. Y. N* **2019**, *21* (10), 974–988. https://doi.org/10.1016/j.neo.2019.07.009.

(55) Nacarelli, T.; Lau, L.; Fukumoto, T.; Zundell, J.; Fatkhutdinov, N.; Wu, S.; Aird, K. M.; Iwasaki, O.; Kossenkov, A. V.; Schultz, D.; Noma, K.; Baur, J. A.; Schug, Z.; Tang, H.-Y.; Speicher, D. W.; David, G.; Zhang, R. NAD + Metabolism Governs the Proinflammatory Senescence-Associated Secretome. *Nat. Cell Biol.* **2019**, *21* (3), 397–407. https://doi.org/10.1038/s41556-019-0287-4.

(56) Sumter, T. F.; Xian, L.; Huso, T.; Koo, M.; Chang, Y.-T.; Almasri, T. N.; Chia, L.; Inglis, C.; Reid, D.; Resar, L. M. S. The High Mobility Group A1 (HMGA1) Transcriptome in Cancer and Development. *Curr. Mol. Med.* **2016**, *16* (4), 353–393. https://doi.org/10.2174/1566524016666160316152147.

(57) Jeong, B.; Park, J. W.; Kim, J. G.; Lee, B. J. FOXO1 Functions in the Regulation of Nicotinamide Phosphoribosyltransferase (Nampt) Expression. *Biochem. Biophys. Res. Commun.* **2019**, *511* (2), 398–403. https://doi.org/10.1016/j.bbrc.2019.02.069.

(58) Zhang, H.; Zhang, N.; Liu, Y.; Su, P.; Liang, Y.; Li, Y.; Wang, X.; Chen, T.; Song, X.; Sang, Y.; Duan, Y.; Zhang, J.; Wang, L.; Chen, B.; Zhao, W.; Guo, H.; Liu, Z.; Hu, G.; Yang, Q. Epigenetic Regulation of NAMPT by NAMPT-AS Drives Metastatic Progression in Triple-Negative Breast Cancer. *Cancer Res.* **2019**, *79* (13), 3347–3359. https://doi.org/10.1158/0008-5472.CAN-18-3418.

(59) Wang, J.; Zhang, M.; Lu, W. Long Noncoding RNA GACAT3 Promotes Glioma Progression by Sponging MiR-135a. *J. Cell. Physiol.* **2019**, *234* (7), 10877–10887. https://doi.org/10.1002/jcp.27946.

(60) Bolandghamat Pour, Z.; Nourbakhsh, M.; Mousavizadeh, K.; Madjd, Z.; Ghorbanhosseini, S. S.; Abdolvahabi, Z.; Hesari, Z.; Mobaser, S. E. Up-Regulation of MiR-381 Inhibits NAD+ Salvage Pathway and Promotes Apoptosis in Breast Cancer Cells. *EXCLI J.* **2019**, *18*, 683–696. https://doi.org/10.17179/excli2019-1431.

(61) Hesari, Z.; Nourbakhsh, M.; Hosseinkhani, S.; Abdolvahabi, Z.; Alipour, M.; Tavakoli-Yaraki, M.; Ghorbanhosseini, S. S.; Yousefi, Z.; Jafarzadeh, M.; Yarahmadi, S. Down-Regulation of NAMPT Expression by Mir-206 Reduces Cell Survival of Breast Cancer Cells. *Gene* **2018**, *673*, 149–158. https://doi.org/10.1016/j.gene.2018.06.021.

(62) Ghorbanhosseini, S. S.; Nourbakhsh, M.; Zangooei, M.; Abdolvahabi, Z.; Bolandghamtpour, Z.; Hesari, Z.; Yousefi, Z.; Panahi, G.; Meshkani, R. MicroRNA-494 Induces Breast Cancer Cell Apoptosis and Reduces Cell Viability by Inhibition of Nicotinamide Phosphoribosyltransferase Expression and Activity. *EXCLI J.* **2019**, *18*, 838–851. https://doi.org/10.17179/excli2018-1748.

(63) Bolandghamat Pour, Z.; Nourbakhsh, M.; Mousavizadeh, K.; Madjd, Z.; Ghorbanhosseini, S. S.; Abdolvahabi, Z.; Hesari, Z.; Ezzati Mobasser, S. Suppression of Nicotinamide Phosphoribosyltransferase Expression by MiR-154 Reduces the Viability of Breast Cancer Cells and Increases Their Susceptibility to Doxorubicin. *BMC Cancer* **2019**, *19* (1), 1027. https://doi.org/10.1186/s12885-019-6221-0.

(64) Lv, R.; Yu, J.; Sun, Q. Anti-Angiogenic Role of MicroRNA-23b in Melanoma by Disturbing NF-KB Signaling Pathway via Targeted Inhibition of NAMPT. *Future Oncol. Lond. Engl.* **2020**, *16* (10), 541–458. https://doi.org/10.2217/fon-2019-0699.

(65) Ju, H.-Q.; Zhuang, Z.-N.; Li, H.; Tian, T.; Lu, Y.-X.; Fan, X.-Q.; Zhou, H.-J.; Mo, H.-Y.; Sheng, H.; Chiao, P. J.; Xu, R.-H. Regulation of the Nampt-Mediated NAD Salvage Pathway and Its Therapeutic Implications in Pancreatic Cancer. *Cancer Lett.* **2016**, *379* (1), 1–11. https://doi.org/10.1016/j.canlet.2016.05.024.

(66) Zhang, C.; Tong, J.; Huang, G. Nicotinamide Phosphoribosyl Transferase (Nampt) Is a Target of MicroRNA-26b in Colorectal Cancer Cells. *PLOS ONE* **2013**, *8* (7), e69963. https://doi.org/10.1371/journal.pone.0069963.

(67) Sociali, G.; Grozio, A.; Caffa, I.; Schuster, S.; Becherini, P.; Damonte, P.; Sturla, L.; Fresia, C.; Passalacqua, M.; Mazzola, F.; Raffaelli, N.; Garten, A.; Kiess, W.; Cea, M.; Nencioni, A.; Bruzzone, S. SIRT6 Deacetylase Activity Regulates NAMPT Activity and NAD(P)(H) Pools in Cancer Cells. *FASEB J. Off. Publ. Fed. Am. Soc. Exp. Biol.* **2019**, *33* (3), 3704–3717. https://doi.org/10.1096/fj.201800321R.

(68) Yoon, M. J.; Yoshida, M.; Johnson, S.; Takikawa, A.; Usui, I.; Tobe, K.; Nakagawa, T.; Yoshino, J.; Imai, S. SIRT1-Mediated ENAMPT Secretion from Adipose Tissue Regulates Hypothalamic NAD+ and Function in Mice. *Cell Metab.* **2015**, *21* (5), 706–717. https://doi.org/10.1016/j.cmet.2015.04.002.

(69) Jung, J.; Kim, L. J.; Wang, X.; Wu, Q.; Sanvoranart, T.; Hubert, C. G.; Prager, B. C.; Wallace, L. C.; Jin, X.; Mack, S. C.; Rich, J. N. Nicotinamide Metabolism Regulates Glioblastoma Stem Cell Maintenance. *JCI Insight* **2017**, *2* (10). https://doi.org/10.1172/jci.insight.90019.

(70) Hasmann, M.; Schemainda, I. FK866, a Highly Specific Noncompetitive Inhibitor of Nicotinamide Phosphoribosyltransferase, Represents a Novel Mechanism for Induction of Tumor Cell Apoptosis. *Cancer Res.* **2003**, *63* (21), 7436–7442.

(71) Wosikowski, K.; Mattern, K.; Schemainda, I.; Hasmann, M.; Rattel, B.; Löser, R. WK175, a Novel Antitumor Agent, Decreases the Intracellular Nicotinamide Adenine Dinucleotide Concentration and Induces the Apoptotic Cascade in Human Leukemia Cells. *Cancer Res.* **2002**, *62* (4), 1057–1062.

(72) Binderup, E.; Björkling, F.; Hjarnaa, P. V.; Latini, S.; Baltzer, B.; Carlsen, M.; Binderup, L. EB1627: A Soluble Prodrug of the Potent Anticancer Cyanoguanidine CHS828. *Bioorg. Med. Chem. Lett.* **2005**, *15* (10), 2491–2494. https://doi.org/10.1016/j.bmcl.2005.03.064.

(73) Olesen, U. H.; Christensen, M. K.; Björkling, F.; Jäättelä, M.; Jensen, P. B.; Sehested, M.; Nielsen, S. J. Anticancer Agent CHS-828 Inhibits Cellular Synthesis of NAD. *Biochem. Biophys. Res. Commun.* **2008**, *367* (4), 799–804. https://doi.org/10.1016/j.bbrc.2008.01.019.

(74) Hjarnaa, P. J.; Jonsson, E.; Latini, S.; Dhar, S.; Larsson, R.; Bramm, E.; Skov, T.; Binderup, L. CHS 828, a Novel Pyridyl Cyanoguanidine with Potent Antitumor Activity in Vitro and in Vivo. *Cancer Res.* **1999**, *59* (22), 5751–5757.

(75) Holen, K.; Saltz, L. B.; Hollywood, E.; Burk, K.; Hanauske, A.-R. The Pharmacokinetics, Toxicities, and Biologic Effects of FK866, a Nicotinamide Adenine Dinucleotide Biosynthesis Inhibitor. *Invest. New Drugs* **2008**, *26* (1), 45–51. https://doi.org/10.1007/s10637-007-9083-2.

(76) Goldinger, S. M.; Gobbi Bischof, S.; Fink-Puches, R.; Klemke, C.-D.; Dréno, B.; Bagot, M.; Dummer, R. Efficacy and Safety of APO866 in Patients With Refractory or Relapsed Cutaneous T-Cell Lymphoma: A Phase 2 Clinical Trial. *JAMA Dermatol.* **2016**, *152* (7), 837–839. https://doi.org/10.1001/jamadermatol.2016.0401.

(77) von Heideman, A.; Berglund, Å.; Larsson, R.; Nygren, P. Safety and Efficacy of NAD Depleting Cancer Drugs: Results of a Phase I Clinical Trial of CHS 828 and Overview of Published Data. *Cancer Chemother. Pharmacol.* **2010**, *65* (6), 1165–1172. https://doi.org/10.1007/s00280-009-1125-3.

(78) Ravaud, A.; Cerny, T.; Terret, C.; Wanders, J.; Bui, B. N.; Hess, D.; Droz, J.-P.; Fumoleau, P.; Twelves, C. Phase I Study and Pharmacokinetic of CHS-828, a Guanidino-Containing Compound, Administered Orally as a Single Dose Every 3weeks in Solid Tumours: An ECSG/EORTC Study. *Eur. J. Cancer* **2005**, *41* (5), 702–707. https://doi.org/10.1016/j.ejca.2004.12.023.

(79) Pishvaian, M. J.; Marshall, J. L.; Hwang, J. H.; Malik, S. M.; He, A. R.; Deeken, J. F.; Kelso, C. B.; Dorsch-Vogel, K.; Berger, M. S. A Phase 1 Trial of GMX1777: An Inhibitor of Nicotinamide Phosphoribosyl Transferase (NAMPRT). *J. Clin. Oncol.* **2008**, *26* (15_suppl), 14568–14568. https://doi.org/10.1200/jco.2008.26.15_suppl.14568.

(80) Zheng, X.; Bauer, P.; Baumeister, T.; Buckmelter, A. J.; Caligiuri, M.; Clodfelter, K. H.; Han, B.; Ho, Y.-C.; Kley, N.; Lin, J.; Reynolds, D. J.; Sharma, G.; Smith, C. C.; Wang, Z.; Dragovich, P. S.; Gunzner-Toste, J.; Liederer, B. M.; Ly, J.; O'Brien, T.; Oh, A.; Wang, L.; Wang, W.; Xiao, Y.; Zak, M.; Zhao, G.; Yuen, P.; Bair, K. W. Structure-Based Discovery of Novel Amide-Containing Nicotinamide Phosphoribosyltransferase (Nampt) Inhibitors. *J. Med. Chem.* **2013**, *56* (16), 6413–6433. https://doi.org/10.1021/jm4008664.

(81) Zheng, X.; Bair, K. W.; Bauer, P.; Baumeister, T.; Bowman, K. K.; Buckmelter, A. J.; Caligiuri, M.; Clodfelter, K. H.; Feng, Y.; Han, B.; Ho, Y.-C.; Kley, N.; Li, H.; Liang, X.; Liederer, B. M.; Lin, J.; Ly, J.; O'Brien, T.; Oeh, J.; Oh, A.; Reynolds, D. J.; Sampath, D.; Sharma, G.; Skelton, N.; Smith, C. C.; Tremayne, J.; Wang, L.; Wang, W.; Wang, Z.; Wu, H.; Wu, J.; Xiao, Y.; Yang, G.; Yuen, P.; Zak, M.; Dragovich, P. S. Identification of Amides Derived from 1H-Pyrazolo[3,4-b]Pyridine-5-Carboxylic Acid as Potent Inhibitors of Human Nicotinamide Phosphoribosyltransferase (NAMPT). *Bioorg. Med. Chem. Lett.* **2013**, *23* (20), 5488–5497. https://doi.org/10.1016/j.bmcl.2013.08.074.

(82) Travelli, C.; Aprile, S.; Rahimian, R.; Grolla, A. A.; Rogati, F.; Bertolotti, M.; Malagnino, F.; di Paola, R.; Impellizzeri, D.; Fusco, R.; Mercalli, V.; Massarotti, A.; Stortini, G.; Terrazzino, S.; Del Grosso, E.; Fakhfouri, G.; Troiani, M. P.; Alisi, M. A.; Grosa, G.; Sorba, G.; Canonico, P. L.; Orsomando, G.; Cuzzocrea, S.; Genazzani, A. A.; Galli, U.; Tron, G. C. Identification of Novel Triazole-Based Nicotinamide Phosphoribosyltransferase (NAMPT) Inhibitors Endowed with Antiproliferative and Antiinflammatory Activity. *J. Med. Chem.* **2017**, *60* (5), 1768–1792. https://doi.org/10.1021/acs.jmedchem.6b01392.

(83) Wilsbacher, J. L.; Cheng, M.; Cheng, D.; Trammell, S. A. J.; Shi, Y.; Guo, J.; Koeniger, S. L.; Kovar, P. J.; He, Y.; Selvaraju, S.; Heyman, H. R.; Sorensen, B. K.; Clark, R. F.; Hansen, T. M.; Longenecker, K. L.; Raich, D.; Korepanova, A. V.; Cepa, S.; Towne, D. L.; Abraham, V. C.; Tang, H.; Richardson, P. L.; McLoughlin, S. M.; Badagnani, I.; Curtin, M. L.; Michaelides, M. R.; Maag, D.; Buchanan, F. G.; Chiang, G. G.; Gao, W.; Rosenberg, S. H.; Brenner, C.; Tse, C. Discovery and Characterization of Novel Nonsubstrate and Substrate NAMPT Inhibitors. *Mol. Cancer Ther.* **2017**, *16* (7), 1236–1245. https://doi.org/10.1158/1535-7163.MCT-16-0819.

(84) Matheny, C. J.; Wei, M. C.; Bassik, M. C.; Donnelly, A. J.; Kampmann, M.; Iwasaki, M.; Piloto, O.; Solow-Cordero, D. E.; Bouley, D. M.; Rau, R.; Brown, P.; McManus, M. T.; Weissman, J. S.; Cleary, M. L. Next-Generation NAMPT Inhibitors Identified by Sequential High-Throughput Phenotypic Chemical and Functional Genomic Screens. *Chem. Biol.* **2013**, *20* (11), 1352–1363. https://doi.org/10.1016/j.chembiol.2013.09.014.

(85) Zhao, G.; Green, C. F.; Hui, Y.-H.; Prieto, L.; Shepard, R.; Dong, S.; Wang, T.; Tan, B.; Gong, X.; Kays, L.; Johnson, R. L.; Wu, W.; Bhattachar, S.; Del Prado, M.; Gillig, J. R.; Fernandez, M.-C.; Roth, K. D.; Buchanan, S.; Kuo, M.-S.; Geeganage, S.; Burkholder, T. P. Discovery of a Highly Selective NAMPT Inhibitor That Demonstrates Robust Efficacy and Improved Retinal Toxicity with Nicotinic Acid Coadministration. *Mol. Cancer Ther.* **2017**, *16* (12), 2677–2688. https://doi.org/10.1158/1535-7163.MCT-16-0674.

(86) Korotchkina, L.; Kazyulkin, D.; Komarov, P. G.; Polinsky, A.; Andrianova, E. L.; Joshi, S.; Gupta, M.; Vujcic, S.; Kononov, E.; Toshkov, I.; Tian, Y.; Krasnov, P.; Chernov, M. V.; Veith, J.; Antoch, M. P.; Middlemiss, S.; Somers, K.; Lock, R. B.; Norris, M. D.; Henderson, M. J.; Haber, M.; Chernova, O. B.; Gudkov, A. V. OT-82, a Novel Anticancer Drug Candidate That Targets the Strong Dependence of Hematological Malignancies on NAD Biosynthesis. *Leukemia* **2020**, *34* (7), 1828–1839. https://doi.org/10.1038/s41375-019-0692-5.

(87) Neumann, C. S.; Olivas, K. C.; Anderson, M. E.; Cochran, J. H.; Jin, S.; Li, F.; Loftus, L. V.; Meyer, D. W.; Neale, J.; Nix, J. C.; Pittman, P. G.; Simmons, J. K.; Ulrich, M. L.; Waight, A. B.; Wong, A.; Zaval, M. C.; Zeng, W.; Lyon, R. P.; Senter, P. D. Targeted Delivery of Cytotoxic NAMPT Inhibitors Using Antibody–Drug Conjugates. *Mol. Cancer Ther.* **2018**, *17* (12), 2633–2642. https://doi.org/10.1158/1535-7163.MCT-18-0643.

(88) Karpov, A. S.; Abrams, T.; Clark, S.; Raikar, A.; D'Alessio, J. A.; Dillon, M. P.; Gesner, T. G.; Jones, D.; Lacaud, M.; Mallet, W.; Martyniuk, P.; Meredith, E.; Mohseni, M.; Nieto-Oberhuber, C. M.; Palacios, D.; Perruccio, F.; Piizzi, G.; Zurini, M.; Bialucha, C. U. Nicotinamide Phosphoribosyltransferase Inhibitor as a Novel Payload for Antibody–Drug Conjugates. *ACS Med. Chem. Lett.* **2018**, *9* (8), 838–842. https://doi.org/10.1021/acsmedchemlett.8b00254.

(89) Böhnke, N.; Berger, M.; Griebenow, N.; Rottmann, A.; Erkelenz, M.; Hammer, S.; Berndt, S.; Günther, J.; Wengner, A. M.; Stelte-Ludwig, B.; Mahlert, C.; Greven, S.; Dietz, L.; Jörißen, H.; Barak, N.; Bömer, U.; Hillig, R. C.; Eberspaecher, U.; Weiske, J.; Giese, A.; Mumberg, D.; Nising, C. F.; Weinmann, H.; Sommer, A. A Novel NAMPT Inhibitor-Based Antibody–Drug Conjugate Payload Class for Cancer Therapy. *Bioconjug. Chem.* **2022**, *33* (6), 1210–1221. https://doi.org/10.1021/acs.bioconjchem.2c00178.

(90) Fratta, S.; Biniecka, P.; Moreno-Vargas, A. J.; Carmona, A. T.; Nahimana, A.; Duchosal, M. A.; Piacente, F.; Bruzzone, S.; Caffa, I.; Nencioni, A.; Robina, I. Synthesis and Structure-Activity Relationship of New Nicotinamide Phosphoribosyltransferase Inhibitors with Antitumor Activity on Solid and Haematological Cancer. *Eur. J. Med. Chem.* **2023**, *250*, 115170. https://doi.org/10.1016/j.ejmech.2023.115170.

(91) Bai, J.-F.; Majjigapu, S. R.; Sordat, B.; Poty, S.; Vogel, P.; Elías-Rodríguez, P.; Moreno-Vargas, A. J.; Carmona, A. T.; Caffa, I.; Ghanem, M.; Khalifa, A.; Monacelli, F.; Cea, M.; Robina, I.; Gajate, C.; Mollinedo, F.; Bellotti, A.; Nahimana, A.; Duchosal, M.; Nencioni, A. Identification of New FK866

Analogues with Potent Anticancer Activity against Pancreatic Cancer. *Eur. J. Med. Chem.* **2022**, *239*, 114504. https://doi.org/10.1016/j.ejmech.2022.114504.

(92) Abu Aboud, O.; Chen, C.-H.; Senapedis, W.; Baloglu, E.; Argueta, C.; Weiss, R. H. Dual and Specific Inhibition of NAMPT and PAK4 By KPT-9274 Decreases Kidney Cancer Growth. *Mol. Cancer Ther.* **2016**, *15* (9), 2119–2129. https://doi.org/10.1158/1535-7163.MCT-16-0197.

(93) Adams, D. J.; Ito, D.; Rees, M. G.; Seashore-Ludlow, B.; Puyang, X.; Ramos, A. H.; Cheah, J. H.; Clemons, P. A.; Warmuth, M.; Zhu, P.; Shamji, A. F.; Schreiber, S. L. NAMPT Is the Cellular Target of STF-31-like Small-Molecule Probes. *ACS Chem. Biol.* **2014**, *9* (10), 2247–2254. https://doi.org/10.1021/cb500347p.

(94) Zhang, W.; Zhang, K.; Yao, Y.; Liu, Y.; Ni, Y.; Liao, C.; Tu, Z.; Qiu, Y.; Wang, D.; Chen, D.; Qiang, L.; Li, Z.; Jiang, S. Dual Nicotinamide Phosphoribosyltransferase and Epidermal Growth Factor Receptor Inhibitors for the Treatment of Cancer. *Eur. J. Med. Chem.* **2021**, *211*, 113022. https://doi.org/10.1016/j.ejmech.2020.113022.

(95) Dong, G.; Chen, W.; Wang, X.; Yang, X.; Xu, T.; Wang, P.; Zhang, W.; Rao, Y.; Miao, C.; Sheng, C. Small Molecule Inhibitors Simultaneously Targeting Cancer Metabolism and Epigenetics: Discovery of Novel Nicotinamide Phosphoribosyltransferase (NAMPT) and Histone Deacetylase (HDAC) Dual Inhibitors. *J. Med. Chem.* **2017**, *60* (19), 7965–7983. https://doi.org/10.1021/acs.jmedchem.7b00467.

(96) Chen, W.; Dong, G.; Wu, Y.; Zhang, W.; Miao, C.; Sheng, C. Dual NAMPT/HDAC Inhibitors as a New Strategy for Multitargeting Antitumor Drug Discovery. *ACS Med. Chem. Lett.* **2018**, *9* (1), 34–38. https://doi.org/10.1021/acsmedchemlett.7b00414.

(97) Wang, K.; Ye, K.; Zhang, X.; Wang, T.; Qi, Z.; Wang, Y.; Jiang, S.; Zhang, K. Dual Nicotinamide Phosphoribosyltransferase (NAMPT) and Indoleamine 2,3-Dioxygenase 1 (IDO1) Inhibitors for the Treatment of Drug-Resistant Nonsmall-Cell Lung Cancer. *J. Med. Chem.* **2023**, *66* (1), 1027–1047. https://doi.org/10.1021/acs.jmedchem.2c01954.

(98) Wu, Y.; Pu, C.; Fu, Y.; Dong, G.; Huang, M.; Sheng, C. NAMPT-Targeting PROTAC Promotes Antitumor Immunity via Suppressing Myeloid-Derived Suppressor Cell Expansion. *Acta Pharm. Sin. B* **2022**, *12* (6), 2859–2868. https://doi.org/10.1016/j.apsb.2021.12.017.

(99) Zhu, X.; Liu, H.; Chen, L.; Wu, C.; Liu, X.; Cang, Y.; Jiang, B.; Yang, X.; Fan, G. Addressing the Enzyme-Independent Tumor-Promoting Function of NAMPT via PROTAC-Mediated Degradation. *Cell Chem. Biol.* **2022**, *29* (11), 1616-1629.e12. https://doi.org/10.1016/j.chembiol.2022.10.007.

(100) Sun, D.; Dong, G.; Wu, Y.; Dong, G.; Du, L.; Li, M.; Sheng, C. Fluorescent and Theranostic Probes for Imaging Nicotinamide Phosphoribosyl Transferase (NAMPT). *Eur. J. Med. Chem.* **2023**, *248*, 115080. https://doi.org/10.1016/j.ejmech.2022.115080.

(101) Dong, G.; Wu, Y.; Cheng, J.; Chen, L.; Liu, R.; Ding, Y.; Wu, S.; Ma, J.; Sheng, C. Ispinesib as an Effective Warhead for the Design of Autophagosome-Tethering Chimeras: Discovery of Potent Degraders of Nicotinamide Phosphoribosyltransferase (NAMPT). *J. Med. Chem.* **2022**, *65* (11), 7619–7628. https://doi.org/10.1021/acs.jmedchem.1c02001.

(102) Galli, U.; Colombo, G.; Travelli, C.; Tron, G. C.; Genazzani, A. A.; Grolla, A. A. Recent Advances in NAMPT Inhibitors: A Novel Immunotherapic Strategy. *Front. Pharmacol.* **2020**, *11*, 656. https://doi.org/10.3389/fphar.2020.00656.

(103) Heske, C. M. Beyond Energy Metabolism: Exploiting the Additional Roles of NAMPT for Cancer Therapy. *Front. Oncol.* **2020**, *9*.

(104) Wei, Y.; Xiang, H.; Zhang, W. Review of Various NAMPT Inhibitors for the Treatment of Cancer. *Front. Pharmacol.* **2022**, *13*, 970553. https://doi.org/10.3389/fphar.2022.970553.

(105) Mitchell, S. R.; Larkin, K.; Grieselhuber, N. R.; Lai, T.-H.; Cannon, M.; Orwick, S.; Sharma, P.; Asemelash, Y.; Zhang, P.; Goettl, V. M.; Beaver, L.; Mims, A.; Puduvalli, V. K.; Blachly, J. S.; Lehman, A.; Harrington, B.; Henderson, S.; Breitbach, J. T.; Williams, K. E.; Dong, S.; Baloglu, E.; Senapedis,

W.; Kirschner, K.; Sampath, D.; Lapalombella, R.; Byrd, J. C. Selective Targeting of NAMPT by KPT-9274 in Acute Myeloid Leukemia. *Blood Adv.* **2019**, *3* (3), 242–255. https://doi.org/10.1182/bloodadvances.2018024182.

(106) Gehrke, I.; Bouchard, E. D. J.; Beiggi, S.; Poeppl, A. G.; Johnston, J. B.; Gibson, S. B.; Banerji, V. On-Target Effect of FK866, a Nicotinamide Phosphoribosyl Transferase Inhibitor, by Apoptosis-Mediated Death in Chronic Lymphocytic Leukemia Cells. *Clin. Cancer Res.* **2014**, *20* (18), 4861–4872. https://doi.org/10.1158/1078-0432.CCR-14-0624.

(107) Cea, M.; Cagnetta, A.; Fulciniti, M.; Tai, Y.-T.; Hideshima, T.; Chauhan, D.; Roccaro, A.; Sacco, A.; Calimeri, T.; Cottini, F.; Jakubikova, J.; Kong, S.-Y.; Patrone, F.; Nencioni, A.; Gobbi, M.; Richardson, P.; Munshi, N.; Anderson, K. C. Targeting NAD+ Salvage Pathway Induces Autophagy in Multiple Myeloma Cells via MTORC1 and Extracellular Signal-Regulated Kinase (ERK1/2) Inhibition. *Blood* **2012**, *120* (17), 3519–3529. https://doi.org/10.1182/blood-2012-03-416776.

(108) Cea, M.; Cagnetta, A.; Patrone, F.; Nencioni, A.; Gobbi, M.; Anderson, K. C. Intracellular NAD+ Depletion Induces Autophagic Death in Multiple Myeloma Cells. *Autophagy* **2013**, *9* (3), 410–412. https://doi.org/10.4161/auto.22866.

(109) Billington, R. A.; Genazzani, A. A.; Travelli, C.; Condorelli, F. NAD Depletion by FK866 Induces Autophagy. *Autophagy* **2008**, *4* (3), 385–387. https://doi.org/10.4161/auto.5635.

(110) Nahimana, A.; Attinger, A.; Aubry, D.; Greaney, P.; Ireson, C.; Thougaard, A. V.; Tjørnelund, J.; Dawson, K. M.; Dupuis, M.; Duchosal, M. A. The NAD Biosynthesis Inhibitor APO866 Has Potent Antitumor Activity against Hematologic Malignancies. *Blood* **2009**, *113* (14), 3276–3286. https://doi.org/10.1182/blood-2008-08-173369.

(111) Travelli, C.; Drago, V.; Maldi, E.; Kaludercic, N.; Galli, U.; Boldorini, R.; Lisa, F. D.; Tron, G. C.; Canonico, P. L.; Genazzani, A. A. Reciprocal Potentiation of the Antitumoral Activities of FK866, an Inhibitor of Nicotinamide Phosphoribosyltransferase, and Etoposide or Cisplatin in Neuroblastoma Cells. *J. Pharmacol. Exp. Ther.* **2011**, *338* (3), 829–840. https://doi.org/10.1124/jpet.111.184630.

(112) Tateishi, K.; Wakimoto, H.; Iafrate, A. J.; Tanaka, S.; Loebel, F.; Lelic, N.; Wiederschain, D.; Bedel, O.; Deng, G.; Zhang, B.; He, T.; Shi, X.; Gerszten, R. E.; Zhang, Y.; Yeh, J.-R. J.; Curry, W. T.; Zhao, D.; Sundaram, S.; Nigim, F.; Koerner, M. V. A.; Ho, Q.; Fisher, D. E.; Roider, E. M.; Kemeny, L. V.; Samuels, Y.; Flaherty, K. T.; Batchelor, T. T.; Chi, A. S.; Cahill, D. P. Extreme Vulnerability of IDH1 Mutant Cancers to NAD+ Depletion. *Cancer Cell* **2015**, *28* (6), 773–784. https://doi.org/10.1016/j.ccell.2015.11.006.

(113) Kozako, T.; Aikawa, A.; Ohsugi, T.; Uchida, Y.; Kato, N.; Sato, K.; Ishitsuka, K.; Yoshimitsu, M.; Honda, S. High Expression of NAMPT in Adult T-Cell Leukemia/Lymphoma and Anti-Tumor Activity of a NAMPT Inhibitor. *Eur. J. Pharmacol.* **2019**, *865*, 172738. https://doi.org/10.1016/j.ejphar.2019.172738.

(114) Zoppoli, G.; Cea, M.; Soncini, D.; Fruscione, F.; Rudner, J.; Moran, E.; Caffa, I.; Bedognetti, D.; Motta, G.; Ghio, R.; Ferrando, F.; Ballestrero, A.; Parodi, S.; Belka, C.; Patrone, F.; Bruzzone, S.; Nencioni, A. Potent Synergistic Interaction between the Nampt Inhibitor APO866 and the Apoptosis Activator TRAIL in Human Leukemia Cells. *Exp. Hematol.* **2010**, *38* (11), 979–988. https://doi.org/10.1016/j.exphem.2010.07.013.

(115) Del Nagro, C.; Xiao, Y.; Rangell, L.; Reichelt, M.; O'Brien, T. Depletion of the Central Metabolite NAD Leads to Oncosis-Mediated Cell Death. *J. Biol. Chem.* **2014**, *289* (51), 35182–35192. https://doi.org/10.1074/jbc.M114.580159.

(116) Jiang, P.; Du, W.; Wu, M. Regulation of the Pentose Phosphate Pathway in Cancer. *Protein Cell* **2014**, *5* (8), 592–602. https://doi.org/10.1007/s13238-014-0082-8.

(117) Patra, K. C.; Hay, N. The Pentose Phosphate Pathway and Cancer. *Trends Biochem. Sci.* **2014**, *39* (8), 347–354. https://doi.org/10.1016/j.tibs.2014.06.005.

(118) Nagaya, M.; Hara, H.; Kamiya, T.; Adachi, T. Inhibition of NAMPT Markedly Enhances Plasma-Activated Medium-Induced Cell Death in Human Breast Cancer MDA-MB-231 Cells. *Arch. Biochem. Biophys.* **2019**, *676*, 108155. https://doi.org/10.1016/j.abb.2019.108155.

(119) Cloux, A.-J.; Aubry, D.; Heulot, M.; Widmann, C.; ElMokh, O.; Piacente, F.; Cea, M.; Nencioni, A.; Bellotti, A.; Bouzourène, K.; Pellegrin, M.; Mazzolai, L.; Duchosal, M. A.; Nahimana, A. Reactive Oxygen/Nitrogen Species Contribute Substantially to the Antileukemia Effect of APO866, a NAD Lowering Agent. *Oncotarget* **2019**, *10* (62), 6723–6738. https://doi.org/10.18632/oncotarget.27336.

(120) Cerna, D.; Li, H.; Flaherty, S.; Takebe, N.; Coleman, C. N.; Yoo, S. S. Inhibition of Nicotinamide Phosphoribosyltransferase (NAMPT) Activity by Small Molecule GMX1778 Regulates Reactive Oxygen Species (ROS)-Mediated Cytotoxicity in a P53- and Nicotinic Acid Phosphoribosyltransferase1 (NAPRT1)-Dependent Manner. *J. Biol. Chem.* **2012**, *287* (26), 22408–22417. https://doi.org/10.1074/jbc.M112.357301.

(121) Somers, K.; Evans, K.; Cheung, L.; Karsa, M.; Pritchard, T.; Kosciolek, A.; Bongers, A.; El-Ayoubi, A.; Forgham, H.; Middlemiss, S.; Mayoh, C.; Jones, L.; Gupta, M.; Kees, U. R.; Chernova, O.; Korotchkina, L.; Gudkov, A. V.; Erickson, S. W.; Teicher, B.; Smith, M. A.; Norris, M. D.; Haber, M.; Lock, R. B.; Henderson, M. J. Effective Targeting of NAMPT in Patient-Derived Xenograft Models of High-Risk Pediatric Acute Lymphoblastic Leukemia. *Leukemia* **2020**, *34* (6), 1524–1539. https://doi.org/10.1038/s41375-019-0683-6.

(122) Moore, Z.; Chakrabarti, G.; Luo, X.; Ali, A.; Hu, Z.; Fattah, F. J.; Vemireddy, R.; DeBerardinis, R. J.; Brekken, R. A.; Boothman, D. A. NAMPT Inhibition Sensitizes Pancreatic Adenocarcinoma Cells to Tumor-Selective, PAR-Independent Metabolic Catastrophe and Cell Death Induced by β-Lapachone. *Cell Death Dis.* **2015**, *6* (1), e1599. https://doi.org/10.1038/cddis.2014.564.

(123) Liu, H.-Y.; Li, Q.-R.; Cheng, X.-F.; Wang, G.-J.; Hao, H.-P. NAMPT Inhibition Synergizes with NQO1-Targeting Agents in Inducing Apoptotic Cell Death in Non-Small Cell Lung Cancer Cells. *Chin. J. Nat. Med.* **2016**, *14* (8), 582–589. https://doi.org/10.1016/S1875-5364(16)30068-1.

(124) Breton, C. S.; Aubry, D.; Ginet, V.; Puyal, J.; Heulot, M.; Widmann, C.; Duchosal, M. A.; Nahimana, A. Combinative Effects of β-Lapachone and APO866 on Pancreatic Cancer Cell Death through Reactive Oxygen Species Production and PARP-1 Activation. *Biochimie* **2015**, *116*, 141–153. https://doi.org/10.1016/j.biochi.2015.07.012.

(125) Oh, G.-S.; Kim, H.-J.; Choi, J.-H.; Shen, A.; Choe, S.-K.; Karna, A.; Lee, S. H.; Jo, H.-J.; Yang, S.-H.; Kwak, T. H.; Lee, C.-H.; Park, R.; So, H.-S. Pharmacological Activation of NQO1 Increases NAD+ Levels and Attenuates Cisplatin-Mediated Acute Kidney Injury in Mice. *Kidney Int.* **2014**, *85* (3), 547–560. https://doi.org/10.1038/ki.2013.330.

(126) Kim, H.-J.; Oh, G.-S.; Shen, A.; Lee, S.-B.; Choe, S.-K.; Kwon, K.-B.; Lee, S.; Seo, K.-S.; Kwak, T. H.; Park, R.; So, H.-S. Augmentation of NAD + by NQO1 Attenuates Cisplatin-Mediated Hearing Impairment. *Cell Death Dis.* **2014**, *5* (6), e1292–1292. https://doi.org/10.1038/cddis.2014.255.

(127) Silvers, M. A.; Deja, S.; Singh, N.; Egnatchik, R. A.; Sudderth, J.; Luo, X.; Beg, M. S.; Burgess, S. C.; DeBerardinis, R. J.; Boothman, D. A.; Merritt, M. E. The NQO1 Bioactivatable Drug, β-Lapachone, Alters the Redox State of NQO1+ Pancreatic Cancer Cells, Causing Perturbation in Central Carbon Metabolism. *J. Biol. Chem.* **2017**, *292* (44), 18203–18216. https://doi.org/10.1074/jbc.M117.813923.

(128) Li, L. S.; Bey, E. A.; Dong, Y.; Meng, J.; Patra, B.; Yan, J.; Xie, X.-J.; Brekken, R. A.; Barnett, C. C.; Bornmann, W. G.; Gao, J.; Boothman, D. A. Modulating Endogenous NQO1 Levels Identifies Key Regulatory Mechanisms of Action of β-Lapachone for Pancreatic Cancer Therapy. *Clin. Cancer Res. Off. J. Am. Assoc. Cancer Res.* **2011**, *17* (2), 275–285. https://doi.org/10.1158/1078-0432.CCR-10-1983.

(129) Miettinen, T. P.; Björklund, M. NQO2 Is a Reactive Oxygen Species Generating Off-Target for Acetaminophen. *Mol. Pharm.* **2014**, *11* (12), 4395–4404. https://doi.org/10.1021/mp5004866.

(130) Feng, J.; Yan, P.-F.; Zhao, H.; Zhang, F.-C.; Zhao, W.-H.; Feng, M. Inhibitor of Nicotinamide Phosphoribosyltransferase Sensitizes Glioblastoma Cells to Temozolomide via Activating ROS/JNK Signaling Pathway. *BioMed Res. Int.* **2016**, *2016*. https://doi.org/10.1155/2016/1450843.

(131) Touat, M.; Sourisseau, T.; Dorvault, N.; Chabanon, R. M.; Garrido, M.; Morel, D.; Krastev, D. B.; Bigot, L.; Adam, J.; Frankum, J. R.; Durand, S.; Pontoizeau, C.; Souquère, S.; Kuo, M.-S.; Sauvaigo, S.; Mardakheh, F.; Sarasin, A.; Olaussen, K. A.; Friboulet, L.; Bouillaud, F.; Pierron, G.; Ashworth, A.; Lombès, A.; Lord, C. J.; Soria, J.-C.; Postel-Vinay, S. DNA Repair Deficiency Sensitizes Lung Cancer Cells to NAD$^+$ Biosynthesis Blockade. *J. Clin. Invest.* **2018**, *128* (4), 1671–1687. https://doi.org/10.1172/JCI90277.

(132) Tateishi, K.; Higuchi, F.; Miller, J. J.; Koerner, M. V. A.; Lelic, N.; Shankar, G. M.; Tanaka, S.; Fisher, D. E.; Batchelor, T. T.; Iafrate, A. J.; Wakimoto, H.; Chi, A. S.; Cahill, D. P. The Alkylating Chemotherapeutic Temozolomide Induces Metabolic Stress in *IDH1* -Mutant Cancers and Potentiates NAD $^+$ Depletion–Mediated Cytotoxicity. *Cancer Res.* **2017**, *77* (15), 4102–4115. https://doi.org/10.1158/0008-5472.CAN-16-2263.

(133) Barraud, M.; Garnier, J.; Loncle, C.; Gayet, O.; Lequeue, C.; Vasseur, S.; Bian, B.; Duconseil, P.; Gilabert, M.; Bigonnet, M.; Maignan, A.; Moutardier, V.; Garcia, S.; Turrini, O.; Delpero, J.-R.; Giovannini, M.; Grandval, P.; Gasmi, M.; Ouaissi, M.; Secq, V.; Poizat, F.; Guibert, N.; Iovanna, J.; Dusetti, N. A Pancreatic Ductal Adenocarcinoma Subpopulation Is Sensitive to FK866, an Inhibitor of NAMPT. *Oncotarget* **2016**, *7* (33), 53783–53796. https://doi.org/10.18632/oncotarget.10776.

(134) Espindola-Netto, J. M.; Chini, C. C. S.; Tarragó, M.; Wang, E.; Dutta, S.; Pal, K.; Mukhopadhyay, D.; Sola-Penna, M.; Chini, E. N. Preclinical Efficacy of the Novel Competitive NAMPT Inhibitor STF-118804 in Pancreatic Cancer. *Oncotarget* **2017**, *8* (49), 85054–85067. https://doi.org/10.18632/oncotarget.18841.

(135) Chan, M.; Gravel, M.; Bramoullé, A.; Bridon, G.; Avizonis, D.; Shore, G. C.; Roulston, A. Synergy between the NAMPT Inhibitor GMX1777(8) and Pemetrexed in Non-Small Cell Lung Cancer Cells Is Mediated by PARP Activation and Enhanced NAD Consumption. *Cancer Res.* **2014**, *74* (21), 5948–5954. https://doi.org/10.1158/0008-5472.CAN-14-0809.

(136) Li, N.; Lopez, M. A.; Linares, M.; Kumar, S.; Oliva, S.; Martinez-Lopez, J.; Xu, L.; Xu, Y.; Perini, T.; Senapedis, W.; Baloglu, E.; Shammas, M. A.; Hunter, Z.; Anderson, K. C.; Treon, S. P.; Munshi, N. C.; Fulciniti, M. Dual PAK4-NAMPT Inhibition Impacts Growth and Survival, and Increases Sensitivity to DNA-Damaging Agents in Waldenström Macroglobulinemia. *Clin. Cancer Res. Off. J. Am. Assoc. Cancer Res.* **2019**, *25* (1), 369–377. https://doi.org/10.1158/1078-0432.CCR-18-1776.

(137) Elf, A.-K.; Bernhardt, P.; Hofving, T.; Arvidsson, Y.; Forssell-Aronsson, E.; Wängberg, B.; Nilsson, O.; Johanson, V. NAMPT Inhibitor GMX1778 Enhances the Efficacy of 177Lu-DOTATATE Treatment of Neuroendocrine Tumors. *J. Nucl. Med. Off. Publ. Soc. Nucl. Med.* **2017**, *58* (2), 288–292. https://doi.org/10.2967/jnumed.116.177584.

(138) Zerp, S. F.; Vens, C.; Floot, B.; Verheij, M.; van Triest, B. NAD$^+$ Depletion by APO866 in Combination with Radiation in a Prostate Cancer Model, Results from an in Vitro and in Vivo Study. *Radiother. Oncol. J. Eur. Soc. Ther. Radiol. Oncol.* **2014**, *110* (2), 348–354. https://doi.org/10.1016/j.radonc.2013.10.039.

(139) Kato, H.; Ito, E.; Shi, W.; Alajez, N. M.; Yue, S.; Lee, C.; Chan, N.; Bhogal, N.; Coackley, C. L.; Vines, D.; Green, D.; Waldron, J.; Gullane, P.; Bristow, R.; Liu, F.-F. Efficacy of Combining GMX1777 with Radiation Therapy for Human Head and Neck Carcinoma. *Clin. Cancer Res. Off. J. Am. Assoc. Cancer Res.* **2010**, *16* (3), 898–911. https://doi.org/10.1158/1078-0432.CCR-09-1945.

(140) Bajrami, I.; Kigozi, A.; Van Weverwijk, A.; Brough, R.; Frankum, J.; Lord, C. J.; Ashworth, A. Synthetic Lethality of PARP and NAMPT Inhibition in Triple-Negative Breast Cancer Cells. *EMBO Mol. Med.* **2012**, *4* (10), 1087–1096. https://doi.org/10.1002/emmm.201201250.

(141) Heske, C. M.; Davis, M. I.; Baumgart, J. T.; Wilson, K.; Gormally, M. V.; Chen, L.; Zhang, X.; Ceribelli, M.; Duveau, D. Y.; Guha, R.; Ferrer, M.; Arnaldez, F. I.; Ji, J.; Tran, H.-L.; Zhang, Y.; Mendoza, A.; Helman, L. J.; Thomas, C. J. Matrix Screen Identifies Synergistic Combination of PARP Inhibitors and Nicotinamide Phosphoribosyltransferase (NAMPT) Inhibitors in Ewing Sarcoma. *Clin. Cancer Res. Off. J. Am. Assoc. Cancer Res.* **2017**, *23* (23), 7301–7311. https://doi.org/10.1158/1078-0432.CCR-17-1121.

(142) Gibson, A. E.; Yeung, C.; Issaq, S. H.; Collins, V. J.; Gouzoulis, M.; Zhang, Y.; Ji, J.; Mendoza, A.; Heske, C. M. Inhibition of Nicotinamide Phosphoribosyltransferase (NAMPT) with OT-82 Induces DNA Damage, Cell Death, and Suppression of Tumor Growth in Preclinical Models of Ewing Sarcoma. *Oncogenesis* **2020**, *9* (9), 80. https://doi.org/10.1038/s41389-020-00264-0.

(143) Bruzzone, S.; Fruscione, F.; Morando, S.; Ferrando, T.; Poggi, A.; Garuti, A.; D'Urso, A.; Selmo, M.; Benvenuto, F.; Cea, M.; Zoppoli, G.; Moran, E.; Soncini, D.; Ballestrero, A.; Sordat, B.; Patrone, F.; Mostoslavsky, R.; Uccelli, A.; Nencioni, A. Catastrophic NAD+ Depletion in Activated T Lymphocytes through Nampt Inhibition Reduces Demyelination and Disability in EAE. *PloS One* **2009**, *4* (11), e7897. https://doi.org/10.1371/journal.pone.0007897.

(144) Li, M.; Kirtane, A. R.; Kiyokawa, J.; Nagashima, H.; Lopes, A.; Tirmizi, Z. A.; Lee, C. K.; Traverso, G.; Cahill, D. P.; Wakimoto, H. Local Targeting of NAD+ Salvage Pathway Alters the Immune Tumor Microenvironment and Enhances Checkpoint Immunotherapy in Glioblastoma. *Cancer Res.* **2020**, canres.1094.2020. https://doi.org/10.1158/0008-5472.CAN-20-1094.

(145) Travelli, C.; Consonni, F. M.; Sangaletti, S.; Storto, M.; Morlacchi, S.; Grolla, A. A.; Galli, U.; Tron, G. C.; Portararo, P.; Rimassa, L.; Pressiani, T.; Mazzone, M.; Trovato, R.; Ugel, S.; Bronte, V.; Tripodo, C.; Colombo, M. P.; Genazzani, A. A.; Sica, A. Nicotinamide Phosphoribosyltransferase Acts as a Metabolic Gate for Mobilization of Myeloid-Derived Suppressor Cells. *Cancer Res.* **2019**, *79* (8), 1938–1951. https://doi.org/10.1158/0008-5472.CAN-18-1544.

(146) Cea, M.; Soncini, D.; Fruscione, F.; Raffaghello, L.; Garuti, A.; Emionite, L.; Moran, E.; Magnone, M.; Zoppoli, G.; Reverberi, D.; Caffa, I.; Salis, A.; Cagnetta, A.; Bergamaschi, M.; Casciaro, S.; Pierri, I.; Damonte, G.; Ansaldi, F.; Gobbi, M.; Pistoia, V.; Ballestrero, A.; Patrone, F.; Bruzzone, S.; Nencioni, A. Synergistic Interactions between HDAC and Sirtuin Inhibitors in Human Leukemia Cells. *PLOS ONE* **2011**, *6* (7), e22739. https://doi.org/10.1371/journal.pone.0022739.

(147) Cea, M.; Cagnetta, A.; Acharya, C.; Acharya, P.; Tai, Y.-T.; Yang, G.; Lovera, D.; Soncini, D.; Miglino, M.; Fraternali-Orcioni, G.; Mastracci, L.; Nencioni, A.; Montecucco, F.; Ballestrero, A.; Hideshima, T.; Chauhan, D.; Gobbi, M.; Lemoli, R. M.; Munshi, N.; Treon, S. P.; Anderson, K. C. Dual NAMPT and BTK Targeting Leads to Synergistic Killing of Waldenstrom's Macroglobulinemia Cells Regardless of MYD88 and CXCR4 Somatic Mutations Status. *Clin. Cancer Res. Off. J. Am. Assoc. Cancer Res.* **2016**, *22* (24), 6099–6109. https://doi.org/10.1158/1078-0432.CCR-16-0630.

(148) Cagnetta, A.; Cea, M.; Calimeri, T.; Acharya, C.; Fulciniti, M.; Tai, Y.-T.; Hideshima, T.; Chauhan, D.; Zhong, M. Y.; Patrone, F.; Nencioni, A.; Gobbi, M.; Richardson, P.; Munshi, N.; Anderson, K. C. Intracellular NAD+ Depletion Enhances Bortezomib-Induced Anti-Myeloma Activity. *Blood* **2013**, *122* (7), 1243–1255. https://doi.org/10.1182/blood-2013-02-483511.

(149) Mpilla, G.; Aboukameel, A.; Muqbil, I.; Kim, S.; Beydoun, R.; Philip, P. A.; Mohammad, R. M.; Kamgar, M.; Shidham, V.; Senapedis, W.; Baloglu, E.; Li, J.; Dyson, G.; Xue, Y.; El-Rayes, B.; Azmi, A. S. PAK4-NAMPT Dual Inhibition as a Novel Strategy for Therapy Resistant Pancreatic Neuroendocrine Tumors. *Cancers* **2019**, *11* (12), 1902. https://doi.org/10.3390/cancers11121902.

(150) Cagnetta, A.; Caffa, I.; Acharya, C.; Soncini, D.; Acharya, P.; Adamia, S.; Pierri, I.; Bergamaschi, M.; Garuti, A.; Fraternali, G.; Mastracci, L.; Provenzani, A.; Zucal, C.; Damonte, G.; Salis, A.;

Montecucco, F.; Patrone, F.; Ballestrero, A.; Bruzzone, S.; Gobbi, M.; Nencioni, A.; Cea, M. APO866 Increases Antitumor Activity of Cyclosporin-A by Inducing Mitochondrial and Endoplasmic Reticulum Stress in Leukemia Cells. *Clin. Cancer Res.* **2015**, *21* (17), 3934–3945. https://doi.org/10.1158/1078-0432.CCR-14-3023.

(151) Piacente, F.; Caffa, I.; Ravera, S.; Sociali, G.; Passalacqua, M.; Vellone, V. G.; Becherini, P.; Reverberi, D.; Monacelli, F.; Ballestrero, A.; Odetti, P.; Cagnetta, A.; Cea, M.; Nahimana, A.; Duchosal, M.; Bruzzone, S.; Nencioni, A. Nicotinic Acid Phosphoribosyltransferase Regulates Cancer Cell Metabolism, Susceptibility to NAMPT Inhibitors, and DNA Repair. *Cancer Res.* **2017**, *77* (14), 3857–3869. https://doi.org/10.1158/0008-5472.CAN-16-3079.

(152) ElMokh, O.; Matsumoto, S.; Biniecka, P.; Bellotti, A.; Schaeuble, K.; Piacente, F.; Gallart-Ayala, H.; Ivanisevic, J.; Stamenkovic, I.; Nencioni, A.; Nahimana, A.; Duchosal, M. A. Gut Microbiota Severely Hampers the Efficacy of NAD-Lowering Therapy in Leukemia. *Cell Death Dis.* **2022**, *13* (4), 320. https://doi.org/10.1038/s41419-022-04763-3.

(153) Fons, N. R.; Sundaram, R. K.; Breuer, G. A.; Peng, S.; McLean, R. L.; Kalathil, A. N.; Schmidt, M. S.; Carvalho, D. M.; Mackay, A.; Jones, C.; Carcaboso, Á. M.; Nazarian, J.; Berens, M. E.; Brenner, C.; Bindra, R. S. PPM1D Mutations Silence NAPRT Gene Expression and Confer NAMPT Inhibitor Sensitivity in Glioma. *Nat. Commun.* **2019**, *10* (1), 3790. https://doi.org/10.1038/s41467-019-11732-6.

(154) Lee, J.; Kim, H.; Lee, J. E.; Shin, S.-J.; Oh, S.; Kwon, G.; Kim, H.; Choi, Y. Y.; White, M. A.; Paik, S.; Cheong, J.-H.; Kim, H. S. Selective Cytotoxicity of the NAMPT Inhibitor FK866 Toward Gastric Cancer Cells With Markers of the Epithelial-Mesenchymal Transition, Due to Loss of NAPRT. *Gastroenterology* **2018**, *155* (3), 799-814.e13. https://doi.org/10.1053/j.gastro.2018.05.024.

(155) Peterse, E. F. P.; van den Akker, B. E. W. M.; Niessen, B.; Oosting, J.; Suijker, J.; de Jong, Y.; Danen, E. H. J.; Cleton-Jansen, A.-M.; Bovée, J. V. M. G. NAD Synthesis Pathway Interference Is a Viable Therapeutic Strategy for Chondrosarcoma. *Mol. Cancer Res.* **2017**, *15* (12), 1714–1721. https://doi.org/10.1158/1541-7786.MCR-17-0293.

(156) Shames, D. S.; Elkins, K.; Walter, K.; Holcomb, T.; Du, P.; Mohl, D.; Xiao, Y.; Pham, T.; Haverty, P. M.; Liederer, B.; Liang, X.; Yauch, R. L.; O'Brien, T.; Bourgon, R.; Koeppen, H.; Belmont, L. D. Loss of NAPRT1 Expression by Tumor-Specific Promoter Methylation Provides a Novel Predictive Biomarker for NAMPT Inhibitors. *Clin. Cancer Res.* **2013**, *19* (24), 6912–6923. https://doi.org/10.1158/1078-0432.CCR-13-1186.

(157) Duarte-Pereira, S.; Pereira-Castro, I.; Silva, S. S.; Correia, M. G.; Neto, C.; da Costa, L. T.; Amorim, A.; Silva, R. M. Extensive Regulation of Nicotinate Phosphoribosyltransferase (NAPRT) Expression in Human Tissues and Tumors. *Oncotarget* **2016**, *7* (2), 1973–1983. https://doi.org/10.18632/oncotarget.6538.

(158) Managò, A.; Audrito, V.; Mazzola, F.; Sorci, L.; Gaudino, F.; Gizzi, K.; Vitale, N.; Incarnato, D.; Minazzato, G.; Ianniello, A.; Varriale, A.; D'Auria, S.; Mengozzi, G.; Politano, G.; Oliviero, S.; Raffaelli, N.; Deaglio, S. Extracellular Nicotinate Phosphoribosyltransferase Binds Toll like Receptor 4 and Mediates Inflammation. *Nat. Commun.* **2019**, *10* (1), 4116. https://doi.org/10.1038/s41467-019-12055-2.

(159) Hara, N.; Yamada, K.; Shibata, T.; Osago, H.; Hashimoto, T.; Tsuchiya, M. Elevation of Cellular NAD Levels by Nicotinic Acid and Involvement of Nicotinic Acid Phosphoribosyltransferase in Human Cells. *J. Biol. Chem.* **2007**, *282* (34), 24574–24582. https://doi.org/10.1074/jbc.M610357200.

(160) Kanarek, N.; Petrova, B.; Sabatini, D. M. Dietary Modifications for Enhanced Cancer Therapy. *Nature* **2020**, *579* (7800), 507–517. https://doi.org/10.1038/s41586-020-2124-0.

(161) Gaut, Z. N.; Solomon, H. M. Inhibition of Nicotinate Phosphoribosyl Transferase by Nonsteroidal Anti-Inflammatory Drugs: A Possible Mechanism of Action. *J. Pharm. Sci.* **1971**, *60* (12), 1887–1888. https://doi.org/10.1002/jps.2600601230.

(162) Gaut, Z. N.; Solomon, H. M. Inhibition of Nicotinate Phosphoribosyltransferase in Human Platelet Lysate by Nicotinic Acid Analogs. *Biochem. Pharmacol.* **1971**, *20* (10), 2903–2906. https://doi.org/10.1016/0006-2952(71)90202-4.

(163) Gaut, Z. N.; Solomon, H. M. Uptake and Metabolism of Nicotinic Acid by Human Blood Platelets. Effects of Structure Analogs and Metabolic Inhibitors. *Biochim. Biophys. Acta* **1970**, *201* (2), 316–322. https://doi.org/10.1016/0304-4165(70)90306-5.

(164) Galassi, L.; Di Stefano, M.; Brunetti, L.; Orsomando, G.; Amici, A.; Ruggieri, S.; Magni, G. Characterization of Human Nicotinate Phosphoribosyltransferase: Kinetic Studies, Structure Prediction and Functional Analysis by Site-Directed Mutagenesis. *Biochimie* **2012**, *94* (2), 300–309. https://doi.org/10.1016/j.biochi.2011.06.033.

(165) Marletta, A. S.; Massarotti, A.; Orsomando, G.; Magni, G.; Rizzi, M.; Garavaglia, S. Crystal Structure of Human Nicotinic Acid Phosphoribosyltransferase. *FEBS Open Bio* **2015**, *5*, 419–428. https://doi.org/10.1016/j.fob.2015.05.002.

(166) Vichai, V.; Kirtikara, K. Sulforhodamine B Colorimetric Assay for Cytotoxicity Screening. *Nat. Protoc.* **2006**, *1* (3), 1112–1116. https://doi.org/10.1038/nprot.2006.179.

(167) Bradford, M. M. A Rapid and Sensitive Method for the Quantitation of Microgram Quantities of Protein Utilizing the Principle of Protein-Dye Binding. *Anal. Biochem.* **1976**, *72*, 248–254. https://doi.org/10.1006/abio.1976.9999.

(168) Marini, C.; Ravera, S.; Buschiazzo, A.; Bianchi, G.; Orengo, A. M.; Bruno, S.; Bottoni, G.; Emionite, L.; Pastorino, F.; Monteverde, E.; Garaboldi, L.; Martella, R.; Salani, B.; Maggi, D.; Ponzoni, M.; Fais, F.; Raffaghello, L.; Sambuceti, G. Discovery of a Novel Glucose Metabolism in Cancer: The Role of Endoplasmic Reticulum beyond Glycolysis and Pentose Phosphate Shunt. *Sci. Rep.* **2016**, *6*, 25092. https://doi.org/10.1038/srep25092.

(169) Becherini, P.; Caffa, I.; Piacente, F.; Damonte, P.; Vellone, V. G.; Passalacqua, M.; Benzi, A.; Bonfiglio, T.; Reverberi, D.; Khalifa, A.; Ghanem, M.; Guijarro, A.; Tagliafico, L.; Sucameli, M.; Persia, A.; Monacelli, F.; Cea, M.; Bruzzone, S.; Ravera, S.; Nencioni, A. SIRT6 Enhances Oxidative Phosphorylation in Breast Cancer and Promotes Mammary Tumorigenesis in Mice. *Cancer Metab.* **2021**, *9* (1), 6. https://doi.org/10.1186/s40170-021-00240-1.

(170) Ravera, S.; Vigliarolo, T.; Bruno, S.; Morandi, F.; Marimpietri, D.; Sabatini, F.; Dagnino, M.; Petretto, A.; Bartolucci, M.; Muraca, M.; Biasin, E.; Haupt, R.; Zecca, M.; Fagioli, F.; Cilloni, D.; Podestà, M.; Frassoni, F. Identification of Biochemical and Molecular Markers of Early Aging in Childhood Cancer Survivors. *Cancers* **2021**, *13* (20), 5214. https://doi.org/10.3390/cancers13205214.

(171) Marini, C.; Cossu, V.; Bauckneht, M.; Carta, S.; Lanfranchi, F.; D'Amico, F.; Ravera, S.; Orengo, A. M.; Ghiggi, C.; Ballerini, F.; Durando, P.; Chiesa, S.; Miceli, A.; Donegani, M. I.; Morbelli, S.; Bruno, S.; Sambuceti, G. Mitochondrial Generated Redox Stress Differently Affects the Endoplasmic Reticulum of Circulating Lymphocytes and Monocytes in Treatment-Naïve Hodgkin's Lymphoma. *Antioxid. Basel Switz.* **2022**, *11* (4), 762. https://doi.org/10.3390/antiox11040762.

(172) Graeff, R.; Lee, H. C. A Novel Cycling Assay for Cellular CADP-Ribose with Nanomolar Sensitivity. *Biochem. J.* **2002**, *361* (Pt 2), 379. https://doi.org/10.1042/bj3610379.

(173) Huang, J.; Cui, L.; Natarajan, M.; Barone, P. W.; Wolfrum, J. M.; Lee, Y. H.; Rice, S. A.; Springs, S. L. The Ratio of Nicotinic Acid to Nicotinamide as a Microbial Biomarker for Assessing Cell Therapy Product Sterility. *Mol. Ther. - Methods Clin. Dev.* **2022**, *25*, 410–424. https://doi.org/10.1016/j.omtm.2022.04.006.

(174) Seiner, D. R.; Hegde, S. S.; Blanchard, J. S. Kinetics and Inhibition of Nicotinamidase from Mycobacterium Tuberculosis. *Biochemistry* **2010**, *49* (44), 9613–9619. https://doi.org/10.1021/bi1011157.

(175) French, J. B.; Cen, Y.; Vrablik, T. L.; Xu, P.; Allen, E.; Hanna-Rose, W.; Sauve, A. A. Characterization of Nicotinamidases: Steady State Kinetic Parameters, Classwide Inhibition by Nicotinaldehydes,

and Catalytic Mechanism. *Biochemistry* **2010**, *49* (49), 10421–10439. https://doi.org/10.1021/bi1012518.

(176) Matsumoto, S.; Biniecka, P.; Bellotti, A.; Duchosal, M. A.; Nahimana, A. Nicotinaldehyde, a Novel Precursor of NAD Biosynthesis, Abrogates the Anti-Cancer Activity of an NAD-Lowering Agent in Leukemia. *Cancers* **2023**, *15* (3), 787. https://doi.org/10.3390/cancers15030787.

(177) Reeves, P. G.; Nielsen, F. H.; Fahey, G. C. AIN-93 Purified Diets for Laboratory Rodents: Final Report of the American Institute of Nutrition Ad Hoc Writing Committee on the Reformulation of the AIN-76A Rodent Diet. *J. Nutr.* **1993**, *123* (11), 1939–1951. https://doi.org/10.1093/jn/123.11.1939.

(178) O'Brien, T.; Oeh, J.; Xiao, Y.; Liang, X.; Vanderbilt, A.; Qin, A.; Yang, L.; Lee, L. B.; Ly, J.; Cosino, E.; LaCap, J. A.; Ogasawara, A.; Williams, S.; Nannini, M.; Liederer, B. M.; Jackson, P.; Dragovich, P. S.; Sampath, D. Supplementation of Nicotinic Acid with NAMPT Inhibitors Results in Loss of In Vivo Efficacy in NAPRT1-Deficient Tumor Models. *Neoplasia* **2013**, *15* (12), 1314-IN3. https://doi.org/10.1593/neo.131718.

(179) Cercillieux, A.; Ciarlo, E.; Canto, C. Balancing NAD+ Deficits with Nicotinamide Riboside: Therapeutic Possibilities and Limitations. *Cell. Mol. Life Sci.* **2022**, *79* (8), 463. https://doi.org/10.1007/s00018-022-04499-5.

(180) Reikvam, D. H.; Erofeev, A.; Sandvik, A.; Grcic, V.; Jahnsen, F. L.; Gaustad, P.; McCoy, K. D.; Macpherson, A. J.; Meza-Zepeda, L. A.; Johansen, F.-E. Depletion of Murine Intestinal Microbiota: Effects on Gut Mucosa and Epithelial Gene Expression. *PLOS ONE* **2011**, *6* (3), e17996. https://doi.org/10.1371/journal.pone.0017996.

(181) Savjani, K. T.; Gajjar, A. K.; Savjani, J. K. Drug Solubility: Importance and Enhancement Techniques. *ISRN Pharm.* **2012**, *2012*, 195727. https://doi.org/10.5402/2012/195727.

(182) Daina, A.; Michielin, O.; Zoete, V. SwissADME: A Free Web Tool to Evaluate Pharmacokinetics, Drug-Likeness and Medicinal Chemistry Friendliness of Small Molecules. *Sci. Rep.* **2017**, *7* (1), 42717. https://doi.org/10.1038/srep42717.

(183) Nanayakkara, A. K.; Follit, C. A.; Chen, G.; Williams, N. S.; Vogel, P. D.; Wise, J. G. Targeted Inhibitors of P-Glycoprotein Increase Chemotherapeutic-Induced Mortality of Multidrug Resistant Tumor Cells. *Sci. Rep.* **2018**, *8* (1), 967. https://doi.org/10.1038/s41598-018-19325-x.

(184) Watson, M.; Roulston, A.; Bélec, L.; Billot, X.; Marcellus, R.; Bédard, D.; Bernier, C.; Branchaud, S.; Chan, H.; Dairi, K.; Gilbert, K.; Goulet, D.; Gratton, M.-O.; Isakau, H.; Jang, A.; Khadir, A.; Koch, E.; Lavoie, M.; Lawless, M.; Nguyen, M.; Paquette, D.; Turcotte, É.; Berger, A.; Mitchell, M.; Shore, G. C.; Beauparlant, P. The Small Molecule GMX1778 Is a Potent Inhibitor of NAD+ Biosynthesis: Strategy for Enhanced Therapy in Nicotinic Acid Phosphoribosyltransferase 1-Deficient Tumors. *Mol. Cell. Biol.* **2009**, *29* (21), 5872–5888. https://doi.org/10.1128/MCB.00112-09.

(185) Olesen, U. H.; Thougaard, A. V.; Jensen, P. B.; Sehested, M. A Preclinical Study on the Rescue of Normal Tissue by Nicotinic Acid in High-Dose Treatment with APO866, a Specific Nicotinamide Phosphoribosyltransferase Inhibitor. *Mol. Cancer Ther.* **2010**, *9* (6), 1609–1617. https://doi.org/10.1158/1535-7163.MCT-09-1130.

(186) Taylor, S. R.; Falcone, J. N.; Cantley, L. C.; Goncalves, M. D. Developing Dietary Interventions as Therapy for Cancer. *Nat. Rev. Cancer* **2022**, *22* (8), 452–466. https://doi.org/10.1038/s41568-022-00485-y.

(187) Kang, G. B.; Bae, M.-H.; Kim, M.-K.; Im, I.; Kim, Y.-C.; Eom, S. H. Crystal Structure of Rattus Norvegicus Visfatin/PBEF/Nampt in Complex with an FK866-Based Inhibitor. *Mol. Cells* **2009**, *27* (6), 667–671. https://doi.org/10.1007/s10059-009-0088-x.

(188) Khan, J. A.; Tao, X.; Tong, L. Molecular Basis for the Inhibition of Human NMPRTase, a Novel Target for Anticancer Agents. *Nat. Struct. Mol. Biol.* **2006**, *13* (7), 582–588. https://doi.org/10.1038/nsmb1105.

(189) Parenti, M. D.; Grozio, A.; Bauer, I.; Galeno, L.; Damonte, P.; Millo, E.; Sociali, G.; Franceschi, C.; Ballestrero, A.; Bruzzone, S.; Del Rio, A.; Nencioni, A. Discovery of Novel and Selective SIRT6 Inhibitors. *J. Med. Chem.* **2014**, *57* (11), 4796–4804. https://doi.org/10.1021/jm500487d.

(190) Franco, J.; Piacente, F.; Walter, M.; Fratta, S.; Ghanem, M.; Benzi, A.; Caffa, I.; Kurkin, A. V.; Altieri, A.; Herr, P.; Martínez-Bailén, M.; Robina, I.; Bruzzone, S.; Nencioni, A.; Del Rio, A. Structure-Based Identification and Biological Characterization of New NAPRT Inhibitors. *Pharmaceuticals* **2022**, *15* (7), 855. https://doi.org/10.3390/ph15070855.

(191) Sliwoski, G.; Kothiwale, S.; Meiler, J.; Lowe, E. W. Computational Methods in Drug Discovery. *Pharmacol. Rev.* **2014**, *66* (1), 334–395. https://doi.org/10.1124/pr.112.007336.

(192) Ghanem, M. S.; Monacelli, F.; Nencioni, A. Advances in NAD-Lowering Agents for Cancer Treatment. *Nutrients* **2021**, *13* (5), 1665. https://doi.org/10.3390/nu13051665.

(193) Ghanem, M. S.; Caffa, I.; Del Rio, A.; Franco, J.; Parenti, M. D.; Monacelli, F.; Cea, M.; Khalifa, A.; Nahimana, A.; Duchosal, M. A.; Ravera, S.; Bertola, N.; Bruzzone, S.; Nencioni, A.; Piacente, F. Identification of NAPRT Inhibitors with Anti-Cancer Properties by In Silico Drug Discovery. *Pharm. Basel Switz.* **2022**, *15* (7), 848. https://doi.org/10.3390/ph15070848.